DYNAMIC RESPONSE OF CONCRETE RECTANGULAR LIQUID STORAGE TANKS

by

Jun Zheng Chen, P.ENG.

B.ENG., Tong Ji University, Shanghai, China, 1995

A thesis

presented to Ryerson University

in partial fulfillment of the

requirement for the degree of

Master of Applied Science

in the program of

Civil Engineering

Toronto, Ontario, Canada, 2003

National Library
of Canada

Bibliothèque nationale
du Canada

Acquisitions and
Bibliographic Services

Acquisisitons et
services bibliographiques

395 Wellington Street
Ottawa ON K1A 0N4
Canada

395, rue Wellington
Ottawa ON K1A 0N4
Canada

Canadä

AUTHOR'S DECLARATION

I hereby declare that I am the sole author of this thesis.

I authorize Ryerson University to lend this thesis to other institutions or individuals for

the purpose of scholarly research.

Jun Zheng Chen, P.ENG.

Department of Civil Engineering

Ryerson University

I further authorize Ryerson University to reproduce this thesis by photocopying or by

other means, in total or in part, at the request of other institutions or individuals for the

purpose of scholarly research.

Jun Zheng Chen, P.ENG.

Department of Civil Engineering

Ryerson University

BORROWER'S PAGE

Ryerson University requires the signatures of all persons using or photocopying this thesis. Please sign below, and give address and date.

Name of Borrowers	Date	Address	Signature

DYNAMIC RESPONSE OF CONCRETE RECTANGULAR

LIQUID STORAGE TANKS

Jun Zheng Chen P.Eng.
Master of Applied Science, 2003
Department of Civil Engineering
Ryerson University

ABSTRACT

In this thesis, the dynamic response of concrete rectangular liquid storage tanks is investigated. In previous studies, the tank wall has been assumed as rigid in the calculation of hydrodynamic pressures. The effect of flexibility of tank wall is considered in this study. The analytical solutions for both impulsive pressure and convective pressure induced by both horizontal and vertical ground motions are presented.

A 2-D coupled analysis model of tank wall is proposed. The hydrodynamic pressures are considered as external forces applied on the tank wall. Through a technique called the sequential method, the two fields of fluid and structure are coupled. The time-history analysis using the mode superposition method and the direct step-by-step integration method are carried out. Two rectangular tanks are analyzed. From the comparison of the results obtained from the proposed model with those proposed by other researchers, such as added mass model based on the rigid wall boundary condition, it shows that the lumped mass approach overestimates the base shear and wall displacement. The effect of wall flexibility on displacements, base shears and base moments are also discussed.

A combination of the added mass method and the sequential method is used to study liquid storage tanks subjected to the vertical ground motion. It is found that the effect of the vertical acceleration should be considered in dynamic analysis of rectangular tanks. It is concluded that the total response of the structures should be based on the sum of the response under both horizontal and vertical components of ground motion.

ACKNOWLEDGEMENTS

I would like to express my thanks to Professor M. Reza Kianoush for his encouragement, support and supervision of this research work.

In addition, deep gratitude is expressed to my parents for their encouragement in the past years, which led me to this achievement.

TABLE OF CONTENTS

LIST OF TABLES

LIST OF FIGURES

LIST OF SYMBOLS

A	=	area of the plane stress element
$\{A^n\}$	=	amplitude of vibration
[B]	=	strain-displacement matrix
C_i	=	period-dependent spectral amplification factor
$[C]$	=	matrix of damping coefficient
d	=	displacement
d_A	=	displacement at the top of tank wall
D	=	Damping
$[D]$	=	matrix of material constants
E	=	Young's modulus
E_c	=	modulus of elasticity of concrete
F	=	generalized force
F_B	=	base shear of tank wall
$\{F\}$	=	vector of generalized force
g	=	acceleration due to gravity
G	=	shear modulus of material
h_i	=	height above the base of the wall to the center of the gravity of the impulsive lateral force
h_w	=	height from the base of the wall to the center of gravity of tank wall
	=	gravity of the impulsive lateral force
H	=	height of tank
H_l	=	height of fluid
H_w	=	height of tank wall

I	=	important factor
$[k]$	=	element stiffness matrix
$[K]$	=	matrix of stiffness coefficient
L_x, L_z	=	half inside length of a rectangular tank in the directions of x and z
M_B	=	base moment
M_i	=	impulsive mass of contained liquid per unit width of a rectangular tank wall
M_w	=	mass per unit width of a rectangular tank wall
$[m]$	=	element mass matrix
$[M]$	=	matrix of inertia coefficient
$[N]$	=	matrix of shape function
p	=	hydrodynamic pressure (Chapter 3)
P	=	hydrodynamic pressure function (Chapter 3)
P_B	=	the lateral inertial forces of wall and lateral impulsive force
p_x, p_y	=	components of the applied boundary forces per unit length of the boundary (Chapter 4)
R_w	=	response modification factor
s	=	the boundary of the plane stress element
S	=	site profile coefficient representing the soil characteristic as they pertain to the structure
t	=	time
t_w	=	thickness of tank wall
T	=	kinetic energy
T_n	=	period of vibration in the nth mode.

$\dot{u}(t)$, $\ddot{u}(t)$ = velocity and acceleration of fluid in horizontal

direction respectively (Chapter 3)

$u, \dot{u}, \ddot{u}$ = displacement, velocity and acceleration respectively

in x direction (Chapter 4)

$v, \dot{v}, \ddot{v}$ = displacement, velocity and acceleration respectively

in y direction (Chapter 4)

$\{u\}, \{\dot{u}\}, \{\ddot{u}\}$ = matrix of system displacement, velocity

and acceleration respectively (Chapter 4)

U = strain energy

ν = Poisson's ratio

V_x, V_y = velocity component in the directions of x, y

x, y, z = Cartesian coordinates

W_{nc} = virtual work done by the non-conservative forces

Z = seismic zone factor

ϕ = velocity potential function for liquid

γ = shear strain

ε = normal strain

ε = effective mass coefficient (Chapter 7)

η = function for mean level of the free surface

λ = wavelength

λ_c = wavelength for convective pressure

λ_I = wavelength for impulsive pressure

λ_n = proportion of critical damping in the nth mode

ρ = mass density of material

ρ_l = mass density of liquid

ρ_w = mass density of tank wall

σ = normal stress

τ = shear stress

ω = natural frequency

ω_i = natural frequency of the impulsive mode of vibration

ω_c = natural frequency of the convective mode of sloshing

ξ = damping ratio

Chapter 1 Introduction

1.1 Introduction

Liquid storage tanks are essential facilities in lifeline and environmental engineering systems. They also play an important role in the rescue work after earthquakes. Any damage of such tanks after an earthquake may cause consequential loss to the society. Although major studies have been conduct in the past, as most of them are related to circular liquid storage tanks, especially steel tanks, little attention has been focused on the dynamic response of concrete rectangular tanks. In this study, the dynamic response of concrete rectangular liquid storage tanks is investigated.

The problem related to liquid storage tanks involves many fundamental subjects which are of concern. One of them is the interaction between the fluid and structures under the seismic loading. Usually the hydrodynamic pressures induced by earthquakes can be separated into convective pressure and impulsive pressure. The boundary condition in the calculation of hydrodynamic pressures has been treated as rigid wall such as those in the current design standards and codes e.g. ACI 350.3 (2001) and New Zealand Code NZS3106 (1986). For the case of concrete tanks, the effect of tank flexibility on dynamic response is still questionable. In this study, this problem is investigated.

1.2 Objectives and Scope of the Study

The main purpose of the present study is to investigate the dynamic response of liquid storage tanks. As mentioned before, though some general principles of dynamic response of liquid storage tanks are studied, the major emphasis is on the dynamic response of concrete rectangular liquid storage tanks. In this thesis, a finite element model is developed to consider the magnitude of hydrodynamic pressures due to the flexibility of wall in the dynamic analysis. In order to implement this proposed model, a

sequential method is used and a computer program is developed. On this basis, the dynamic response of liquid storage tanks is easily analyzed. Finally some recommendations are provided.

The scope of the present study is summarized below:

(1) Study the hydrodynamic pressures in the flexible wall boundary condition.

(2) Develop a finite element model for the analysis of the dynamic response of liquid storage tanks.

(3) Establish the dynamic analysis techniques for computer analysis.

(4) Develop a computer program HYDRO which can calculate the impulsive pressure. Incorporate this program into a general purpose structural analysis software SAPIV.

(5) Analyze rectangular tanks under horizontal and vertical ground motion. Study different models in order to verify the validity of the proposed model.

(6) Study the load combination of liquid storage tanks subjected to earthquakes.

1.3 Thesis Layout

The thesis is divided into eight chapters. In Chapter 1 the objectives and the scope of research are described. A summary of the research work on dynamic response of liquid storage tanks is presented in Chapter 2.

Chapter 3 discusses how to calculate hydrodynamic pressures in the flexible wall boundary condition. The basic theory in relation to surface wave or potential flow is presented. Two-dimensional analytical solutions for both impulsive and convective hydrodynamic pressure are provided. The results include hydrodynamic pressures induced by both horizontal and vertical ground motions.

In Chapter 4, the dynamic response of an empty tank is investigated. The dynamic analysis is carried out using time history analysis. Both the mode superposition method and the direct step-by-step integration method are used.

Chapter 5 presents a finite element model for the analysis of fluid-structure

interaction problem. The sequential method used in the analysis for the proposed model is described.

In Chapter 6, the subroutine HYDRO is presented. The linear structural analysis software SAPIV is used to carry out dynamic analysis. The incorporation of subroutine HYDRO into SAPIV is described.

Chapter 7 presents the results of series of parametric studies on the dynamic response of rectangular storage tanks. A rectangular tank studied by other researchers is used to verify the efficiency of proposed model.

Finally, a summary and the major conclusions reached from the study are described in Chapter 8. Some recommendations for further study are also given in this chapter.

Chapter 2 Literature Review

2.1 Introduction

The previous research work related to the dynamic response of liquid storage tanks is presented in this chapter. Section 2.2 describes the damages and failures of the fluid storage tanks during past earthquakes. Some figures describing the failure mechanism are presented for understanding of this problem. A brief summary of historical research in this field is presented in Section 2.3. Different models used in the analysis of fluid storage tanks and the major contributions from past studies are described in this section. Finally some related information is presented as this subject links to many other engineering fields. The design codes and the related documents are introduced in Section 2.4.

2.2 Failure of Fluid Storage Tanks under Earthquakes

Liquid storage tanks are very important components of lifeline and industrial facilities. The damage of such tanks may not mean the loss of economic value of the tank and content. Without the assured water supply, some consequential damage such as uncontrolled fires may occur. In addition, as these structures are used extensively for the storage of a variety of liquids and liquid-material such as oil, liquefied natural gas, chemical fluids, and wastes of different forms, any collapse during earthquake can be a disaster to the environment. This will lead to the even worse condition in which the loss may be more than the earthquake itself.

The failure modes of fluid storage tanks in past earthquakes can be summarized into the following categories.

For steel storage tanks, it may be:

(1) Elephant-foot buckling of bottom shell due to overload stresses. Figure 2.1 shows the elephant foot deformation of one steel tank after San Fernando, California, Earthquake of February 9, 1971.

(2) Diamond-shaped buckling of tanks with very thin shells. Figure 2.2 shows such deformation in a winery after Livermore, California earthquake, Jan. 24, 1980. All these filled stainless steel tanks buckled.

(3) Damage to the roof caused by sloshing of the fluid or failure of frangible joints between wall and roof. Such collapse of roof occurred frequently in San Fernando, California Earthquake 1971. For example Granada High Tank, which is a 55-foot diameter by 45-foot high riveted steel tank, was damaged by the collapse of the roof trusses which were constructed of light-gauge steel angle.

(4) Fracture of wall-base connection in tanks partially restrained or tanks unrestrained against up-lift. Figure 2.3 shows a fracture failure at the bottom of large tank in Kobe, Japan earthquake, Jan. 17, 1995.

(5) The rocking of the tank resulting from the sloshing of the fluid inside may pull out or cause tension failure of the anchor bolts. Figure 2.4 shows an anchor bolt pulled out about 13 inches in Joseph Jensen Filtration Plant wash-water tank in San Fernando, California, Earthquake of February 9, 1971.

(6) Failure of a tanks support system for elevated tanks. Figure 2.5 shows the collapse of an elevated steel storage bin anchorage in Alaska earthquake, Mar. 27, 1964.

Concrete liquid storage tanks have also suffered severe damages to the roofs, columns and wall systems due to excessive initial forces in past earthquakes. In San Fernando, California, Earthquake of February 9, 1971, a finished underground water reservoir of Joseph Jensen Filtration Plant was subjected to a maximum horizontal inertial force estimated about 0.4g which would be about 450 to 500 psi applied to the roof due to the filled cover. Figures 2.6 and 2.7 show the damage to the wall and column of this reservoir respectively.

The concrete support system is commonly used in elevated fluid storage tanks. The failure of such a system, for example the failure of beam and column plastic hinges in the circular frames, can also frequently be found after strong earthquakes. In the Chilean

earthquake of May 1960, a 700,000-liter capacity elevated reinforced concrete water tank suffered strut damage throughout. The actual water content at the time of the earthquake was 600,000 liters. Figure 2.8 shows the damaged tank after the earthquake. This phenomenon has also been observed in a recent earthquake of Izmit (Kocaeli), Turkey earthquake, Aug. 17, 1999 as shown in Figure 2.9.

Besides, there are many other types of damages to both steel and concrete liquid storage tanks such as foundation failure due to liquefaction of soil beneath the tank and failure of connection between the tank and piping or other accessory systems.

Based on observation from previous earthquakes, it is concluded that liquid storage tanks can be subjected to large hydrodynamic pressures during earthquakes. Consequently, high stresses can cause buckling failure in the steel tanks. In concrete tanks, due to large inertial mass of concrete, the stresses could be large and result in cracking, leakage or even collapsing of the structure. These damages and failures of liquid storage tanks in past earthquakes attract many practicing engineers and researchers to study this problem in order to improve the behaviors of those structures.

2.3 Previous Research

Intensive research work on the dynamic response of liquid storage tanks commenced in the late 1940's, but originally it was in the study of dynamic response of the fuel tank in aerospace engineering. Later Housner (1957, 1963), Hounser and Haroun (1979, 1980), Haroun and Housner (1981), Haroun (1983, 1984), Haroun and Tayel (1985), Haroun and Abou-Izzeddine (1992A, 1992B), Veletsos and Yang (1976) and Veletsos and Tang (1986, 1987, 1990), Veletsos et al. (1992A, 1992B), Nash et al. (1987), Park et al. (1990), Kim et al. (1996) and many others carried out research work in this area. However, these studies were mostly related to cylindrical steel tanks which were more commonly used in the civil engineering especially in the oil and water supply industry. Little attention was drawn to the seismic response of concrete tanks, especially to rectangular tanks.
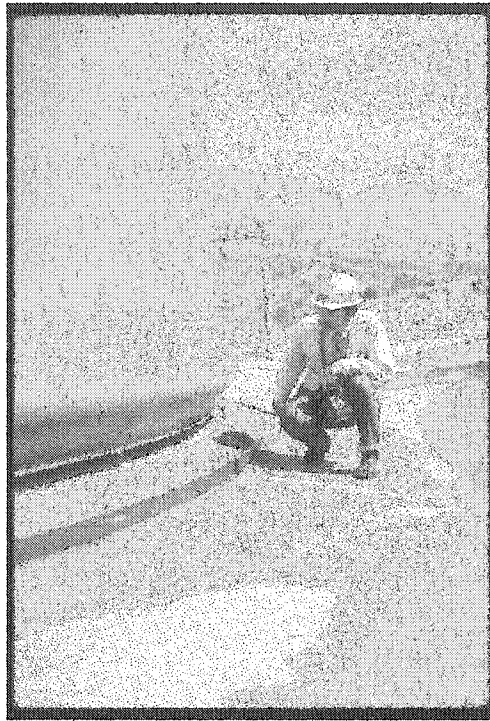
Figure 2.1 Elephant Foot Deformation of Water Tank on the Hill behind Olive

View Hospital (San Fernando, California, Earthquake of February 9, 1971)
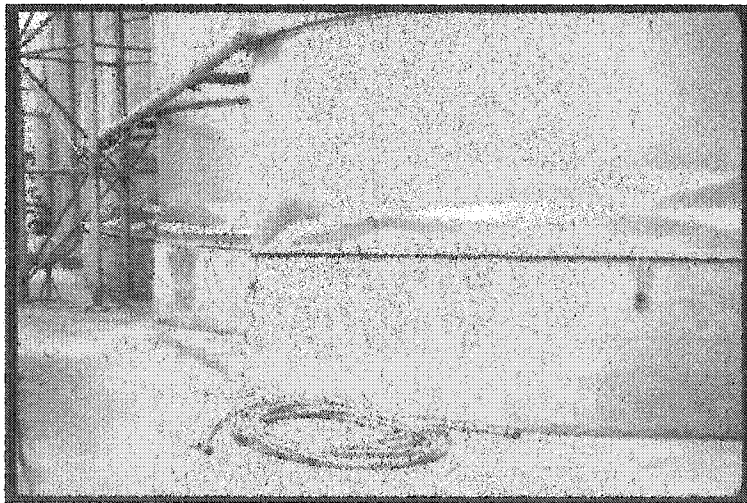
Figure 2.2 All Filled Stainless Steel Tanks Buckled. (Livermore, California

Earthquake, Jan. 24, 1980)

Figure 2.3 Displaced Collar Ring around a Large Tank in the Karumojima Tank Farm (Kobe, Japan Earthquake, Jan. 17, 1995).
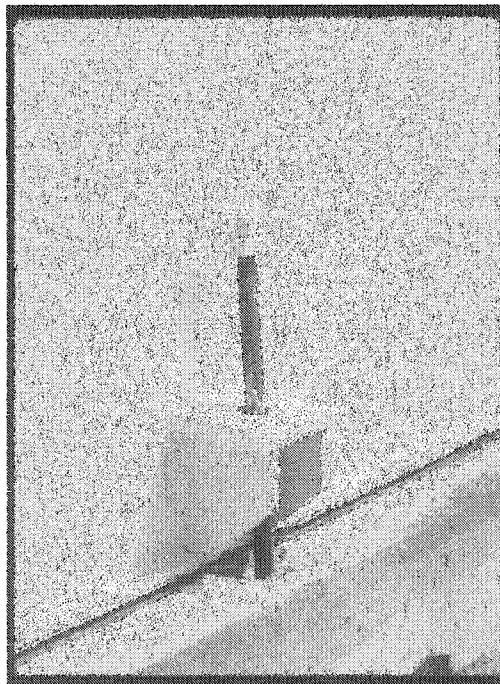
Figure 2.4 A 13-inch Anchor Bolt Stretch in Jensen Filtration Plant, Metropolitan Water District. (San Fernando, California, Earthquake of February 9, 1971)
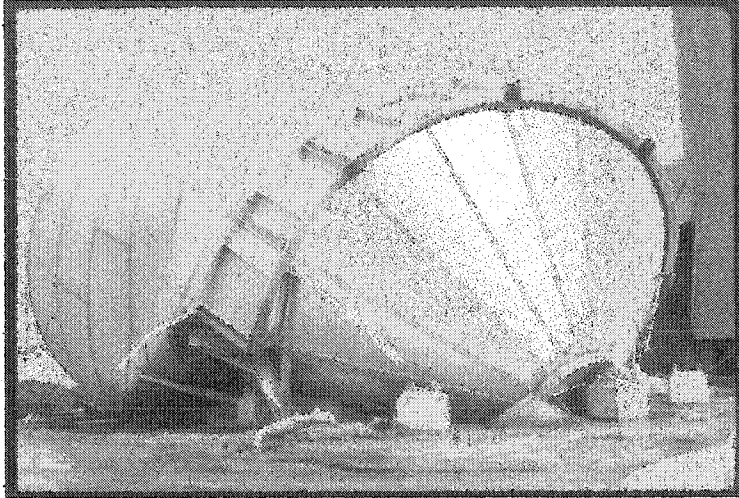
Figure 2.5 Collapse of Elevated Steel Storage Bin Anchorage

(Alaska Earthquake, Mar. 27, 1964)
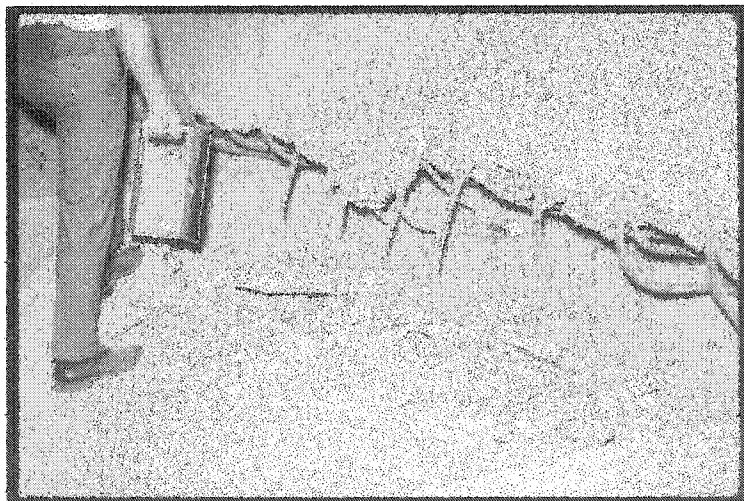
Figure 2.6 Joseph Jensen Filtration Plant -Collapse of Concrete Wall of

Underground Reservoir

(San Fernando, California, Earthquake of February 9, 1971)
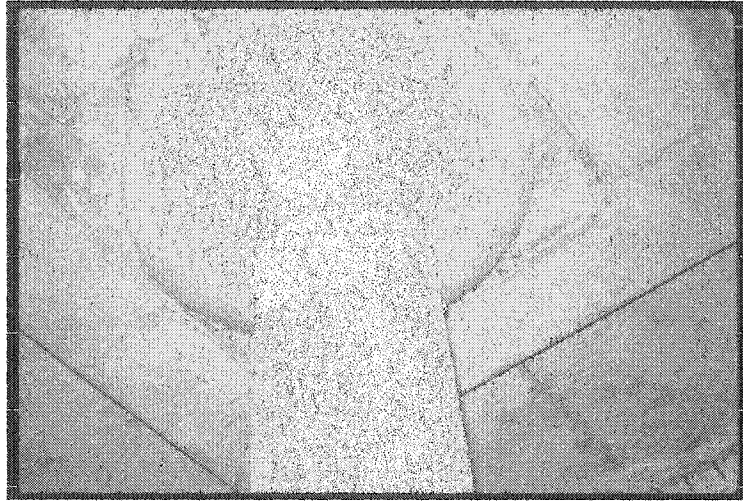
Figure 2.7 Joseph Jensen Filtration Plant - Damage of Column of Concrete

Underground Reservoir

(San Fernando, California, Earthquake of February 9, 1971)
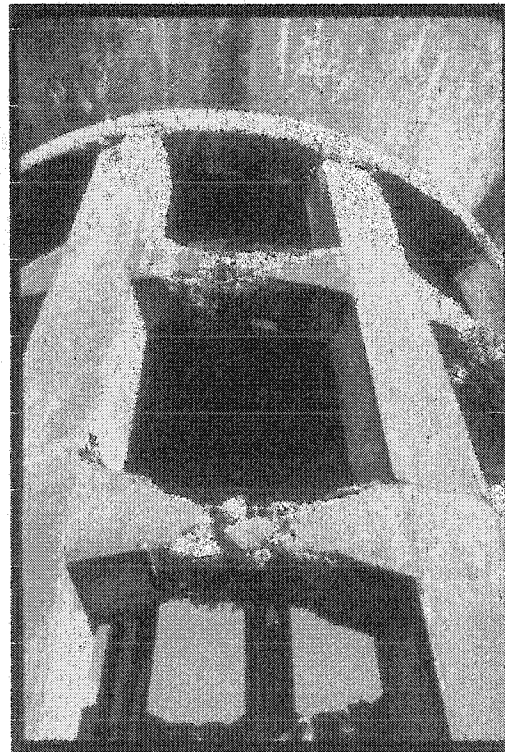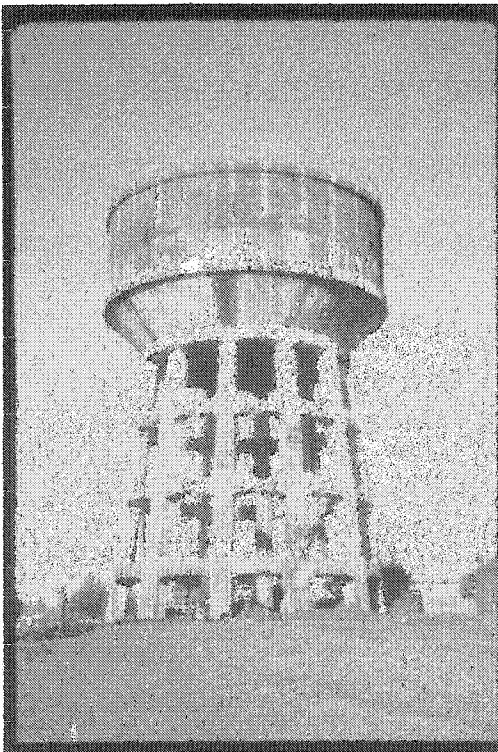
Figure 2.8 Damage of a 700,000-liter Capacity Elevated Reinforced Concrete Water

Tank (Chilean Earthquake of May 1960)
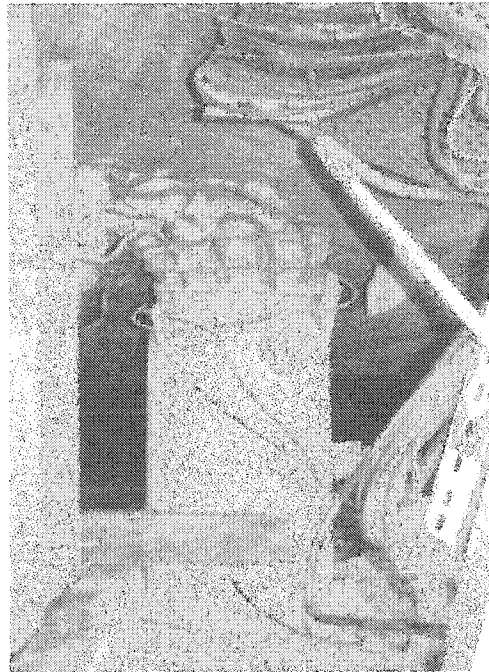
Figure 2.9 Damage of Concrete Supports under Tank, Habas Liquid Gas Plant

(Izmit (Kocaeli), Turkey Earthquake, Aug. 17, 1999)

The main difference between the research on dynamic response of fuel tanks in aerospace engineering and those in civil earthquake engineering is that the later more concerned with response in the lower frequencies as the size of the such tanks are so lager that the dynamic response resulting from the lower frequencies dominates the critical stresses and deformation of the tanks.

Housner (1957) developed the most commonly used model as indicated in Figure 2.10. He assumed the incompressible liquid underwent small displacement. The hydrodynamic pressures induced by earthquake were separated into two parts: impulsive pressure - the portion of the liquid accelerating with the tank, and convective pressure - the portion of the liquid sloshing in the tank. On this basis, he developed simplified expressions to approximate these pressures by added masses. The added mass in terms of impulsive pressure is rigidly connected with the tank wall and the added mass in terms of

convective pressure is connected to the tank wall using springs. The boundary condition in calculation of hydrodynamic pressures was treated as rigid in his model. Later, Epstein (1976) presented the design curves according to the Housner's model for estimating the bending and overturning moment induced by the hydrodynamic pressures for both cylindrical and rectangular tanks.

(a) Fluid Motion in Tank   (b) Dynamic Model for Rigid Wall Tank
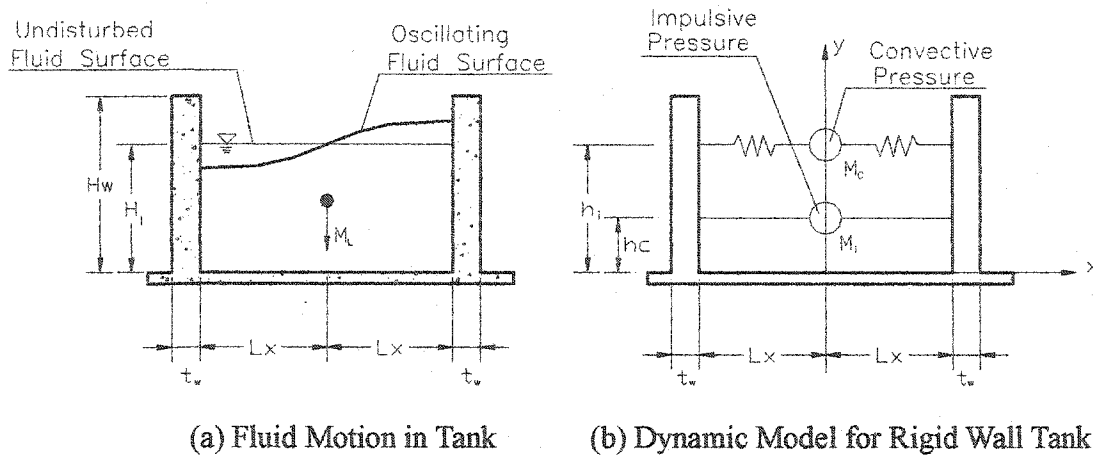
Figure 2.10 Hounser's Model

Yang and Veletsos (1976) considered the effect of wall flexibility on the magnitude and distribution of the hydrodynamic pressures and associated tank forces. They assumed that the tank-fluid system behaved like a single degree of freedom system and the base shear and moment were evaluated for several prescribed modes of vibration. They used Flüggle's shell theory to analyze the dynamic response of tank. The displacement component of the arbitrary point on the shell were expressed in terms of natural modes of the vibration of a uniform cantilever beam with shear and bending flexibilities, and the effect of the container liquid was approximated by assuming that a portion of the mass of liquid was attached to the shell. It is found that for tanks with realistic flexibility, the impulsive forces are considerable higher than those in rigid tanks.

Both of the above studies used an analytical method which consists of the high order differential equations in fluid mechanics and structural dynamic problem. But due to the

limitation of solving such differential equations, the results were less accurate. In order to analyze the dynamic response of the contained liquid system more accurately, Balendra and Nash (1975) used the Finite Element Method to discrete the tank wall and considered it to be a thin elastic shell element. The effect of sloshing was neglected. Thus the problem was reduced to an empty cylindrical tank with mass matrix augmented by an "added mass" representing the effect of the contained liquid. The program "EXDOMTANK" based on the reference (Balendra and Nash, 1975) gave the time history of displacement and stress in the shell due to impulsive forces. Later Yu and Nash (1986) used Finite Element-Perturbation Method which was based on the perturbation technique to study the non-linear sloshing of liquid and the stability. The response of solid tank is solved by nonlinear finite element method. The technique, which was called sequential method, was used to simulate the interaction between fluid and wall. But no time history response concerned by Civil Engineering was demonstrated in their study. The commercial finite element software ANSYS was used in their research.

Haroun has done many theoretical and experimental investigations on the dynamic behavior of the fluid storage tanks. He used liquid-shell system in which the shell wall was discretized by using cylindrical finite element and the fluid region was treated as a continuum by the boundary solution techniques (Haroun, 1981). Also, he presented a very detailed analytical method in the typical systems of loadings in the rectangular tanks (Haroun, 1984). The hydrodynamic pressures were calculated by classical potential flow approach. The formulas of hydrodynamic pressures only considered the rigid wall boundary condition. In addition, Haroun (1983) carried out the experiments at University of California, Berkeley. A series of ambient and forced vibration tests of three, full scale water storage tanks were conducted to determine the natural frequencies and the mode shapes of vibration. Two tanks were selected in which permanent instruments were installed to record the possible future earthquakes. This research work significantly improved the understanding of dynamic response of fluid storage tanks and provided

practicing engineers with simple and sufficiently accurate tools to estimate such response.

Park et al. (1990) performed research studies on dynamic response of the rectangular tanks. They used the boundary element method to calculate the hydrodynamic pressures and finite element method to analyze the solid wall. The governing equation for the coupled system was given. The time history analysis was used to obtain the dynamic response of fluid storage tanks. Both impulsive and convective effects were considered. Later, Kim et al. (1996) used an analytical method to solve this problem. They presented formulas for the 3-D hydrodynamic pressures calculation and applied the Rayleigh-Ritz method using assumed vibration modes of rectangular plate with suitable boundary conditions as admissible functions for dynamic analysis. The results obtained from the analytical solution agreed well with those from the coupled boundary element – finite element method.

The study of liquid storage tanks still remains to be a hot topic in the earthquake engineering. With the development of numerical method and computer technology, Finite Element Method is more widely used in the dynamic analysis. Variable elements are available in the commercial software to solve the fluid and solid mechanics problem. High-speed computer provides a powerful tool to calculate thousands of nodal stresses and displacements only within several minutes. The time history analysis of random vibration such as oscillation under earthquake is possible in the present software. On the other side, more real scale experiments of fluid storage tanks are carried out to verify the correct of the theory and design method. The results of these studies can increase the safety of new fluid storage tanks and reduce the loss in future earthquakes.

2.4 Other Related Studies

Hydrodynamic loads and other fluid-structure interaction effects will be considered in the design of structures which contain, surround, or submerge in fluid when subject the seismic excitation. Therefore, the results of this research may not only be applied in the

design of fluid storage tanks, but they can also be used in the design of hydro or marine facilities.

Another area that includes liquid structure interaction effect is related to dams. The safety of dams during earthquake is of concern by many structural engineers. The difference in the behavior between a dam and a tank is that the fluid is considered as infinite on one side of boundary for the dam. However, the basic hydrodynamic pressure calculation is similar. The added mass method is also used in the analysis, except that only part of water is considered as inertial forces applied on the dams while the rest of water in the reservoir remains inactive.

Nuclear reactor facilities typically include numerous fluid containers of variety of geometries and sizes. The geometry of the container can be cylindrical, rectangular, or even a complicated one such as horizontal cylindrical, annular cylindrical, toroidal, and spherical or any other geometry. Also, some research groups studied the dynamic response of such tanks (ASCE, 1984).

There are many design standards and codes available for engineering practice purpose, however, most of them are for steel tank design. In 2001 ACI Committee 350 published ACI 350.3 (2001) "Seismic Design Of Liquid-Containing Concrete Structures and Commentary". This standard prescribes procedures for the seismic analysis and design of concrete liquid - containing structures. The hydrodynamic pressures are calculated based on the Housner model in which the boundary condition is considered rigid and hydrodynamic pressures are treated as added masses applied on the tank wall. The dynamic response of tank wall is analyzed by modeling the tank wall as an equivalent cantilever beam. Such model is also used in the earlier New Zealand Code NZS3106 (1986) "Practice for Concrete Structures for the Storage of Liquids". In these codes and standards, the amplitude of hydrodynamic pressures due to the flexibility of wall is not considered.

Portland Cement Association published a document "Design of Liquid-Containing

Concrete Structures for the Earthquake Forces" (Munshi, 2002). It provides requirement and guideline for the design and detailing of the liquid –containing structure for earthquake forces using the IBC 2000, UBC 1997, UBC 1994, BOCA 1996 and SBC 1997 model codes. The analysis method is as the same as ACI 350.3.

Chapter 3 Hydrodynamic Pressures in Rectangular Tanks

3.1 Introduction

The calculation of hydrodynamic pressures is the key issue in the analysis of fluid-structure system. This problem is studied in this chapter. In section 3.2 the previous methods of analysis used in the calculation of hydrodynamic pressures are discussed. In this study, the surface wave or flow potential method is used. Section 3.3 introduces the basic concepts of surface wave in order to understand the advantages and disadvantages of different methods used in the calculation of hydrodynamic pressures. The basic formulation of fluid motion in a rectangular tank due to the horizontal acceleration is established in Section 3.4. The two dimensional formulas of impulsive and convective pressure are deducted by considering the effect of wall flexibility. In Section 3.5 the formulas in terms of the vertical acceleration are deducted. Overall, this chapter provides the analytical solutions of hydrodynamic pressures in rectangular tanks.

3.2 Previous Analysis

The effect of hydrodynamic pressures on the structures has been studied for long time. Westergaard (1933) gave the first solution of pressures on a rectangular, vertical dam subjected to horizontal acceleration. In his analysis, Westergaard showed that the hydrodynamic pressures exerted on the face of the dam due to the earthquake ground motion was equivalent to the inertial force of the body of the water attached to the dam and moving back and forth with dam while the rest of the reservoir remained inactive. He suggested a parabolic shape for this body of the water with a base width equal to 7/8 of the height, as shown in Figure 3.1. Jacobsen (1949) solved the corresponding problem for a cylindrical tank containing fluid and for the cylindrical pier surrounded by fluid.

Later, Housner (1957) gave the more detailed solutions on the impulsive and convective hydrodynamic pressure in both rectangular tanks and cylindrical tanks. He

assumed the incompressible liquid underwent small displacement. Yang and Veletsos (1976) considered amplitude of hydrodynamic pressures due to the flexibility of the wall. Horoun (1981) used boundary solution to analyze the hydrodynamic pressures in rectangular tanks. But only rigid wall boundary condition was considered. Park et al. (1990) used the boundary element method to model the boundary condition of the liquid in the rectangular tanks and later Kim et al. (1996) gave the analytical formulas for the hydrodynamic pressures in rectangular tanks including the flexible wall.
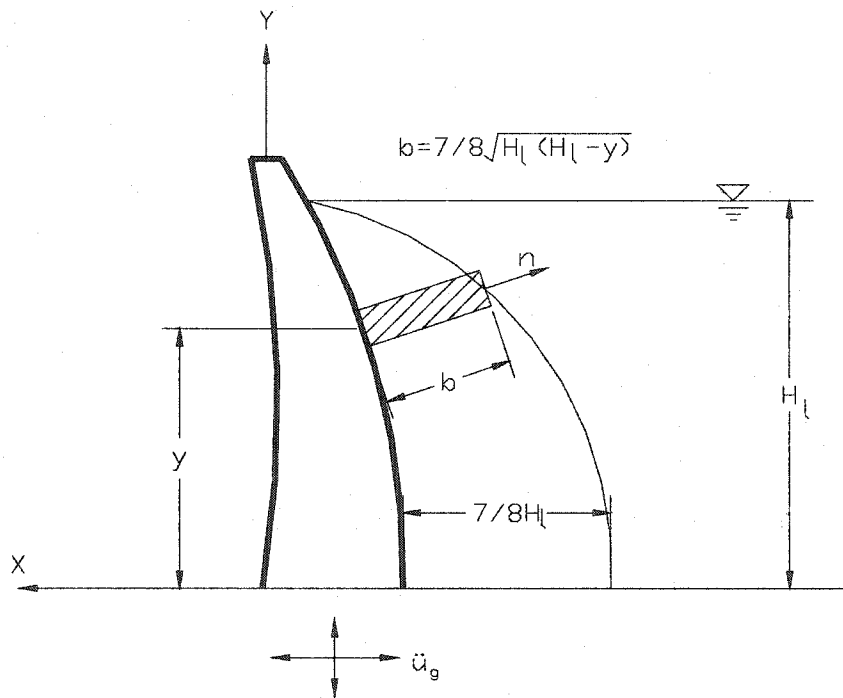
Figure 3.1 Generalized Westergaard Added Hydrodynamic Mass Model for Dams

From the fluid mechanics point of view, the fluid motion in a vessel can be treated as surface waves. The principle of such free-surface phenomena can be assumed as potential in nature. Although the hydrodynamic pressures can be solved by finite element method, in this study an analytical method is used. The reason is discussed in the next section.

3.3 Fluid Motion in Rectangular Tanks

The response of body of fluid to an earthquake is a very complex phenomenon. When earthquake occurs, fluid is excited and gravity waves are generated on its free surface. The motion induced by the surface waves may be considered to be irrotational in most instances. Then the velocity vector may be expressed as the gradient of velocity potential $\phi(x, y, z, t)$ which must satisfy Laplace's equation:

$$\nabla^2 \phi = 0 \tag{3.1}$$

After the boundary condition is established, the hydrodynamic pressures can be obtained from solving the velocity potential equation.

Figure 3.2 shows the waves on the free surface of the liquid in a rectangular tank subjected to vibration. The x-axis of a coordinate system is located at the mean level of the free surface, which is defined by the equation $y=\eta(x,z,t)$ and the mean depth of the liquid is H_l.
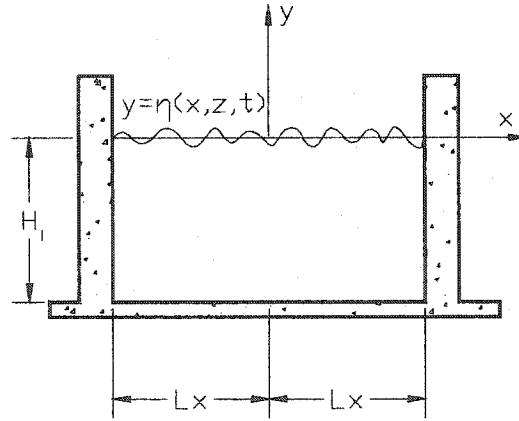
Figure 3.2 Coordinate System for Surface -Wave Problems

Two boundary conditions must be imposed on the free surface, kinematic surface condition and dynamic condition. The kinematic surface condition is to specify that a particle of fluid which is at some time on the free surface, will always remain on the free surface. Because the equation of the free surface is $y-\eta=0$, in the eulerian coordinates

system it can be expressed as that:

$$\frac{\partial}{\partial t}(y - \eta) + \mathbf{u} \, \nabla(y - \eta) = 0 \tag{3.2}$$

where in the eulerian frame $\mathbf{u} \, \nabla(y - \eta)$ is denoted as:

$$\mathbf{u} \, \nabla \alpha = u \frac{\partial \alpha}{\partial x} + v \frac{\partial \alpha}{\partial y} + w \frac{\partial \alpha}{\partial z} \tag{3.3}$$

α can be any field variables such as function of the independent variables *x, y, z* and u is a vector.

In the eulerian coordinates system and with respect to the velocity potential ϕ, the kinematic surface condition becomes:

$$\frac{\partial \eta}{\partial t} + \frac{\partial \phi}{\partial x} \cdot \frac{\partial \eta}{\partial x} + \frac{\partial \phi}{\partial z} \cdot \frac{\partial \eta}{\partial z} = \frac{\partial \phi}{\partial y} \tag{3.4}$$

For the dynamic condition, it is to specify that the pressure is constant at the surface. It is implemented from the Bernouli equation which is for unsteady, irrotational motion. Since gravitational forces are intrinsically important in free-surface waves, gravity g must be included in the body force term. So the boundary condition *p=P(x,z,t)* on *y=η* is:

$$\frac{\partial \phi}{\partial t} + \frac{P}{\rho} + \frac{1}{2} \cdot \nabla \phi \cdot \nabla \phi + g \eta = F(t) \tag{3.5}$$

It assumed that the fluid is incompressible and inviscid. The boundary condition at the flat bed is that:

$$\frac{\partial \phi}{\partial y} = 0 \qquad \text{on} \quad y = -\text{H}_l \tag{3.6}$$

and boundary condition at the surface of the wall is that:

$$\frac{\partial \phi}{\partial x} = \dot{u}(t) \qquad \text{on} \qquad x = \pm \, \text{L}_x \tag{3.7}$$

It may be seen that the most difficulties to get hydrodynamic pressure is to solve the boundary conditions rather than differential equation. By linearizing the problem we can get some analytical solution (discussed later), while the basic features of the flow are not

20

destroyed.

In recent studies, the finite element method has become more popular to simulate the fluid motion. In some cases, the finite element is used to analyze the fluid in which no special fluid elements are used. The shear modulus may be specified to be zero in the standard solid element or using the stress-strain relation of solid material to calculate the hydrodynamic pressure. As no special treatment of the fluid domain is needed, the element matrices may be assembled and the system can be solved just as for a solid analysis. The disadvantage of such solution is that the special treatment is needed on the fluid structure boundary. Here continuity of the normal displacement is required, while the fluid must be allowed to slip relative to the structure in the tangential direction. If no special boundary condition is specified, as stress-strain relation of solid material does not agree well with that in the fluid condition, the results will be great less than the analytical method such as results shown in Figure 3.3 (Dogangun et al., 1996).
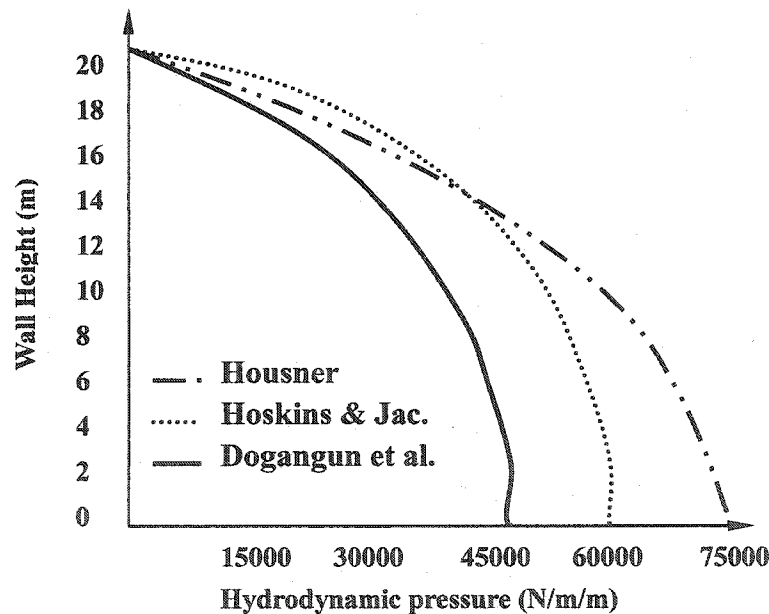
Figure 3.3 Hydrodynamic Pressure Distribution For Rigid Tank

(Dogangun et al., 1996)

The fluid can also be modeled as a steady-state flow in the vessel using pure

pressure formulations for the fluid. The fluid can be considered an incompressible, invisid liquid with mass density ρ_l. The equations governing the fluid domain are:

(1) Conservative of mass:

$$\frac{\partial u_i}{\partial x_i} = 0 \tag{3.8}$$

(2) Conservative of Momentum:

$$\rho_l \left(\frac{\partial u_i}{\partial t} + u_j \frac{\partial u_i}{\partial x_j} \right) - \frac{\partial}{\partial x_j} \left[-P\delta_{ij} + \mu \left(\frac{\partial u_i}{\partial x_j} + \frac{\partial u_j}{\partial x_i} \right) \right] + \rho \cdot f_i = 0 \tag{3.9}$$

(3) Constitutive Equations:

$$\sigma_{ij} = \tau_{ij} - P\delta_{ij}$$
$$\tau_{ij} = \mu D_{ij} \tag{3.10}$$
$$D_{ij} = \frac{1}{2} \left(\frac{\partial u_i}{\partial x_j} + \frac{\partial u_j}{\partial x_i} \right)$$

In the above equation u_i, u_j denotes the velocity vector, σ_{ij} is the total stress tensor, τ_{ij} is the viscous stress tensor, P is the pressure, f is the body force vector (per unit mass), ρ is the density, and μ is the shear viscosity of the fluid. The boundary condition is the same as that in the surface wave. It can be solved using the finite element method (Reddy, 1993, 2001), but the use of non-symmetric matrix is not favor in the analysis. Although the finite element software such as ANSYS can solve some parts of this problem, the difficulties still exist in the specifying the boundary conditions. More complex computational fluid dynamics (CFD) techniques may be needed to truly simulate the motion of the fluid subjected to earthquakes.

Due to the difficulties in modeling the exact fluid motion in the body of liquid, it is preferred to calculate hydrodynamic pressures based on the boundary conditions. This method is called boundary solution which is of two types. It can be either the analytical method (Haroun, 1984) or Boundary Element Method (Park et al., 1990). In this study, the analytical method is used.

3.4 Hydrodynamic Pressures – Horizontal Acceleration Condition

Before solving the problem of two-dimensional hydrodynamic pressures in rectangular tanks, one assumption must be paid attention to. It is assumed that the waves in rectangular tanks are of small amplitude waves in order to make the surface boundary condition more tractable. It means that η is small compared with the wavelength λ and the liquid depth H_l. Thus the high order term with respect to the Taylor expansion can be neglected in the general equations presented in previous section. Then the linearized boundary conditions can be more easily handled in the analysis.

3.4.1 Governing Equation

Figure 3.4 shows the tank geometry of width $L = 2L_x$ and depth of fluid H_l for liquid in a two-dimensional rectangular tank. The mass density of fluid is ρ_l.
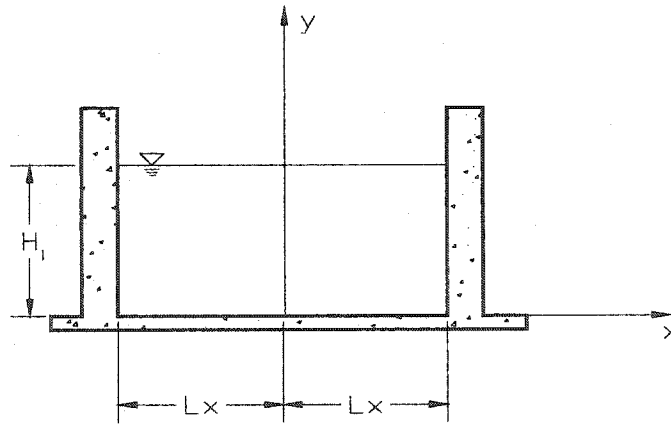
Figure 3.4 Geometry for Liquid in a Rectangular Tank

The satisfied partial different equation is that:

$$\frac{\partial^2 \phi}{\partial x^2} + \frac{\partial^2 \phi}{\partial y^2} = 0 \tag{3.11}$$

in which ϕ is the velocity potential function. The velocity components v_x, v_y in the directions of x , y are that:

$$v_x = \frac{\partial \phi}{\partial x} \tag{3.12.1}$$

$$v_y = \frac{\partial \phi}{\partial y} \tag{3.12.2}$$

The hydrodynamic pressure is expressed by:

$$p(x,y,t) = -\rho_l \frac{\partial \phi(x,y,t)}{\partial t} \tag{3.13}$$

The boundary conditions are:

$$\frac{\partial^2 \phi}{\partial t^2}(x,H_l,t) + g\frac{\partial \phi}{\partial y}(x,H_l,t) = 0 \tag{3.14}$$

$$\frac{\partial \phi}{\partial y}(x,0,t) = 0 \tag{3.15}$$

$$\frac{\partial \phi}{\partial x}(\pm L_x,y,t) = \dot{u}(t) \tag{3.16}$$

The velocity potential can be separated into two partial solutions in order to make it easier to solve the problem. ϕ_1 represents the impulsive pressure and ϕ_2 represents the convective pressure. The velocity potential equation and the corresponding boundary conditions are given:

$$\phi_1 + \phi_2 = \phi \tag{3.17}$$

For ϕ_1, the boundary conditions are that:

$$\frac{\partial \phi_1}{\partial t}(x,H_l,t) = 0 \tag{3.18}$$

$$\frac{\partial \phi_1}{\partial y}(x,0,t) = 0 \tag{3.19}$$

$$\frac{\partial \phi_1}{\partial x}(\pm L_x,y,t) = \dot{u}(t) \tag{3.20}$$

For ϕ_2, the boundary conditions are that:

$$\frac{\partial^2 \phi_2}{\partial t^2}(x,H_l,t) + g\frac{\partial \phi_2}{\partial y}(x,H_l,t) = -g\frac{\partial \phi_1}{\partial y}(x,H_l,t) \tag{3.21}$$

$$\frac{\partial \phi_2}{\partial y}(x,0,t) = 0 \tag{3.22}$$

$$\frac{\partial \phi_2}{\partial x}(\pm L_x, y, t) = 0 \tag{3.23}$$

The significant difference between ϕ_1 and ϕ_2 in boundary condition is that the surface pressure is equal to zero in impulsive condition ϕ_1, while in convective condition ϕ_2 it is combined with the free surface and the effect due to the impulsive pressure. The other difference is that the velocity of fluid at the surface of sidewall is equal to the velocity of flexible wall in impulsive condition ϕ_1, while in convective condition ϕ_2 it is equal to zero.

3.4.2 Impulsive Solution ϕ_1

The solution for the impulsive pressure in terms of ϕ_1 is that (the detailed derivation of Eq.3.24 is in Appendix A):

$$\phi_1 = -\sum_{n=1}^{\infty} \frac{2 \cdot \sinh(\lambda_{i,n} x)}{\lambda_{i,n} \cdot H_l \cdot \cosh(\lambda_{i,n} L_x)} \cos(\lambda_{i,n} y) \int_0^{H_l} \cos(\lambda_{i,n} y) \cdot \dot{u}(t) dy \tag{3.24}$$

Then the impulsive pressure can be obtained by the application of Eq.3.13, then:

$$p = -\rho_l \frac{\partial \phi_1}{\partial t} = \sum_{n=1}^{\infty} \frac{2 \cdot \rho_l}{\lambda_{i,n} \cdot H_l} \tanh(\lambda_{i,n} L_x) \cos(\lambda_{i,n} y) \int_0^{H_l} \cos(\lambda_{i,n} y) \, \ddot{u}(t) dy \tag{3.25}$$

The vertical component of the velocity at the surface $y=H_l$ is:

$$v_y = \frac{\partial \phi_1}{\partial y} = -\sum_{n=1}^{\infty} \frac{2 \cdot \sinh(\lambda_{i,n} x)}{H_l \cdot \cosh(\lambda_{i,n} L_x)} \int_0^{H_l} \cos(\lambda_{i,n} y) \cdot \dot{u}(t) dy \tag{3.26}$$

For $\int_0^{H_l} \cos(\lambda_{i,n} y) \, \dot{u}(t) dy = const.$ at specific time t.

By integration Eq.3.26 with time, the vertical displacement of particle at the free surface of the fluid is that:

$$d(t) = \int_0^t v_y dt = -\sum_{n=1}^{\infty} \frac{2 \cdot \sinh(\lambda_{i,n} x)}{H_l \cdot \cosh(\lambda_{i,n} L_x)} \int_0^{H_l} \cos(\lambda_{i,n} y) \, u(t) dy \tag{3.27}$$

3.4.3 Convective Solution ϕ_2

The velocity potential function ϕ_2 with respect to the harmonic response is given below (the detailed derivation of Eq.3.28 is in Appendix B):

$$\phi_2 = \dot{u}_0 \cdot \sin(\omega \cdot t) \cdot \sum_{m=1}^{\infty} \sum_{n=1}^{\infty} \frac{1}{(\omega^2 - \omega_{c,m}^2) \cdot \cosh(\lambda_{c,m} H_l) \cdot L_x} \cdot \frac{2 \cdot g}{\lambda_{i,n} \cdot H_l \cdot \cosh(\lambda_{i,n} L_x)} \cdot \frac{2}{\lambda_{i,n}^2 + \lambda_{c,m}^2} \cdot$$

$$[(-1)^m \cdot \lambda_{i,n} \cdot \cosh(\lambda_{i,n} L_x) - \lambda_{c,m} \sinh(\lambda_{i,n} L_x)] \cdot \sin(\lambda_{c,m} x) \cdot \cosh(\lambda_{c,m} y)$$

$$(3.28)$$

The harmonic convective pressure in the rectangular tank is that:

$$p = -\frac{\partial \phi_2}{\partial t} = \ddot{u}_0 \cdot \sin(\omega \cdot t) \cdot \sum_{m=1}^{\infty} \sum_{n=1}^{\infty} \frac{1}{(\omega^2 - \omega_{c,m}^2) \cdot \cosh(\lambda_{c,m} H_l) \cdot L_x} \cdot \frac{2 \cdot g}{\lambda_{i,n} \cdot H_l \cdot \cosh(\lambda_{i,n} L_x)} \cdot$$

$$\frac{2}{\lambda_{i,n}^2 + \lambda_{c,m}^2} \cdot [(-1)^m \cdot \lambda_{i,n} \cdot \cosh(\lambda_{i,n} L_x) - \lambda_{c,m} \sinh(\lambda_{i,n} L_x)] \cdot \sin(\lambda_{c,m} x) \cdot \cosh(\lambda_{c,m} y)$$

$$(3.29)$$

The natural frequencies of sloshing fluid is that:

$$\omega_{c,m}^2 = \lambda_{c,m} \cdot g \cdot \tanh(\lambda_{c,m} H_l) \qquad (3.30)$$

The vertical velocity component for the particles at the surface of the fluid $y=H_l$ is that:

$$v_y = -\frac{\partial \phi_2}{\partial y}$$

$$= \dot{u}_0 \cdot \sin(\omega \cdot t) \cdot \sum_{m=1}^{\infty} \sum_{n=1}^{\infty} \frac{1}{(\omega^2 - \omega_{c,m}^2) \cdot \cosh(\lambda_{c,m} H_l) \cdot L_x} \cdot \frac{2 \cdot g}{\lambda_{i,n} \cdot H_l \cdot \cosh(\lambda_{i,n} L_x)} \cdot$$

$$\frac{2}{(\lambda_{i,n}^2 + \lambda_{c,m}^2) \lambda_{c,m}} \cdot [(-1)^m \cdot \lambda_{i,n} \cdot \cosh(\lambda_{i,n} L_x) - \lambda_{c,m} \sinh(\lambda_{i,n} L_x)] \cdot \sin(\lambda_{c,m} x) \cdot \sinh(\lambda_{c,m} y)$$

$$(3.31)$$

And the corresponding displacement component d is given below:

$$d(t) = \int_0^t v_y dt$$

$$= -\frac{u_0}{\omega} \cdot \cos(\omega \cdot t) \cdot \sum_{m=1}^{\infty} \sum_{n=1}^{\infty} \frac{1}{(\omega^2 - \omega_{c,m}^2) \cdot \cosh(\lambda_{c,m} H_l) \cdot L_x} \cdot \frac{2 \cdot g}{\lambda_{i,n} \cdot H_l \cdot \cosh(\lambda_{i,n} L_x)} \cdot$$

$$\frac{2}{(\lambda_{i,n}^2 + \lambda_{c,m}^2) \lambda_{c,m}} \cdot [(-1)^m \cdot \lambda_{i,n} \cdot \cosh(\lambda_{i,n} L_x) - \lambda_{c,m} \sinh(\lambda_{i,n} L_x)] \cdot \sin(\lambda_{c,m} x) \cdot \sinh(\lambda_{c,m} y)$$

$$(3.32)$$

The velocity potential function ϕ_2 with respect to the random earthquake vibration can be obtained by the Fourier Transform and the Duhamel's integration. For the frequency, the response of pressure $p(\omega)$ can be defined as simple form as shown below:

$$p(\omega) = \sum_{m=1}^{\infty} \frac{f(x,y)}{(\omega^2 - \omega_{c,m}^2)} \qquad (3.33)$$

Then apply the Fourier Transform in Eq.3.33 to get the impulsive pressure:

$$p(\omega) = \frac{1}{2\pi} \sum_{m=1}^{\infty} \int_{-\infty}^{+\infty} \frac{f(x,y)}{(\omega^2 - \omega_{c,m}^2)} d\omega \qquad (3.34)$$

For an arbitrary acceleration input the pressure is obtained by application of Duhamel's integration shown below:

$$p(t) = \frac{1}{2\pi} \sum_{m=1}^{\infty} f(x,y) \int_0^t \omega_n \cdot \ddot{u}(t) \cdot \sin[\omega_n(t-\tau)] \cdot d\tau \qquad (3.35)$$

And the final formula in terms of convective pressure p, vertical velocity component v and the displacement component d are indicated below:

$$p = \sum_{m=1}^{\infty} \sum_{n=1}^{\infty} \frac{1}{\cosh(\lambda_{c,m}H_l) \cdot L_x} \cdot \frac{2 \cdot g}{\lambda_{i,n} \cdot H_l \cdot \cosh(\lambda_{i,n}L_x)} \cdot$$
$$\frac{2}{\lambda_{i,n}^2 + \lambda_{c,m}^2} \cdot [(-1)^m \cdot \lambda_{i,n} \cdot \cosh(\lambda_{i,n}L_x) - \lambda_{c,m} \sinh(\lambda_{i,n}L_x)] \cdot \sin(\lambda_{c,m}x) \cdot \cosh(\lambda_{c,m}y) \cdot A_n(t)$$

$$(3.36)$$

$$v_y = \sum_{m=1}^{\infty} \sum_{n=1}^{\infty} \frac{1}{\cosh(\lambda_{c,m}H_l) \cdot L_x} \cdot \frac{2 \cdot g}{\lambda_{i,n} \cdot H_l \cdot \cosh(\lambda_{i,n}L_x)} \cdot$$
$$\frac{2}{(\lambda_{i,n}^2 + \lambda_{c,m}^2)\lambda_{c,m}} \cdot [(-1)^m \cdot \lambda_{i,n} \cdot \cosh(\lambda_{i,n}L_x) - \lambda_{c,m} \sinh(\lambda_{i,n}L_x)] \cdot \sin(\lambda_{c,m}x) \cdot \sinh(\lambda_{c,m}y) \cdot V_n(t)$$

$$(3.37)$$

$$d(t) = \sum_{m=1}^{\infty} \sum_{n=1}^{\infty} \frac{1}{(\omega^2 - \omega_{c,m}^2) \cdot \cosh(\lambda_{c,m}H_l) \cdot L_x} \cdot \frac{2 \cdot g}{\lambda_{i,n} \cdot H_l \cdot \cosh(\lambda_{i,n}L_x)} \cdot$$
$$\frac{2}{(\lambda_{i,n}^2 + \lambda_{c,m}^2)\lambda_{c,m}} \cdot [(-1)^m \cdot \lambda_{i,n} \cdot \cosh(\lambda_{i,n}L_x) - \lambda_{c,m} \sinh(\lambda_{i,n}L_x)] \cdot \sin(\lambda_{c,m}x) \cdot \sinh(\lambda_{c,m}y) \cdot D_n(t)$$

$$(3.38)$$

3.5 Hydrodynamic Pressures – Vertical Acceleration Condition

The hydrodynamic pressures induced by the vertical acceleration include three pressure components, the long-period contributed by the convective fluid motion (sloshing), the impulsive fluid pressure component which varies in synchronism with the vertical ground acceleration and the short period component contributed by the vibration of the tank wall. Based on an experimental study conducted by Haroun and Tayel (1985), little or no sloshing occurred due to the transient vertical motion. Therefore, the sloshing can be neglected due to the vertical acceleration condition and only the last two components are considered in this study.

In this study, it is assumed that the base of the concrete rectangular tank is rigid. The soil is considered as rigid as well and rigid connect with the base of tank. Therefore, the tank base moves with soil during the earthquake. There is no interaction between the soil and base at the bottom of tank.

When the rectangular tank is subjected to the vertical ground acceleration, the boundary conditions are governed by the following boundary conditions:

(1) At the liquid free surface, the atmospheric pressure is assumed to be zero. Then the boundary condition at the surface of fluid can be expressed as:

$$\frac{\partial \phi}{\partial t}(x, H_l, t) = 0 \tag{3.39}$$

(2) The vertical velocity on the rigid base of the rectangular fluid storage tank is equal to vertical ground velocity, then

$$\frac{\partial \phi}{\partial y}(x, 0, t) = \dot{v}_g(t) \tag{3.40}$$

(3) At the interaction surface between the fluid and the flexible tank wall, the boundary condition must satisfy the compatibility along the height of the wall:

$$\frac{\partial \phi}{\partial x}(\pm L_x, y, t) = \dot{u}(t) \tag{3.41}$$

The hydrodynamic pressure can be obtained by the application of Eq.3.13 and shown below (the detailed derivation is in Appendix C):

$$p = \rho_l (H_l - y) \cdot \ddot{v}_g(t) + \sum_{n=1}^{\infty} \frac{2 \cdot \rho_l}{\lambda_{i,n} \cdot H_l} \coth(\lambda_{i,n} L_x) \cos(\lambda_{i,n} y) \int_0^{H_l} \cos(\lambda_{i,n} y) \cdot \ddot{u}(t) dy$$

$$(3.42)$$

It can be observed that the first part in the right hand side of Eq.3.42 is only related to the vertical acceleration of the ground motion and the second part is corresponding to the transverse vibration of the flexible wall.

Chapter 4 Structural Dynamic Analysis of Tank Walls

4.1 Introduction

The dynamic response of empty tank (tank wall) is considered in this chapter. In this case, the tank is analyzed using the finite element method. The behavior of tank wall is assumed to be linear-elastic. The plane strain element is used to model the tank wall and the Rayleigh-Ritz method is used for the dynamic analysis. For time history analysis, both the mode superposition method and the direct step-by-step integration method are used. The algorithm of unconditional stable Wilson θ method is applied. The difference in specifying damping and analysis results between the mode superposition method and the direct step-by-step method is discussed.

4.2 Finite Element Modeling of Rectangular Tank (Tank Wall)

The concrete tank consists of rectangular walls connected to the base to contain the liquid. The connections between the base and the walls can be either fixed base connection or hinged (pin) as shown in Figures 4.1 and 4.2. Also these tanks may contain roofs which are not shown. In this study it is assumed that the tank wall is fixed to the base and free at the top.

Dynamic response of tank wall subject to earthquake is analyzed using the finite element method. Only the two-dimensional model is considered in this study. The plane strain element is used in the analysis. Figure 4.3 (a) shows a three dimensional rectangular tank. A Cartesian coordinate system (x, y, z) is used with the origin located at the center of the tank base. In addition, it is assumed that the length to width ratio of the tank is so large that the unit length of tank can represent the tank. The corresponding 2-D model is shown in Figure 4.3 (b).

It is assumed that the earthquake ground motion excites the liquid storage tank in the X-direction. The two walls parallel to this direction are considered to be rigid; the walls

in the direction of earthquake are flexible and oscillate in this direction.
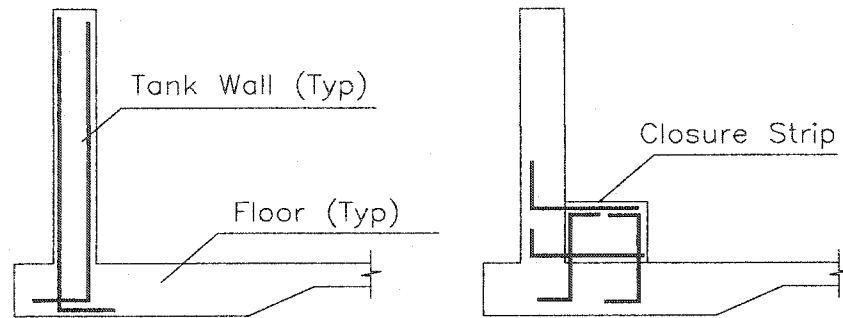
Figure 4.1 Fixed Base Connection
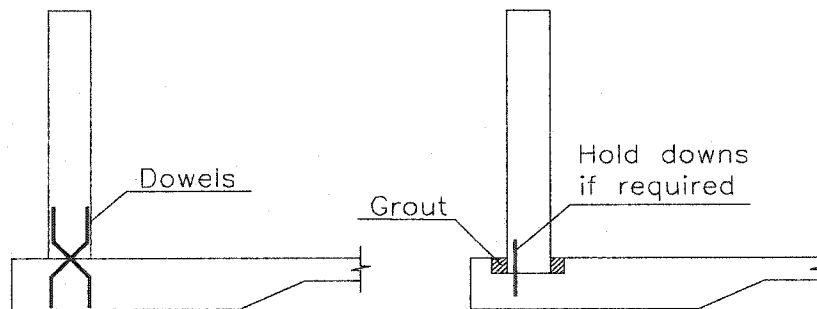
Figure 4.2 Hinged or Pinned Base Connection
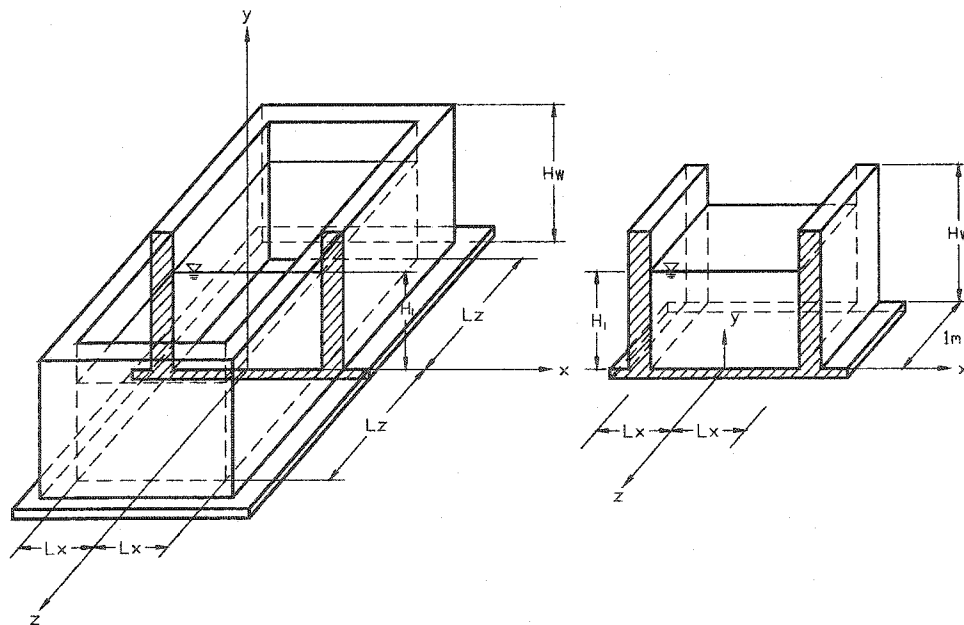
(a) 3-D Model of Rectangular Tank   (b) 2-D Model of Rectangular Tank

Figure 4.3 Model of Rectangular Tank

4.3 Governing Equation of Motion

Equations of motion of the structure system are derived from Hamilton's principle. It can be expressed by:

$$\int_{t_1}^{t_2} (\delta(T-U) + \delta W_{nc}) dt = 0 \tag{4.1}$$

where T is kinetic energy

U is strain energy

W_{nc} is the virtual work done by the non-conservative forces.

The Hamilton principle can be applied to the equation of motion for any system such as discrete, multi-degree of freedom system and continuous system. The advantage of this formulation is that it uses scalar energy quantities. Vector quantities may only be required in calculating the work done by the non-conservative forces.

When the Hamilton's principle is applied to discrete systems, it can be expressed in Lagrange's equations. In the case of multi-degree of freedom system, the deformation of which is described by n independent displacements $u_1, u_2, ..., u_n$, then the kinetic energy is only a function of the velocities $\dot{u}_i$ (i=1,2, ..., n), and strain energy is only a function of the displacement u_i (i = 1,2, ..., n), that is:

$$T = T(\dot{u}_1, \dot{u}_2, ..., \dot{u}_n) \tag{4.2}$$

$$U = U(u_1, u_2, ..., u_n) \tag{4.3}$$

Similarly, the dissipation function is a function of the velocities $\dot{u}_i$ (i=1,2, ..., n) that is

$$D = D(\dot{u}_1, \dot{u}_2, ..., \dot{u}_n) \tag{4.4}$$

Also, the work done by the non-conservative forces can be written in the form

$$\delta W_{nc} = \sum_{i=1}^{n} (F_i - \frac{\partial D}{\partial \dot{u}_i}) \delta u_i \tag{4.5}$$

where the F_i are the generalized forces.

Then the Eq. 4.1 can be expressed as Lagrange's equation:

$$\frac{d}{dt}(\frac{\partial T}{\partial \dot{u}_i}) + \frac{\partial D}{\partial \dot{u}_i} + \frac{\partial U}{\partial u_i} = F_i \qquad i = 1,2,...,n \qquad (4.6)$$

If the previous procedure is written in matrix form, the kinetic energy, dissipation function and strain energy can be the following forms:

$$T = \frac{1}{2}\{\dot{u}\}^T [M]\{\dot{u}\} \qquad (4.7a)$$

$$D = \frac{1}{2}\{\dot{u}\}^T [C]\{\dot{u}\} \qquad (4.7b)$$

$$U = \frac{1}{2}\{u\}^T [K]\{u\} \qquad (4.7c)$$

where $\{u\}$ = matrix of system displacement

$\{\dot{u}\}$ = matrix of system velocities

$\{\ddot{u}\}$ = matrix of system acceleration

$[M]$ = matrix of inertia coefficient

$[C]$ = matrix of damping coefficient

$[K]$ = matrix of stiffness coefficient

Using equation (4.7), the separate terms in Lagrange's equations become

$$\left\{\frac{d}{dt}(\frac{\partial T}{\partial \dot{u}_i})\right\} = [M]\cdot\{\ddot{u}\} \qquad (4.8a)$$

$$\left\{\frac{\partial D}{\partial \dot{u}_i}\right\} = [C]\cdot\{\dot{u}\} \qquad (4.8b)$$

$$\left\{\frac{\partial U}{\partial u_i}\right\} = [K]\cdot\{u\} \qquad (4.8c)$$

Therefore, the governing equation of motion derived from Lagrange's equation in the matrix form can be expressed that:

$$[M]\cdot\{\ddot{u}\} + [C]\cdot\{\dot{u}\} + [K]\cdot\{u\} = \{F\} \qquad (4.9)$$

It can be seen that it is only necessary to obtain the energy expressions in matrix form in order to determine the matrix coefficient in the equation of motion.

4.4 Plane Strain Element

The derivation of energy in Hamilton's principle in this study is based on the linear elastic theory. The plane strain element is used in 2D modal as shown in Figure 4.4:
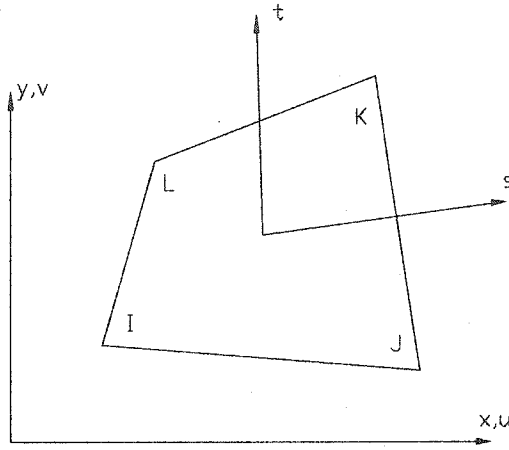
Fig. 4.4 Geometry of Plane Stress Element

(1) The strain energy stored in the element is:

$$U = \frac{1}{2}t\int_A (\sigma_x \varepsilon_x + \sigma_y \varepsilon_y + \tau_{xy}\gamma_{xy})dA \qquad (4.10)$$

Which can be expressed in the following matrix form:

$$U = \frac{1}{2}t\int_A \{\sigma\}^T \{\varepsilon\}dA \qquad (4.11)$$

where $\{\sigma\}^T = \lfloor \sigma_x, \sigma_y, \tau_{xy} \rfloor$

$\{\varepsilon\}^T = \lfloor \varepsilon_x, \varepsilon_y, \gamma_{xy} \rfloor$

t = thickness of element

The stress-strain relationship is that:

$$\{\sigma\} = [D]\{\varepsilon\} \qquad (4.12)$$

34

For isotropic material the elastic properties are the same in all direction. Then the matrix of material constants is:

$$[D] = \frac{E}{(1+v)(1-2v)} \begin{bmatrix} 1-v & v & 0 \\ v & 1-v & 0 \\ 0 & 0 & \dfrac{1-2v}{2} \end{bmatrix} \tag{4.13}$$

E = Young's modulus

v = Poisson's ratio

Substituting equation Eq. 4.12 into the energy expression Eq. 4.11 gives

$$U = \frac{1}{2} t \int_A \{\varepsilon\}^T [D]\{\varepsilon\} dA \tag{4.14}$$

The strains can be expressed in terms of displacement as follows:

$$\{\varepsilon\} = \begin{bmatrix} \dfrac{\partial u}{\partial x} \\ \dfrac{\partial v}{\partial y} \\ \dfrac{\partial u}{\partial y} + \dfrac{\partial v}{\partial x} \end{bmatrix} \tag{4.15}$$

(2) The kinetic energy:

$$T = \frac{1}{2} t \int_A \rho(\dot{u}^2 + \dot{v}^2) dA \tag{4.16}$$

(3) The virtual work:

$$\delta W = \int_s (p_x \delta u + p_y \delta v) ds \tag{4.17}$$

where p_x, p_y are the components of the applied boundary forces per unit length of the boundary and s is the boundary of the element.

The dynamic analysis is carried out using the software SAPIV in this study. It is a computer program for static and dynamic analysis of linear structural system. For quadrilateral plane strain element in SAPIV, the isoparametric formulation is used. The strains in terms of the unknown nodal displacement is:

$$\{\varepsilon\} = [B]\{d\} \tag{4.18}$$

where [B] is the strain-displacement matrix. The related linear shape function in the natural s-t coordinate system is defined below:

$$N_1 = \frac{(1-s)(1-t)}{4}$$

$$N_2 = \frac{(1+s)(1-t)}{4}$$

$$N_3 = \frac{(1+s)(1+t)}{4}$$

$$N_4 = \frac{(1-s)(1+t)}{4} \tag{4.19}$$

Then the element stiffness matrix can be derived by:

$$[k] = \iint_A [B]^T [D][B] t\, dxdy \tag{4.20}$$

and the element mass matrix is:

$$[m] = \iint_A [N]^T [N] \rho \cdot t\, dxdy \tag{4.21}$$

Finally, the global stiffness and mass matrix can be obtained by assembling the element matrix using direct method.

4.5 Rayleigh Ritz Method

The technique for determining approximate solutions to the Hamilton's principal is Rayleigh-Ritz method. It approximates the solution of the virtual displacement such as $u(t)$ with a finite expansion of the form:

$$u^n(t) = \sum_{j=1}^{n} \phi_j q_j^n(t) \tag{4.22}$$

where the $q_j^n(t)$ are unknown functions of time t, and the ϕ_j are prescribed functions of vibration, which must satisfy the geometric boundary condition.

In finite element method the continuous system can be discreted into a system with a finite number of degrees of element. Then the application of Hamilton's principle leads to Lagrange's equations as the following matrix form formula:

$$[M]\{\ddot{u}^n\}+[C]\{\dot{u}^n\}+[K]\{u^n\}=\{F^n\}$$ (4.23)

Where

$$\{u^n\}^T =\lfloor u_1^n \quad u_2^n \quad ... \quad u_n^n \rfloor$$ (4.24)

The mass matrix and stiffness matrix are derived from the corresponding element matrix in Eq.4.20 and Eq.4.21 respectively.

The natural frequencies and modes of free vibration of structure are determined by considering the virtual work done by external force equal to zero. It results in:

$$[M]\{\ddot{u}^n\}+[K]\{u^n\}=0$$ (4.25)

Since the motion is harmonic then,

$$\{u^n(t)\}=\{A^n\}\sin \omega \cdot t$$ (4.26)

where the amplitudes $\{A^n\}$ are independent of time and ω is the frequency of the vibration. Substituting Eq.4.26 into Eq.4.25, it gives:

$$[K-\omega^2 M]\{A^n\}=0$$ (4.27)

The condition that Eq.4.27 has a none-zero solution is that the determined of coefficient should be vanished. It is:

$$|K-\omega^2 M|=0$$ (4.28)

Eq. 4.28 can be expanded to give a polynomial of degree n in ω^2. This polynomial equation will have n roots $\omega_1^2 \quad \omega_2^2 ... \omega_n^2$. These values are called eigenvalues. SAPIV provided the solution of such eigenvalue calculation. In this study only first two natural frequencies are considered.

4.5 Time-History Analysis

Time-history analysis is used to calculate the response of liquid storage tanks subjected to earthquake in this study. Acceleration time history is used as the seismic

input. A complete response history of the structure for the entire duration of the earthquake ground motion is computed. The advantage of such analysis is that it can analyze time dependent characteristics of the dynamic response. It not only provides the maximum stress values, but also acceleration, velocity and displacement at each time step, which are the boundary conditions of fluid domain in liquid-structure interaction problem. Both the mode superposition method and the direct step-by step integration method are used in the study.

Mode superposition method is based on the fact that for certain forms of damping, the response in each natural mode of vibration can be computed separately. The total response is obtained by combining the effects of every mode. Each mode responds with its own particular pattern of deformation or mode shape ϕ_n; with its own natural frequency of vibration ω_n, and with its own modal damping ratio ξ_n. As the lower modes of vibration are essential to the dynamic response of structures, only the response in the first few modes need be considered. In this study the first two modes are analyzed.

In the direct step-by-step integration method, the equations are not transferred into a different form prior to the numerical integration as the mode superposition method does. The equations of motion are satisfied at each discrete time intervals Δt. Therefore, analysis results from the direct step-by-step integration method cannot provide natural frequencies which mode superposition method can calculate. In this study both methods are carried out using linear static and dynamic structural analysis software SAPIV.

The step-by-step integration technique determines the stability, accuracy and efficiency of dynamic analysis. Many techniques are available such as central difference method, Houbolt method, Wilson θ method and Newmark method etc. The numerical integration procedure can be either explicit or implicit. When the solution at time $t + \Delta t$ is based on the equilibrium condition at the previous time step t, the integration method is called an explicit integration method. If the solution at time $t + \Delta t$ is obtained from equilibrium at time $t + \Delta t$, it is called implicit. The main advantage of the implicit

method is that it is unconditionally stable. The time interval Δt has no special mathematical limitation in it. The Δt can be much larger than that in the explicit method, but it still must be small enough in order to assure the accuracy of calculation. In this study the time interval Δt used for dynamic analysis is the range of 0.01 sec and 0.02 sec.

In SAPIV unconditionally stable Wilson θ method is used. The algorithm is summarized below (Bathe et al., 1974)

1. Initial Calculation:

(a) Calculate the following constants (assume $C=\alpha M+\beta K$):

$$\theta = 1.4 \qquad\qquad \tau = \theta \cdot \Delta t \qquad\qquad b_1 = \beta \cdot a_4$$

$$a_0 = (6+3\alpha \cdot \tau)/(\tau^2 +3\beta \cdot \tau) \qquad\qquad a_5 = 3b_1/\tau - 6/(\tau^2 \cdot \theta)$$

$$b_0 = \alpha \cdot - \beta \cdot a_0 \qquad\qquad a_6 = 2b_1 - 6/(\tau \cdot \theta)$$

$$a_1 = 6/\tau^2 + 3b_0/\tau \qquad\qquad a_7 = b_1 \cdot \tau/2 + 1 - 3/\theta$$

$$a_2 = 6/\tau + 2b_0 \qquad\qquad a_8 = \Delta t/2$$

$$a_3 = 2 + \tau \cdot b_0/2 \qquad\qquad a_9 = \Delta t^2/3$$

$$a_4 = 6/[\theta \cdot (3\beta \cdot \tau + \tau^2)] \qquad\qquad a_{10} = a_9/2 \qquad\qquad (4.29)$$

(b) Form effective stiffness matrix

$$K^* = K + a_0 \cdot M \qquad\qquad (4.30)$$

(c) Triangularize K^*

2. For each time increment:

(a) Form effective load vector R_t^*:

$$R_t^* = R_t + \theta(R_{t+\Delta t} - R_t) + M(a_1 \cdot u_t + a_2 \cdot \dot{u}_t + a_3 \cdot \ddot{u}_t) \qquad\qquad (4.31)$$

(b) Solve for effective displacement vector u_t^*:

$$K^* \cdot u_t^* = R_t^* \qquad (4.32)$$

(c) Calculate new acceleration, velocity and displacement vectors,

$$\ddot{u}_{t+\Delta t} = a_4 \cdot u_t^* + a_5 \cdot u_t + a_6 \cdot \dot{u}_t + a_7 \cdot \ddot{u}_t \qquad (4.33)$$

$$\dot{u}_{t+\Delta t} = \dot{u}_t + a_8 \left(\ddot{u}_{t+\Delta t} + \ddot{u}_t \right) \qquad (4.34)$$

$$u_{t+\Delta t} = u_t + \Delta t \cdot \dot{u}_t + a_9 \cdot \ddot{u}_t + a_{10} \cdot \ddot{u}_{t+\Delta t} \qquad (4.35)$$

(d) Calculate element stresses if desired

In SAPIV damping is specified in different ways depending on the method of analysis. In the mode superposition method damping is specified by the damping ratio. It is assumed 5% for the concrete wall. In direct step-by-step integration method, Rayleigh damping is used. It can be calculated by the equation shown below:

$$[C] = \alpha [M] + \beta [K] \qquad (4.36)$$

The parameters α, β are obtained by the formulas:

$$\alpha = \frac{4\pi \left(T_j \cdot \lambda_j - T_i \cdot \lambda_i \right)}{T_j^2 - T_i^2} \qquad (4.37)$$

$$\beta = \frac{T_i \cdot T_j \cdot \left(T_j \cdot \lambda_j - T_i \cdot \lambda_i \right)}{T_j^2 - T_i^2} \qquad (4.38)$$

where λ_n is proportion of critical damping in the nth mode, and T_n is period of vibration in the nth mode. The first two modes of vibration are considered in this study.

Chapter 5 Dynamic Analysis of Liquid Storage Tank System

5.1 Introduction

A finite element model is proposed in this chapter, which can consider the effect of flexibility of wall on hydrodynamic pressures. Based on the proposed model, a sequential method is used for dynamic analysis. The proposed model has proved to be equivalent to the Housner's model when the tank wall is assumed to be rigid. Both horizontal and vertical ground motion are considered in the study. Finally, the load combination of the liquid storage tanks subjected to the earthquakes is discussed.
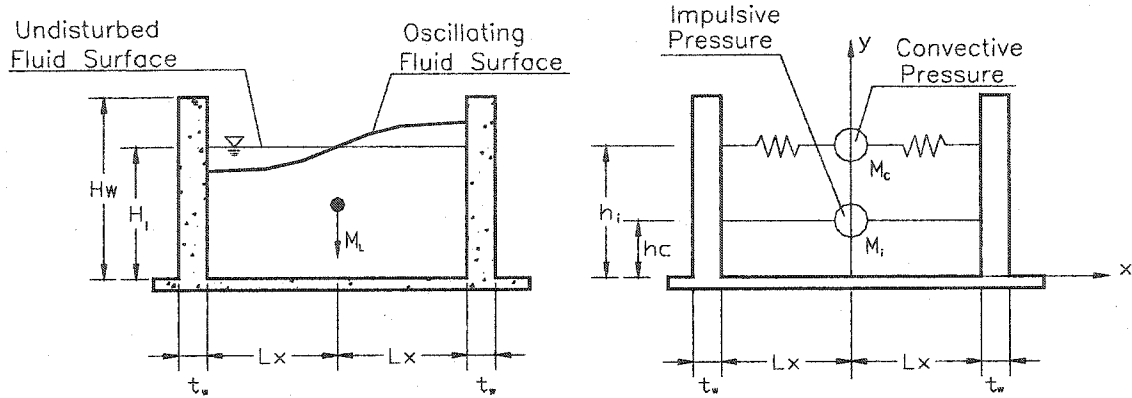
5.2 Finite Element Model for Rectangular Liquid Storage Tank System

As discussed in Chapter 2, many different models are available to analyze the dynamic response of liquid storage tanks subjected to earthquakes. Housner's model is a typical model used widely in the design standards and codes such as ACI 350.3 (2001) and New Zealand Code NZS3106 (1986). Although the Housner's model was discussed in Chapter 2, in order to compare it with the proposed model presented in this study, it is demonstrated in Figure 5.1 again.

Previously, the most popular coupled analysis technique used for analyzing the fluid-structure interaction was the added mass method which means that the hydrodynamic pressures are treated as additional masses attached on the surface of wall. In the Housner's model, the added mass in terms of impulsive pressure is rigidly connected to the tank wall and the added mass in terms of convective pressure is flexibly connected to the wall by means of springs.

In this study, the fluid structure interaction problem is considered as Coupled-Field Analysis, which means an analysis that takes into account the interaction (coupling) between two or more discipline (fields) of engineering, including the fluid structure analysis, thermal-stress analysis, magnetic-thermal analysis, magnetic-structural analysis

and micro-electro mechanical systems etc.

Figure 5.1 Hounser's Model

Figure 5.2 shows a 2-D finite element model proposed in this study. The concrete rectangular tank has width $2L_x$ (in the direction of earthquake), height H_w and wall thickness t_w. It is filled with fluid with the height H_l. The tank wall is discreted into a numbers of finite elements. The plane strain rectangular element is used in the analysis.
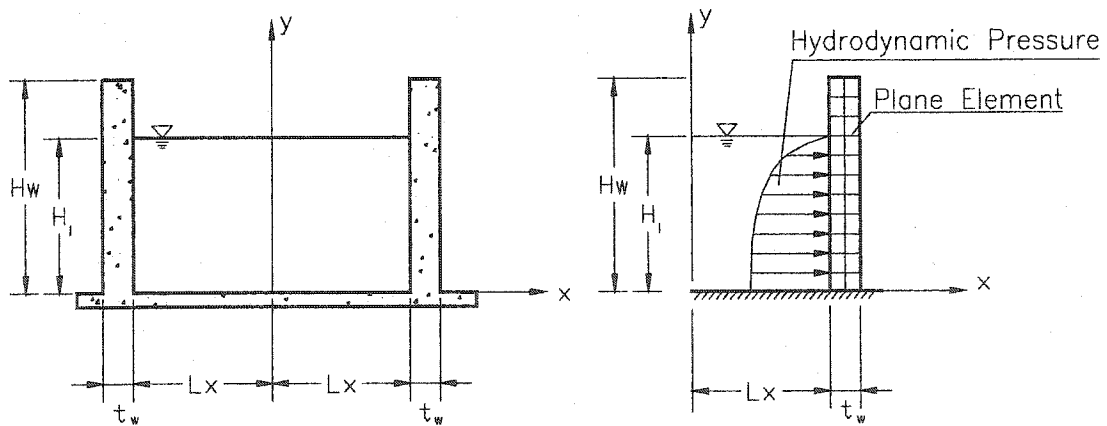
Figure 5.2 Finite Element Model of Rectangular Tank

The difference between the Housner's model and the proposed model is that the hydrodynamic pressures are considered as external forces in the proposed model, while

they are treated as added masses in the Housner's model. In addition, in the proposed model the effect of flexibility of tank wall is considered in the analysis. The advantages of the proposed model will be explained in the following section.

5.3 Dynamic Analysis

5.3.1 Governing Equation of Motion

Earthquake motion is three dimensional in nature. For the horizontal ground motion, the equation of motion of the flexible tank wall in terms of the transverse displacement u relative to the ground can be expressed as the following equation, assuming that the ground excitation is directed along the x-axis as indicated in Figure 5.2:

$$[M]\{\ddot{u}_r\} + [C]\{\dot{u}_r\} + [K]\{u_r\} = -[M]\{\ddot{u}_g\} + \{P\} \tag{5.1}$$

$\{u_r\}, \{\dot{u}_r\}, \{\ddot{u}_r\}$: Displacement, velocity and acceleration of rectangular wall relative to the ground.

$\{\ddot{u}_g\}$: Horizontal ground acceleration in x direction.

$\{P\}$: Hydrodynamic pressure on the wall surface.

$[K]$: Stiffness matrix of rectangular tank wall.

$[M]$: Mass matrix of rectangular tank wall.

$[C]$: Damping matrix of rectangular tank wall

For the vertical ground acceleration, the situation is more complex. As the vertical ground acceleration can be transmitted into horizontal hydrodynamic pressures in the liquid storage tanks, so the rectangular liquid storage tank wall undergoes horizontal displacement in addition to axial displacement. As the transverse vibration of the flexible tank wall is significant, in this study only the horizontal motion due to the vertical acceleration is investigated. The equation of motion in the x direction (horizontal) can be expressed as that:

$$[M]\{\ddot{u}_r\}+[C]\{\dot{u}_r\}+[K]\{u_r\}=\{P\} \tag{5.2}$$

The denotation in this equation is the same as that in Eq.5.1

5.3.2 Coupled Analysis of Horizontal Ground Motion Condition

Using Equation 5.1 and 5.2, the dynamic analysis of the fluid storage tank system can be divided into two engineering problems, fluid mechanic and structural dynamic analysis. In Chapter 3 and 4, these two problems were studied respectively.

Basically the dynamic response of fluid storage tanks must be solved by a "strong" coupled method that data must be transferred or shared between at each step of the solution to maintain accuracy of overall simulation. In the past, coupled analysis is achieved using the added mass method. For the general condition, the impulsive hydrodynamic pressures in terms of the added mass can be calculated by:

$$\{P\}=-[M_i]\{\ddot{u}\}=-[M_i]\{\ddot{u}_g+\ddot{u}_r\} \tag{5.3}$$

where $[M_i]$ is the added mass representing the impulsive pressure.

As a result, the equation of motion in terms of added mass method can be expressed as:

$$[M_w+M_i]\{\ddot{u}_r\}+[C]\{\dot{u}_r\}+[K]\{u_r\}=-[M_w+M_i]\{\ddot{u}_g\} \tag{5.4}$$

The added mass with respect to impulsive pressure can be calculated from Housner's model. For distributed mass it is:

$$m_i(y)=-\frac{\sqrt{3}\cdot\rho_l\cdot H_l}{2}\cdot[1-\frac{y^2}{H_l^2}]\cdot\tanh(\frac{\sqrt{3}\cdot L_x}{H_l}) \tag{5.5}$$

Or lumped mass that is:

$$M_{i,total}=\frac{\tanh[0.866(L_x/H_L)]}{0.866(L_x/H_L)}M_L \tag{5.6}$$

Also it can be obtained from Eq. 3.25 for rigid wall boundary condition which is as same as the Haroun's model (1984) in Eq. A.16. The distributed mass is:

$$m_i(y) = \sum_{i=1}^{\infty} \frac{2 \cdot (-1)^i \cdot \rho_l}{\lambda_i^2 \cdot H_l} \tanh(\lambda_i \cdot L_x) \cdot \cos(\lambda_i \cdot y) \qquad (5.7)$$

and the lumped mass is:

$$M_{i,total} = \sum_{i=1}^{\infty} \frac{2}{\lambda_i^3 \cdot H_l^2 \cdot L_x} \tanh(\lambda_i \cdot L_x) \cdot M_L \qquad (5.8)$$

where M_L is the mass of liquid in the half tank.

If the added mass method is used in the dynamic analysis, the added mass matrix representing the impulsive pressure derived from the rigid wall boundary condition cannot change with the time. Therefore, the amplitude of hydrodynamic pressure due to the flexibility of wall cannot be considered in the structural dynamic analysis. It means the boundary condition for the impulsive pressure is still rigid in the added mass method. Only the tank wall is considered to be flexible in the dynamic analysis.

In order to consider the effects of flexibility of wall in both hydrodynamic pressures calculation and dynamic analysis of tank wall, the sequential method is used in this study. The sequential method is a technique in which the two fields are coupled by applying results from the first analysis as loads or boundary conditions for the second analysis. Principally the dynamic response of liquid storage tanks must be solved by "strong" coupled method. As shown in Equation 5.1, the hydrodynamic pressures are the external forces applied on the surface of the rectangular tank wall. The hydrodynamic pressure is then calculated according to the boundary conditions determined by the dynamic response of tank wall shown in Eq.3.25. Actually Equations 5.1 and 3.25 must be solved simultaneously because the interaction between the tank wall and the hydrodynamic pressure occurs at the same time. Since it is difficult to solve the dynamic response of tank wall and hydrodynamic pressure from these equations directly, the sequential method can be used to approximate it.

The sequential method is carried out by the following procedure. First the dynamic response of the flexible tank wall subjected to an earthquake is analyzed at time step t. Then the hydrodynamic pressure is determined, which also includes the effect of

45

flexibility of the tank wall. Finally the hydrodynamic pressure is applied on the tank wall at the next time step t+Δt. The procedure is then repeated at each time step until the analysis is complete. Figure 5.3 shows in a flowchart format the procedure for analysis and Figure 5.4 shows the transfer of data between the rectangular tank wall and the fluid.
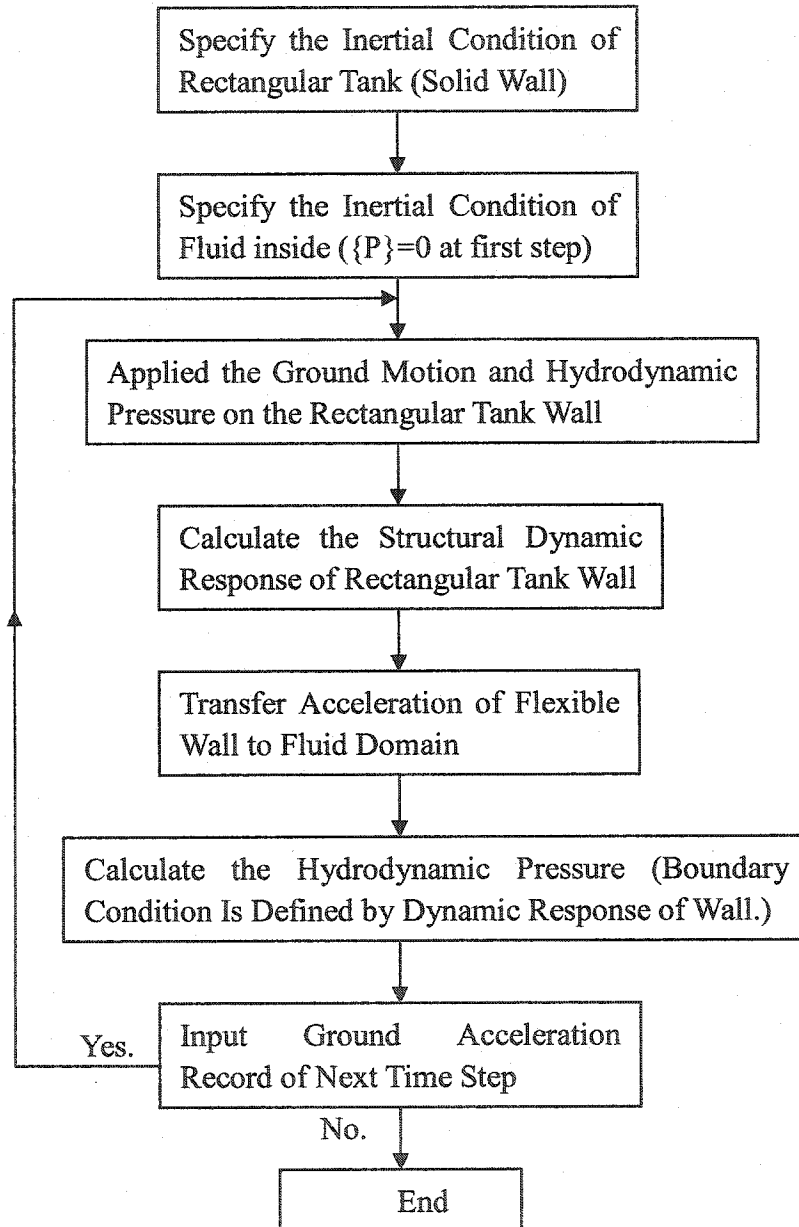
Figure 5.3 Flow Chart of Sequential Analysis
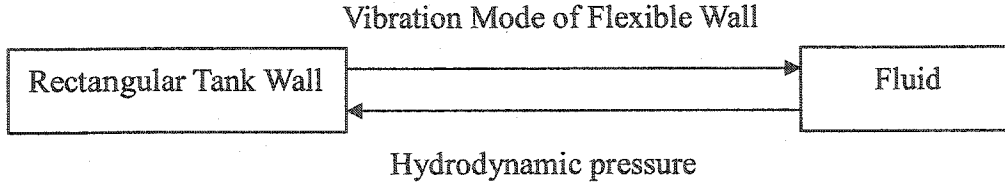
Figure 5.4 Transfer Data in Coupled Fluid Storage Tank System

The equation of motion in terms of the sequential method at time t can be expressed as:

$$[M_w]\{\ddot{u}_{r,t}\} + [C]\{\dot{u}_{r,t}\} + [K]\{u_{r,t}\} = -[M_w]\{\ddot{u}_{g,t}\} - [R_i(t-\Delta t)]\{\ddot{u}_{g,t-\Delta t} + \ddot{u}_{r,t-\Delta t}\} \qquad (5.9)$$

where $R_i(t-\Delta t)$ is time dependent functional for impulsive hydrodynamic pressure and can be derived from the Eq.3.25.

If $R_i(t-\Delta t)$ is treated as $M_i(t-\Delta t)$, time dependent function for added mass related to hydrodynamic pressure at time $t-\Delta t$, Eq.(5.9) becomes:

$$[M_w]\{\ddot{u}_{r,t}\} + [C]\{\dot{u}_{r,t}\} + [K]\{u_{r,t}\} = -[M_w]\{\ddot{u}_{g,t}\} - [M_i(t-\Delta t)]\{\ddot{u}_{g,t-\Delta t} + \ddot{u}_{r,t-\Delta t}\} \qquad (5.10)$$

or

$$[M_w]\{\ddot{u}_{r,t}\} + [M_i(t-\Delta t)]\{\ddot{u}_{r,t-\Delta t}\} + [C]\{\dot{u}_{r,t}\} + [K]\{u_{r,t}\} = -[M_w]\{\ddot{u}_{g,t}\} - [M_i(t-\Delta t)]\{\ddot{u}_{g,t-\Delta t}\}$$
$$(5.11)$$

It can be seen that if the impulsive hydrodynamic pressure due to the acceleration of the flexible wall in Eq. 5.10 is moved to left hand side as shown in Eq.5.11, it is equivalent to Eq. 5.4, except that time t in Eq. 5.10 is replaced by t-Δt in Eq.5.11. If the hydrodynamic pressure at time t-Δt is known, it can be easily applied as external force on the tank wall to obtain the dynamic response of tank wall at the next time step, t. Furthermore, if the time interval Δt is decreased in the analysis, the accuracy of final result can be improved.

There are four major advantages of using the proposed model over the models used by other researches. As discussed before, the hydrodynamic pressure is no longer approximated by the added masses in the proposed model. As a result, the flexibility of tank wall can be considered in both the hydrodynamic pressure calculation and dynamic

analysis of tank wall.

Secondly, in the past, many researchers used the pre-assumed vibration function to calculate the amplitude of hydrodynamic pressure due to the flexibility of tank wall. This method was first proposed by Yang and Veletsos (1976) in the study of dynamic response of circular tanks. In their research, three vibration functions based on the oscillation of vertical cantilever beam were assumed to calculate the hydrodynamic pressures. In fact, for a variety of height-diameter ratios of circular tanks, it is not very accurate to use few vibration functions to approximate the dynamic response of tanks (Nachtigall et al., 2003). Kim et al. (1996) applied Reyleigh-Ritz method using assumed vibration modes of rectangular plate with suitable boundary conditions as admissible function to study the rectangular tank. The added mass method is still used to approximate the hydrodynamic pressures in the structural dynamic analysis due to the complexity of calculations. However, for the proposed model, as the dynamic response of tank wall is analyzed using the finite element method, the dynamic response at each time step can reflect the motion of tank wall more accurately. Thus the boundary conditions used in the hydrodynamic pressure calculation are also more accurate than those from the pre-assumed vibration mode method.

Thirdly, the proposed model has low computation cost in the analysis as compared with the other models. In the past, some researchers proposed 'strong coupled' equation of motion in their research (Balendra et al. 1982). As the governing equations for the fluid dynamics and solid dynamics are absolutely different, these equations were very difficult to be solved directly, especially in the time history analysis. In the proposed model, the two engineering fields are solved separately. Then through sequential analysis, the time history of dynamic response can be easily obtained. But it must be emphasized that in the proposed model the time step Δt must be small enough to guarantee the accuracy of the results.

Finally, in the past, few researches have considered the damping effect in the

dynamic response of liquid storage tanks. However, the effect of damping can be very critical in dynamic analysis of liquid storage tanks. It is possible that resonance may occur resulting in the dynamic response of liquid storage tanks to be extremely large. In the proposed model, damping is considered using a damping ratio or Reyleigh damping.

5.3.3 Coupled Analysis of Vertical Ground Motion Condition

In the vertical ground motion condition, as the vertical ground acceleration can transmit the hydrodynamic pressure in the horizontal direction, some special techniques must be used in the dynamic analysis. Equation 3.42 shows the hydrodynamic pressure induced by the vertical ground acceleration. This equation is repeated as below:

$$p = \rho_l(H_l - y) \cdot \ddot{v}_g(t) + \sum_{n=1}^{\infty} \frac{2 \cdot \rho_l}{\lambda_{i,n} \cdot H_l} \coth(\lambda_{i,n} L_x) \cos(\lambda_{i,n} y) \int_0^{H_l} \cos(\lambda_{i,n} y) \cdot \ddot{u}(t) dy$$

(5.12)

The above equation can be simplified into a matrix form as follows:

$$\{P\} = [R_v] \cdot \{\ddot{v}_g(t)\} + \{P_{flex}\}$$

(5.13)

where $\{P\}$: the total hydrodynamic pressure induced by the vertical ground acceleration

$\{P_{flex}\}$: the part of hydrodynamic pressure due to the flexibility of tank wall. It can be obtained from the formula:

$$P_{flex} = \sum_{n=1}^{\infty} \frac{2 \cdot \rho_l}{\lambda_{i,n} \cdot H_l} \coth(\lambda_{i,n} L_x) \cos(\lambda_{i,n} y) \int_0^{H_l} \cos(\lambda_{i,n} y) \cdot \ddot{u}(t) dy$$

(5.13)

$[R_v]$: Hydrodynamic pressure function due to the vertical ground acceleration. It can be derived from the formula:

$$R_v = \rho_l(H_l - y)$$

(5.14)

The dynamic response of liquid storage tanks subject to the vertical ground motion is analyzed by the combination of the added mass method and the sequential method. As the wall inertial mass due to vertical ground motion has no significant effect in the

49

horizontal direction, the inertial mass matrix of tank wall is equal to zero. The hydrodynamic pressure due the vertical ground acceleration is approximate by the added liquid mass $M_v = R_v$ applied on the tank wall. The hydrodynamic pressure due to the flexibility of tank wall is analyzed by the sequential method. Therefore the governing equation of motion is:

$$[M_v]\{\ddot{u}_r\} + [C]\{\dot{u}_r\} + [K]\{u_r\} = [M_v]\{\ddot{v}_g(t)\} + \{P_{flex}\} \qquad (5.15)$$

It is noted that this method is conservative for the dynamic response of liquid storage tanks subjected to the vertical ground motion due to the approximation of added mass. As the relative acceleration in the tank wall is small in this case, the virtual inertial forces represented by the added mass due to the hydrodynamic pressure are not significant.

5.4 Load Combination

When a rectangular tank is subject to the simultaneous action of three components of earthquake motion, tank walls experience hydrodynamic pressures and inertial forces in addition to the hydrostatic pressure. For 2-D model, it assumed the earthquake wave has only two components, horizontal and vertical. As a result, in the horizontal direction, the loads include hydrostatic pressure, inertial force and hydrodynamic pressures which contain the impulsive pressure and convective pressure induced by both horizontal and vertical ground motion. It is known that the sloshing response in the vertical ground motion is not significant (Kana 1979). Thus it is not included in this study. The corresponding system of loads of rectangular tank wall subjected to earthquake is shown in Figure 5.5.

The combination of dynamic response of liquid storage tanks is calculated by sum of all dynamic load cases in the time history. The convective pressure can be obtained using the response spectrum method as demonstrated in Chapter 3. However, the convective and hydrostatic pressures are not considered in the study.
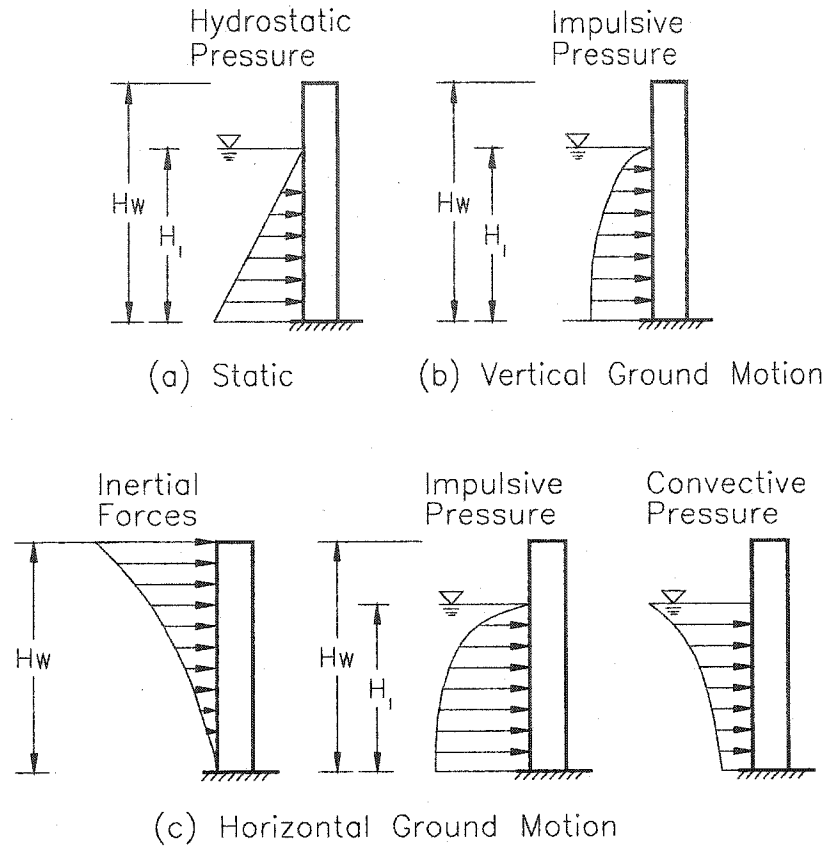
Figure 5.5 Typical Loads Applied on Tank Wall

Chapter 6

Description of the Computer Program for Dynamic Analysis
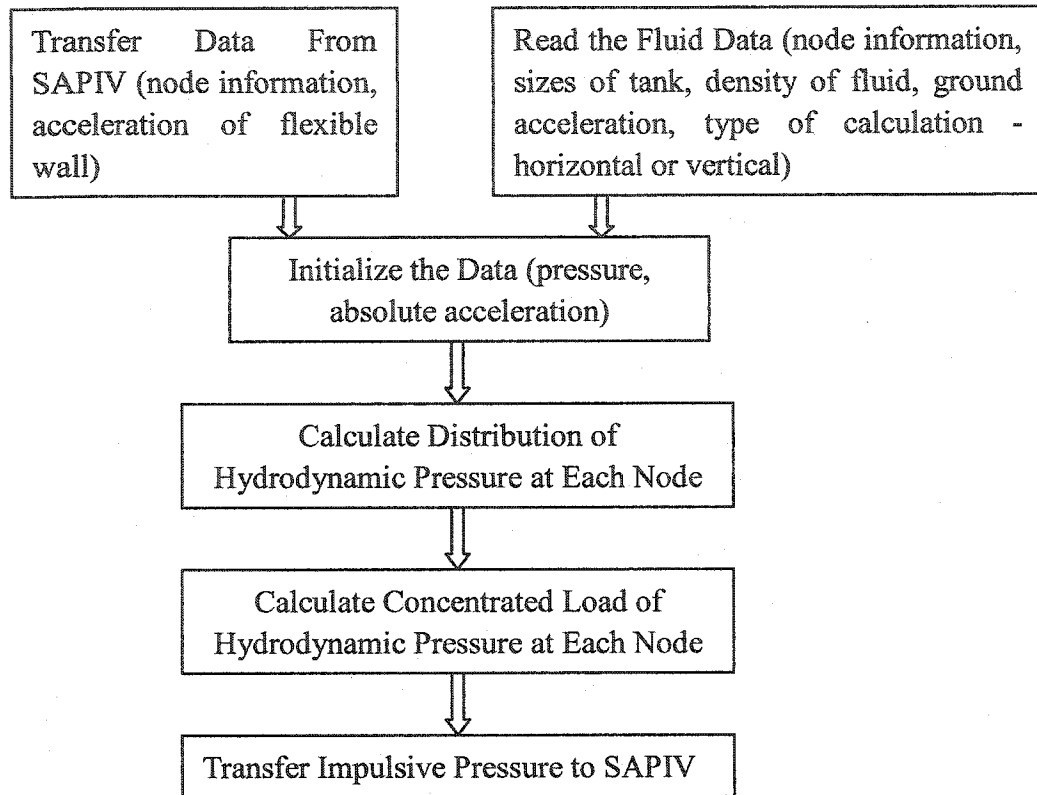
6.1 Introduction

The time history analysis is carried out using linear static and dynamic structural analysis software SAPIV. The Hydrodynamic pressure is calculated using the subroutine HYDRO developed in this study. It is successfully incorporated into SAPIV to obtain the dynamic response of liquid storage tanks. The algorithm and incorporation of HYDRO into SAPIV is presented in this chapter. The program can calculate the response of rectangular tanks due to both horizontal and vertical ground motions. The impulsive pressure is considered in this program. Some numerical methods and computer techniques used in this study are explained. The analysis procedure is described.

6.2 Subroutine HYDRO for Hydrodynamic Pressure Calculation

The subroutine HYDRO is developed to calculate the hydrodynamic pressure applied on the rectangular tank wall. Only impulsive pressure is considered in this program. It is incorporated into SAPIV as a subroutine to calculate the magnitude of the hydrodynamic pressure due to the flexibility of wall. The flow chart of the program is shown in Figure 6.1.

The input data for subroutine can be divided into two parts. One is directly transferred from SAPIV such as node information NEQ, Y(I) and acceleration of flexible wall X(I). The other is obtained from the independent input file "PRE.DAT" which contains information of fluid in the tank. The purpose of using separate data input file is to keep integration of SAPIV and subroutine HYDRO, and less destroy the program structure of SAPIV. The PRE.DAT includes node information - MF, size of tank - HL, XL, YL, density of fluid - DENS, ground acceleration – A(I), and type of calculation - horizontal or vertical. The format of input data file PRE.DAT is described in the

Appendix D.

```
┌─────────────────────────────┐         ┌─────────────────────────────────┐
│ Transfer   Data   From      │         │ Read the Fluid Data (node         │
│ SAPIV (node information,     │         │ information, sizes of tank,       │
│ acceleration of flexible     │         │ density of fluid, ground          │
│ wall)                        │         │ acceleration, type of calculation │
│                              │         │ - horizontal or vertical)         │
└─────────────────────────────┘         └─────────────────────────────────┘
              │                                         │
              └──────────────┐          ┌───────────────┘
                             ▼          ▼
                  ┌──────────────────────────┐
                  │ Initialize the Data (pressure, │
                  │ absolute acceleration)    │
                  └──────────────────────────┘
                             │
                             ▼
              ┌──────────────────────────────────┐
              │ Calculate Distribution of         │
              │ Hydrodynamic Pressure at Each Node │
              └──────────────────────────────────┘
                             │
                             ▼
              ┌──────────────────────────────────┐
              │ Calculate Concentrated Load of     │
              │ Hydrodynamic Pressure at Each Node │
              └──────────────────────────────────┘
                             │
                             ▼
              ┌──────────────────────────────────┐
              │ Transfer Impulsive Pressure to SAPIV │
              └──────────────────────────────────┘
```

Figure 6.1 The Flow Chart of Subroutine HYDRO

The inertial impulsive pressure at each node is equal to zero at the first step in the subroutine HYDRO. It is noted that the acceleration of structure calculated in SAPIV is relative acceleration in the structural dynamic analysis, however the acceleration used in the hydrodynamic pressure calculation is the absolute acceleration. Therefore, after the relative acceleration from SAPIV is calculated, it must be added with ground acceleration to obtain the absolute acceleration as shown in Eq.6.1.

$$\ddot{u}(t) = \ddot{u}_r + \ddot{u}_g \qquad (6.1)$$

This absolute acceleration can be used in the hydrodynamic pressure calculation.

The subroutine HYDRO then calculates the impulsive pressure distribution along

the height of the wall. Afterwards, the impulsive pressure distribution is linearized and the distributed impulsive pressure is concentrated at the nodes in structural dynamics analysis.

In the calculation of impulsive pressure, the subroutine SIMP3 is used for integration. The Simpson three-point integration method is used. It is that if one extra point $f(x_1)$ between $f(x_0)$ and $f(x_2)$, where $f(x)$ is a predefined function, these three points can be connected with a parabola to approximate this function. The formulas that result from taking the integrals under these parabolas are called Simpson three point rules. It can be expressed in mathematical form as below:

$$I = \int_{x_0}^{x_2} f(x)dx \cong \int_{x_0}^{x_2} f_2(x)dx \qquad (6.2)$$

Where $f_2(x)$ is the second order polynomial.

If $f_2(x)$ is represented by a second order Lagrange polynomial, it result in:

$$I = \int_{x_0}^{x_2}[\frac{(x-x_1)(x-x_2)}{(x_0-x_1)(x_0-x_2)}f(x_0) + \frac{(x-x_0)(x-x_2)}{(x_1-x_0)(x_1-x_2)}f(x_1) + \frac{(x-x_0)(x-x_1)}{(x_2-x_0)(x_2-x_1)}f(x_2)]dx$$

$$(6.3)$$

After integration and algebraic manipulation, it becomes:

$$I \cong \frac{h}{3}[f(x_0) + 4f(x_1) + f(x_2)] \qquad (6.4)$$

Where h is the width of the stripe, in this program $h=(x_2-x_0)/2$. So it can also be expressed as that:

$$I \cong (x_2 - x_0)\frac{f(x_0) + 4f(x_1) + f(x_2)}{6} \qquad (6.5)$$

It must be noted that although Simpson three point integration method can calculate both odd and even number segments, for simplifying purpose, only odd number segments are adopted in this program. Therefore the number of finite elements that contact the fluid must be odd. Although it will not affect the accuracy of the calculation, it must be noted in the meshing of tank wall in the part which contacts the fluid.

Finally data of impulsive pressure are transferred to SAPIV. It is noted that if there is

no degree of freedom at the nodes, in SAPIV the numbers of equations are not specified. For example the nodes at the bottom of tank wall rigidly connected to tank base have no numbers of equations. In this situation, the hydrodynamic pressure must be directly transferred to these nodes. Thus the impulsive pressure can be considered as external load applied on the tank wall.

6.3 Incorporation of HYDRO into SAP IV

SAPIV is a computer program for static and dynamic analysis of linear structural system. The detail information about SAPIV including the format of input file can be found in the reference (Bathe et al., 1974).

In SAPIV there are two types of time history analysis, the mode superposition method and the direct step-by-step integration method. For added mass method, the mode superposition method is used, while the direct step-by-step integration method is applied in sequential method. Thus the results of analysis of these two different methods can be compared with each other in order to verify the efficiency of sequential method used in the new model.

Although the direct step-by-step integration method cannot provide the natural frequencies of structure, it can calculate the displacement, velocity and acceleration at each time step. Therefore, it is very convenient to apply the sequential method in the dynamic analysis of liquid storage tank system. In SAPIV the main subroutine for the step-by-step direct integration method is subroutine STEP. The subroutines for such analysis include:

(1) ADDMAS – to read the system mass matrix

(2) PLOAD- to read forcing function dada

(3) EMIDS – to create an integer array mass which flags transnational component number associated with the system freedom

(4) GROUND – to modify the function multiplies and arrival time arrays to input ground

motion

(5) INDLY – to read arrival time values from data input

(6) LOADV – to read time, function from input card

(7) INOUT – to output requests for displacement and element stress components

(8) TRIFAC – to decompose the system matrix in blocks

(9) SOLSTD – to solve for displacement, velocities and acceleration at each solutions
   time step

(10) SDSPLY- to print response table

The subroutine SOLSTD can calculate displacement, velocities and acceleration at each time step. These are boundary conditions used in the impulsive pressure calculation. The subroutine HYDRO for impulsive pressure calculation is incorporated into subroutine SOLSTD.

6.4 Analysis Procedure

The analysis procedure is described in this section. Before the calculation of liquid storage tank, the empty tank must be analyzed. The input file for empty tank is prepared according to the reference (Bathe et al., 1974). Then the output file provides the equation numbers which are used for application of hydrodynamic pressure according to the element nodes. These equation numbers with the Y coordinate of nodes on which hydrodynamic pressure is applied can be specified in Part 3 of PRE.DAT.

In SAPIV the equation numbers will not be specified to the nodes which have no degrees of freedom. Therefore, such equation numbers must be defined as zero in RRE.DAT. For example, the equation numbers of the nodes at the bottom of the rectangular wall rigidly connected to tank base are zero. The impulsive pressure must also be directly added to the base reaction to obtain the total support reaction at each time step.

Although the earthquake time function has already been defined in SAP.DAT, in

order to less destroy the structure of SAPIV, it has to be input again in Part 4 of PRE.DAT. It can be easily achieved by copying it from the input file SAP.DAT directly.

Thus the procedure of analysis can be summarized below:

(1) Prepare the input file SAP.DAT for empty rectangular tank.

(2) Run SAPIV to obtain the equation numbers of nodes which impulsive applied.

(3) Prepare the input file PRE.DAT.

(4) Run SAPIV again to obtain the dynamic response of fluid-rectangular tank system.

(5) Add the hydrodynamic pressure where the nodes are defined as zero to get total support reaction.

(6) Calculate the base shear, base moment and top displacement of rectangular tank wall for design.

Chapter 7

Parameter Analysis and Examples

7.1 Introduction

In this chapter a series of dynamic analyses are carried out in order to verify the efficiency of the proposed model. The validity of SAPIV is first tested by static analysis of tank wall. Then an empty tank is studied to prove the accuracy of time history dynamic analysis. The results from the mode superposition method and the direct step-by-step integration method are compared with each other to confirm the validity of these two methods used in this study.

Several models are used in the dynamic analysis of rectangular liquid storage tanks. The accuracy of analysis is improved by application of the techniques discussed in the previous chapters. A concrete rectangular tank studied by the other researchers (Kim et al., 1996) is also investigated in this study. Dynamic responses of the tank in terms of horizontal and vertical ground motions are investigated. The results of dynamic analysis and impulsive pressure distribution are discussed.

Another rectangular tank is investigated later by the application of the different ground motion record in order to study the response of liquid storage tanks for the vertical ground motion. The load combination of horizontal and vertical ground motion is also studied.

7.2 Dynamic Analysis of Liquid Storage Tanks - Empty Tank

The rectangular tank studied by Park et al. (1990) and Kim et al. (1996) is analyzed in this study. Figure 7.1 shows the dimensions of tank and parameters. Figure 7.2 shows 2-D finite element model.

Prior to dynamic analysis of rectangular tank wall, a static analysis is carried out. A concentrated force equal to 400 KN is applied at top of the wall. The displacement

calculated using SAPIV is 81.15 mm which is similar to the result 83.33 mm calculated by analytical method. The base shear is 399.96 KN. It proves that the static analysis is correct and the 4-nodal plane strain element in SAPIV is valid.

For dynamic analysis, the North-South component of 1940 El Centro Earthquake records is used as input ground record in the horizontal direction. The accelerogram of Imperial Valley (Irrigation District) is shown in Figure 7.3. The time interval between each step is 0.01 sec. The damping ratio in the mode superposition method is 5% for the concrete wall. The Rayleigh damping $[C] = \alpha[M] + \beta[K]$ is used in the direct step-by-step integration method. The parameters α, β are calculated using Equations 4.30 and 4.31 as discussed before.
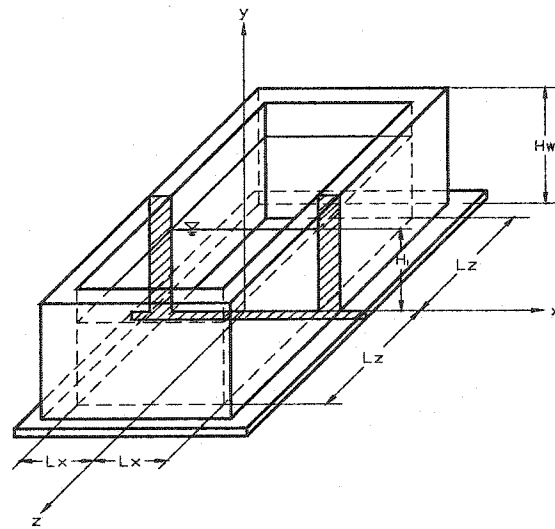
ρ_w = 2300 Kg/m³ t_w = 1.2 m

ρ_l = 1000 Kg/m³ L_x = 9.8 m

E = 2.0776x10⁴ MPa L_z = 28 m

ν = 0.17 H_w = 12.3 m

H_l = 11.2 m

Figure 7.1 Dimensions and Parameters of Rectangular Tank
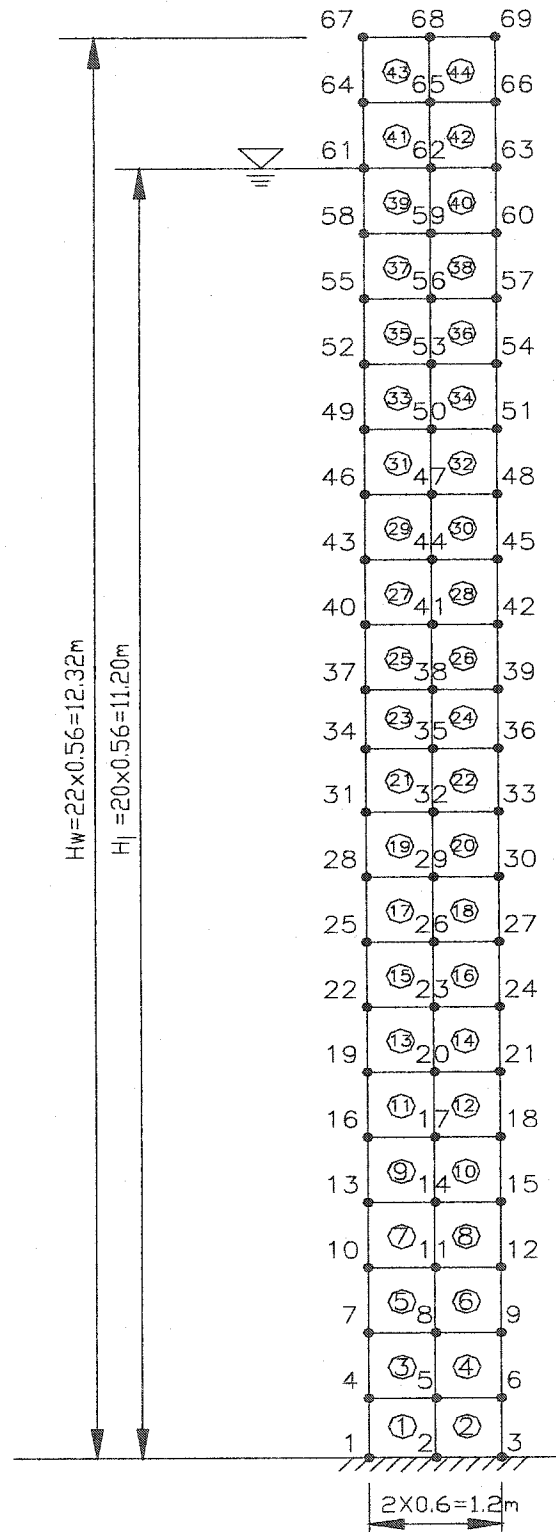
Figure 7.2 Finite Element Model – Tall Tank

60
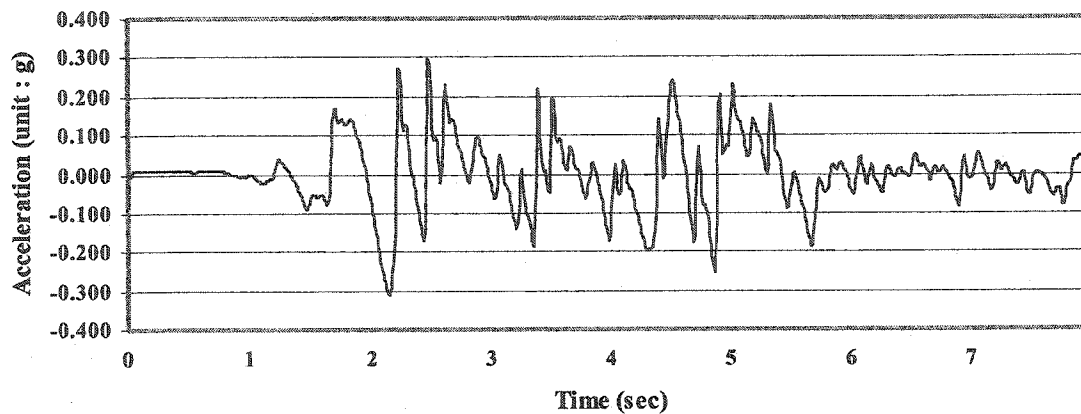
**Figure 7.3 N-S Component of El Centro Accelerogram,
1940 Imperial Valley Earthquake**

For the empty tank, three models are analyzed:

(1) Equivalent lumped mass model based on ACI 350.3. The total mass of rectangular tank wall is lumped on a cantilever wall at the equivalent height.

(2) The model with the mass of rectangular tank wall distributed at each node.

Both of above models are analyzed using the mode superposition method.

(3) This model is the same as model 2 except that it is analyzed using the direct step-by-step integration method.

The results of analysis are summarized in Table 7.1. The time history response in terms of displacement d_A at the top of tank wall and base shear F_B is shown in Figures 7.4-7.6.

The results presented in Table 7.1 and Figures 7.4-7.6 show that the calculation results are almost the same between the mode superposition method and the direct step-by-step integration method with respect to distributed mass model. This indicates that these two methods are equivalent in the dynamic analysis. In addition, the period of first mode in equivalent lumped mass model can also be calculated by the analytical method such as that presented in ACI 350.3. It is 0.1862 sec which is as same as the result of Model 1 calculated by mode superposition method of SAPIV shown in Table 7.1.

That means the results from both the mode superposition method and the direct step-by-step integration method are correct, or the time history dynamic analysis in SAPIV can provide the correct analysis results. The maximum base shear in equivalent lumped mass model is larger than that of distributed mass model. This is due to mass distribution. Basically the results from the distributed mass model are more accurate than those of the lumped mass model. The displacement at the top of tank wall in Model 1 is less than that of Model 2 and 3.
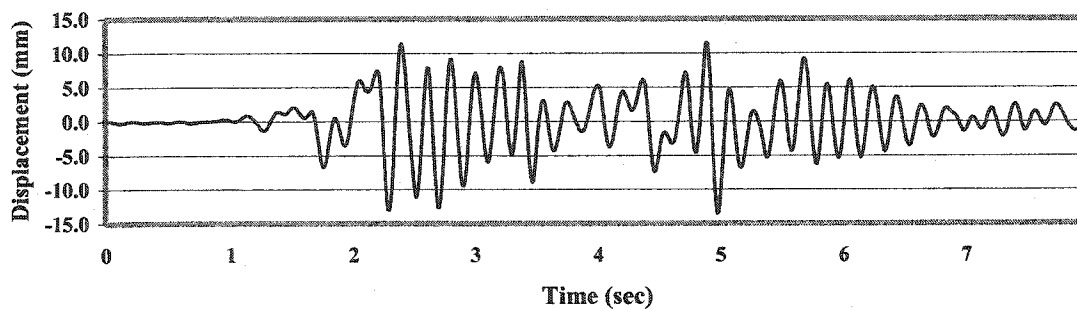
(a) Displacement (Top)
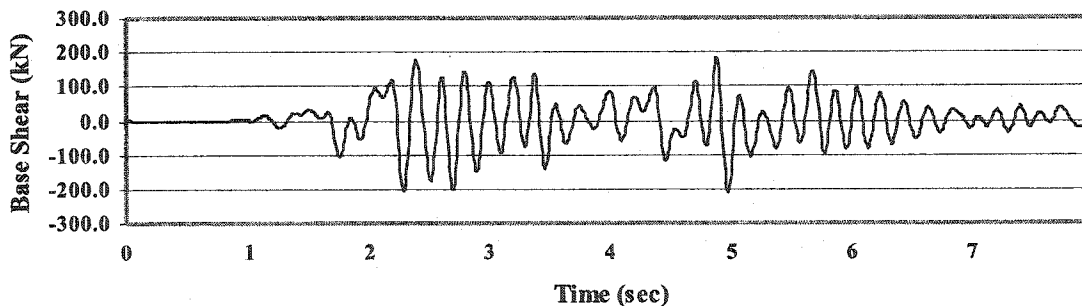
(b) Base Shear

Figure 7.4 Dynamic Response of Empty Tank - Model 1
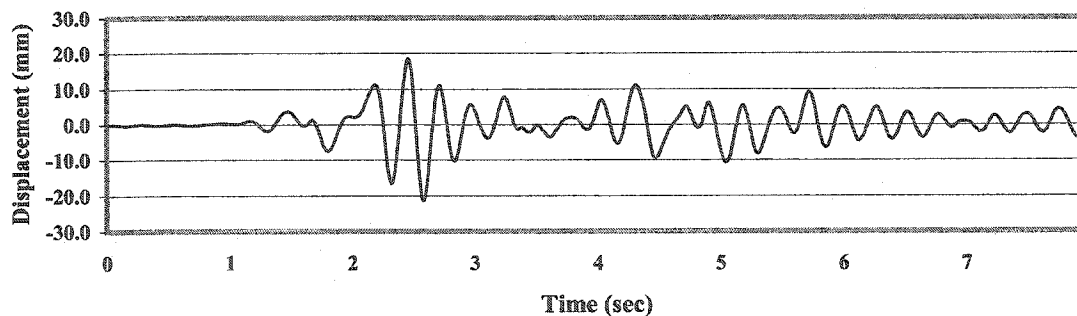
(a) Displacement (Top)
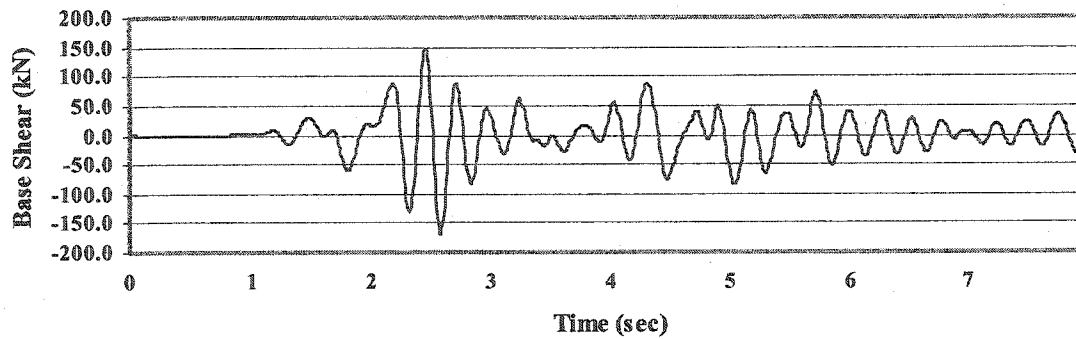
(b) Base Shear

Figure 7.5 Dynamic response of Empty Tank - Model 2
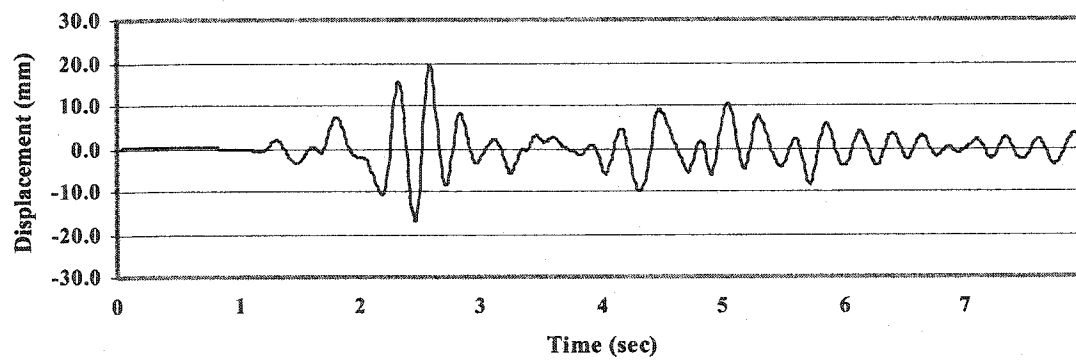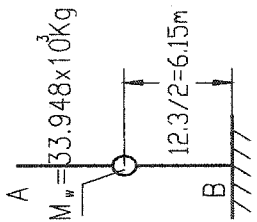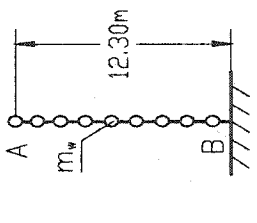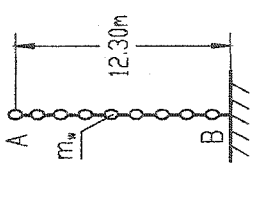
(a) Displacement (Top)
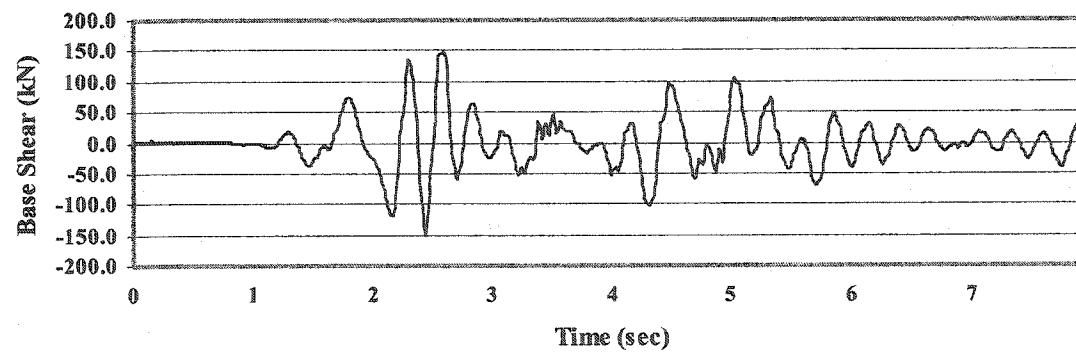
(b) Base Shear

Figure 7.6 Dynamic Response of Empty Tank – Model 3

Table 7.1 Summary of Dynamic Response of Empty Tank

Model	Model.1 – Equivalent Lumped Mass Model	Model.2 – Distributed Mass Model	Model.3 – Distributed Mass Model
Analysis Method	Mode Superposition Method	Mode Superposition Method	Direct step-by-step Integration method
Schematic of Model			
Period (sec)	$T_1 = 0.1850$ $T_2 = 0$	$T_1 = 0.2580$ $T_2 = 0.04247$	---
Damping	5%	5%	$\alpha=2.091, \beta=0.00182$
t_{max} *(sec)	4.98	2.58	2.58
Base Shear F_B (KN)	213.48	169.80	150.72 (t_{max} =2.45 sec)
Displacement d_A (mm)	13.53	21.48	19.49

* t_{max} : the time when the peak values of dynamic response are reached

64

7.3 Dynamic Analysis of Liquid Storage Tanks –Full Tank

7.3.1 Horizontal Ground Motion

For the liquid storage tank, 6 conditions are calculated. The summarized calculation results are list in Table 7.2. For the first 5 models, the time history of displacement d_A at the top of the tank wall and base shear F_B is shown in Figures 7.8-7.12.

The impulsive pressure is applied by the added mass method in Model 2 and Model 3. The added mass is obtained from application of unit acceleration in Eq.5.3. Both of them are analyzed by mode superposition method. The difference between Model 2 and Model 3 is that the different formulas are used in the calculation of lumped added mass representing impulsive pressure. In Model 2 the lumped added mass of impulsive pressure is calculated using Eq.5.6 proposed by Housner (1957). The lumped added mass of impulsive pressure in Model 3 is obtained from Eq.5.8 proposed in this study. It is as same as the results from Haroun (1981) for the rigid wall boundary condition. The distribution of impulsive pressure along the height of wall is shown in Figure 7.7. From the calculation results, we can find that the results from Model 2 and Model 3 are similar. The difference between these two models does not exceed 10%. For this tank, the total added mass in Housner's model is 65.710×10^3 kg, while it is 59.815×10^3 kg in Model 3. The position or height of concentrated mass h_i is 4.20 m calculated by the equation in ACI 350.3. Due to finite element model it is conservatively added at the nearest node (node26).

In Model 4 the distributed added mass is used. It is an improved model compared to Model 3 assuming lumped added mass. It is analyzed by the mode superposition method as well. Though the period of first two modes are not big different with above two models, the base shear is reduced. This is due to the mass distribution discussed in the empty tank. All these three models use the rigid wall boundary condition to calculate the impulsive pressure.

The analysis result of the proposed model is shown in Model 5. The effect of

flexibility of tank wall in both hydrodynamic pressure calculation and structural dynamic analysis are considered. It is achieved by the application of sequential method discussed in Chapter 5. The dynamic analysis is carried out by the direct step-by-step integration method. The top displacement time history of Model 5 is similar to those obtained from the added mass method for rigid wall boundary condition (Model 2, 3, 4). But the base shear is increased due to the flexibility of tank wall compared to Model 4. From calculation results, despite the dynamic response of liquid storage tank has little different between Model 2, 3, 4, 5, the top displacement and base shear at peak value are almost between two periods, 2-3 sec and 4-5sec. That means the sequential method reflects the time history of dynamic response properly.
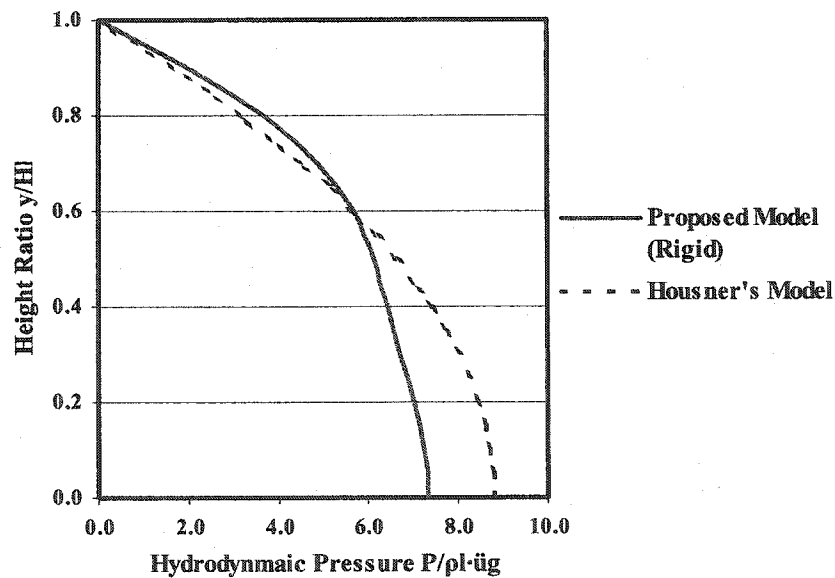
Figure 7.7 Comparison of Impulsive Pressure Distribution in Two Models (Rigid)

Two special cases are considered. One is in Model 6 that the Young's Modulus is specified as infinity to get the dynamic response of absolute rigid wall. The result shows that the wall always moves with the ground motion. The maximum base shear is less than that in the flexible wall. The time history of base shear is shown in Figure 7.13.

Another special case is to specify the damping parameters α, β equal to zero in

Model 5. The dynamic response for both impulsive pressure and tank wall becomes extremely large resulting in meaningless. This reflects that damping ratio is a very significant parameter in the study of dynamic response of liquid storage tanks. Further study must be carried out.

For the case of Model 1 which is based on ACI 350.3, although the period of first mode $T_1 = 0.225$ sec calculated using equation in ACI 350.3 is similar to that calculated using the mode superposition method $T_1 = 0.2389$ sec from SAPIV. However, the base shear is extremely large at time 2.56 sec. This is due to the deficiency in calculation the equivalent height. The equivalent height specified in ACI 350.3 is that:

$$h = \frac{M_i \cdot h_i + M_w \cdot h_w}{h_i + h_w}$$

(7.1)

It also results from the equivalent lumped mass model which couldn't reflect the dynamic response very well compared with the distributed mass model. The Model 1 is not accurate in the analysis.

In ACI 350.3, the base shear is calculated by the equation:

$$P_B = ZSIC_i \times \frac{(\varepsilon \cdot M_w + M_i) \cdot g}{R_w}$$

(7.2)

where P_B: the lateral inertial forces of wall and lateral impulsive force

Z: seismic zone factor assuming 0.4 in this case

S: site profile coefficient representing the soil characteristic as they pertain to the structure

I: important factor

C_i: period-dependent spectral amplification factor. For T<0.31 sec, it is $C_i=2.75/S$.

R_w: response modification factor 2.75 for this case

ε: effective mass coefficient

The final design base shear is modified by the response modification factor R_w, which is a numerical coefficient representing the combined effect of the structure's ductility,

energy-dissipating capacity and structural redundancy. Using Eq. 7.2, the result of base shear P_B is equal to 355.16 KN which is similar to those from this study. But the natural period of liquid storage tank, which reflects the basic properties of dynamic response of structure, is not so accurate compared with those of Model 2 and 3.

The change of hydrodynamic pressure with time in the earthquake is another interesting problem concerned in this study. The maximum impulsive pressure will be increased significantly due to the flexible wall boundary condition. But it may not occur at the same time of the maximum dynamic response of tank wall. The reason is as same as that the maximum dynamic response of tank wall will not appear at the time of maximum ground acceleration. In Figure 7.14(a) it shows the absolute acceleration along the height of wall or mode shape at the time the maximum dynamic response of liquid storage tank is reached for Model 5. The horizontal ground acceleration at the bottom of wall at that time is 1.766 m/sec^2 and the one at the top of wall is 6.990 m/sec^2. The corresponding impulsive pressure distribution is shown in Figure 7.14(b). It can be found that the impulsive pressure is significantly more than that in the rigid boundary condition. Figure 7.15 shows the result for Model 6 at the time the maximum dynamic response is reached. As the wall is absolute rigid, the acceleration along the height is equal to ground acceleration 3.072 m/sec^2 as shown in Figure 7.15(a). The impulsive pressure distribution is indicated in Figure 7.15(b). All these calculation results are obtained from the subroutine HYDRO at each time step.

As mentioned earlier, the tall tank investigated in this study is as the same dimension and properties as that used by Park et al. (1990) and Kim et al. (1996). Results of this study show that maximum response values are somewhat different with their research as demonstrated in Figure 7.16, particular after the 6 sec of ground motion. Results of their study show a type of harmonic motion after 6 sec. This type of response is out of range and in disagreement with the input ground motion from this study.
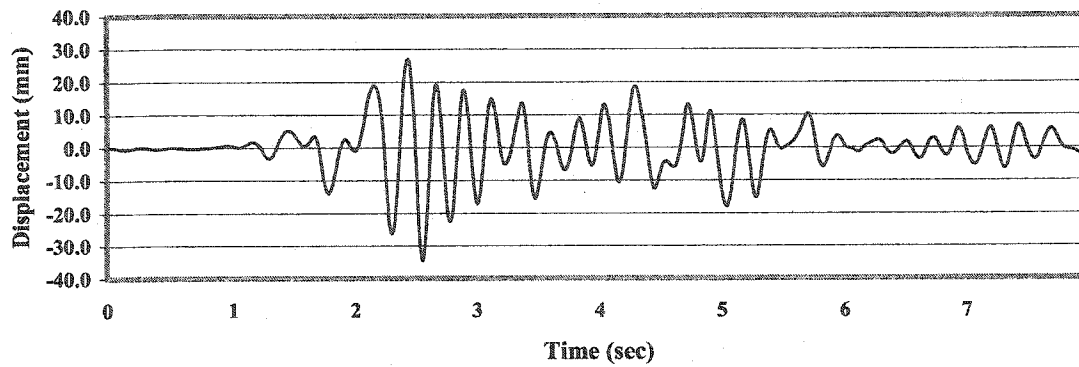
(a) Displacement (Top)
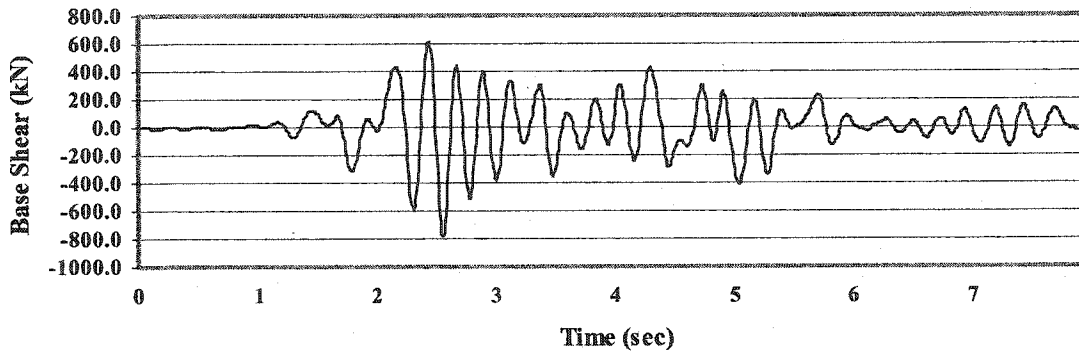
(b) Base Shear

Figure 7.8 Dynamic Response of Tall Tank - Model 1
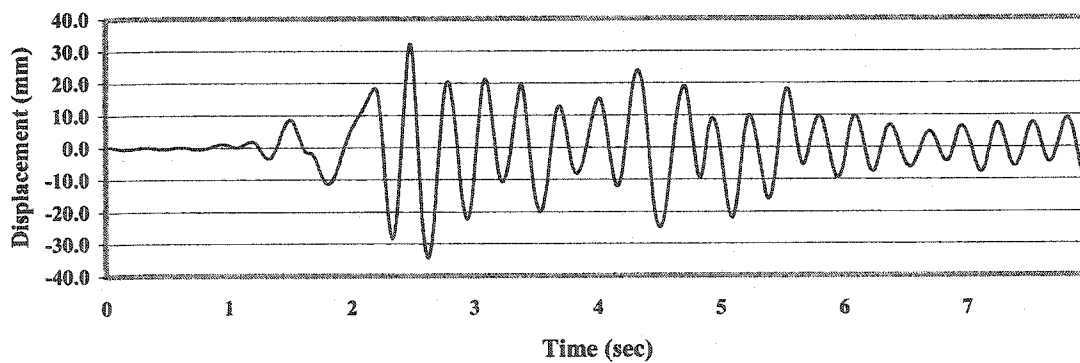
(a) Displacement (Top)
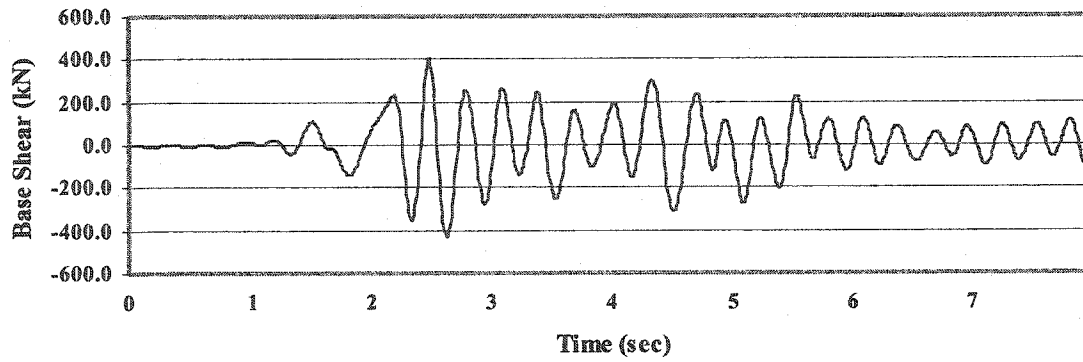
(b) Base Shear

Figure 7.9 Dynamic Response of Tall Tank – Model 2
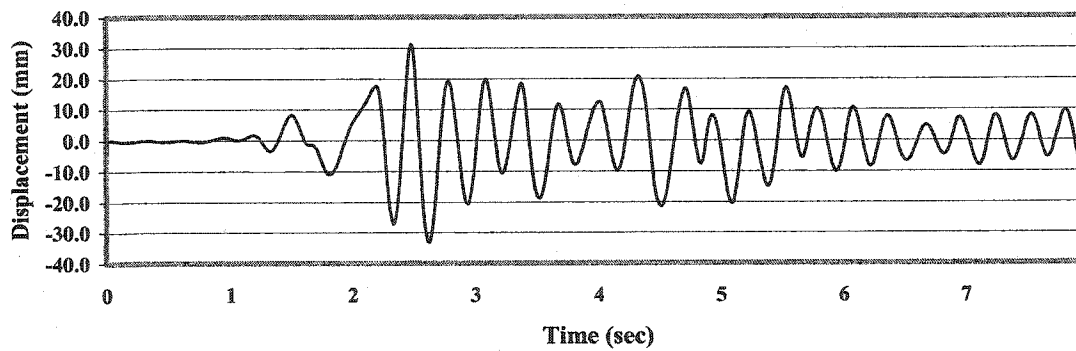
(a) Displacement (Top)
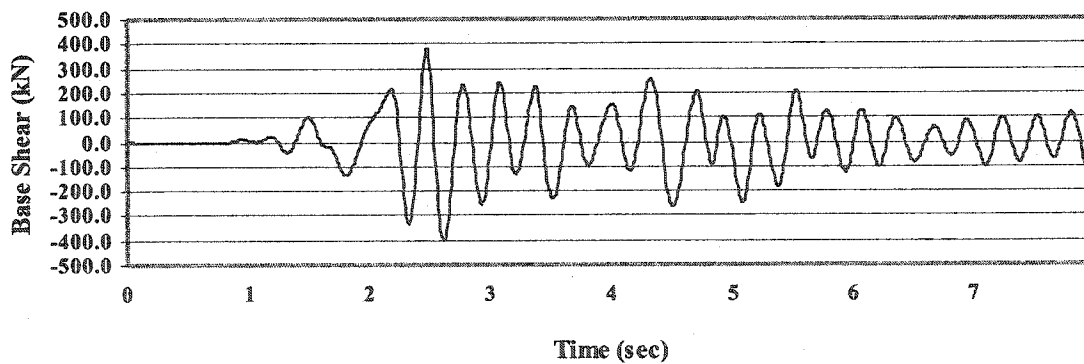
(b) Base Shear

Figure 7.10 Dynamic Response of Tall Tank – Model 3
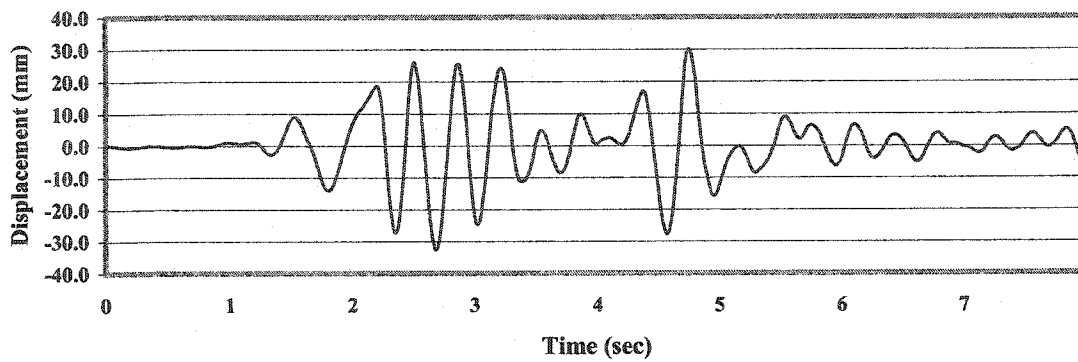
(a) Displacement (Top)
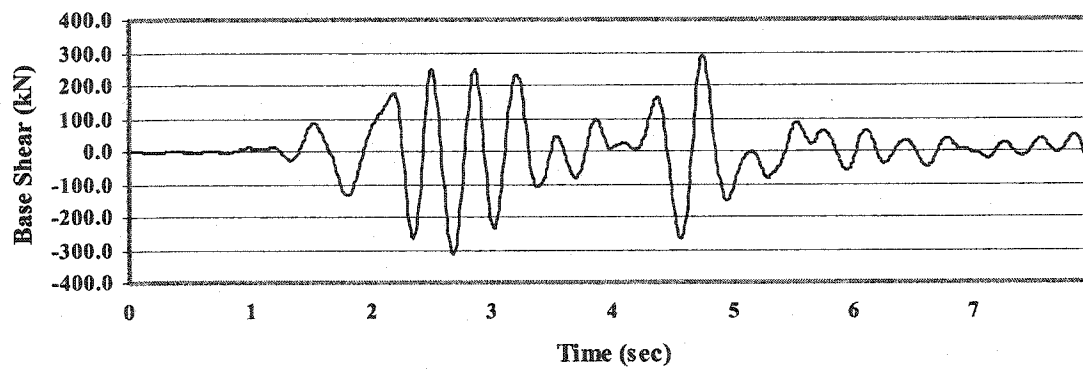
(b) Base Shear

Figure 7.11 Dynamic Response of Tall Tank - Model 4
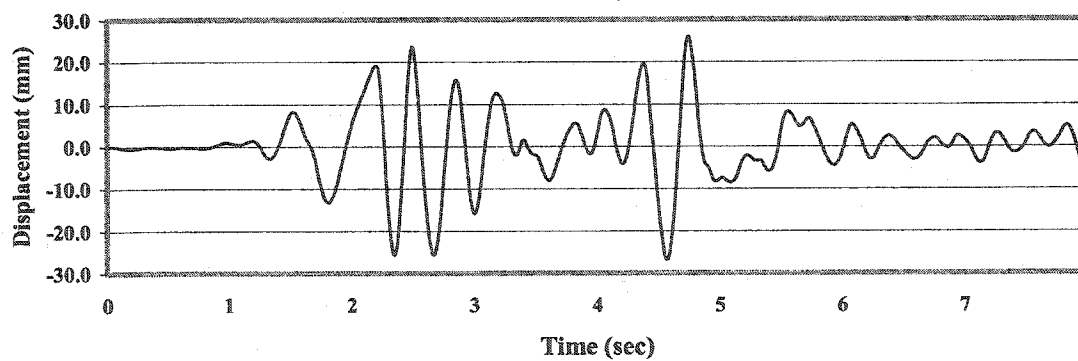
(a) Displacement (Top)
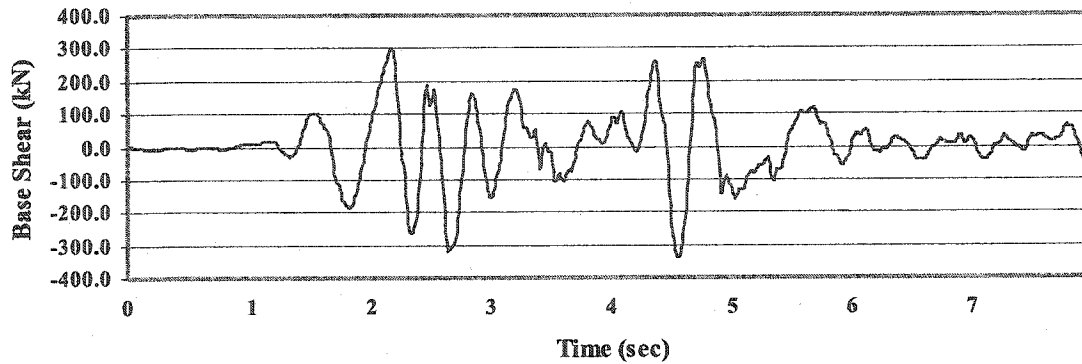
(b) Base Shear

Figure 7.12 Dynamic Response of Tall Tank - Model 5
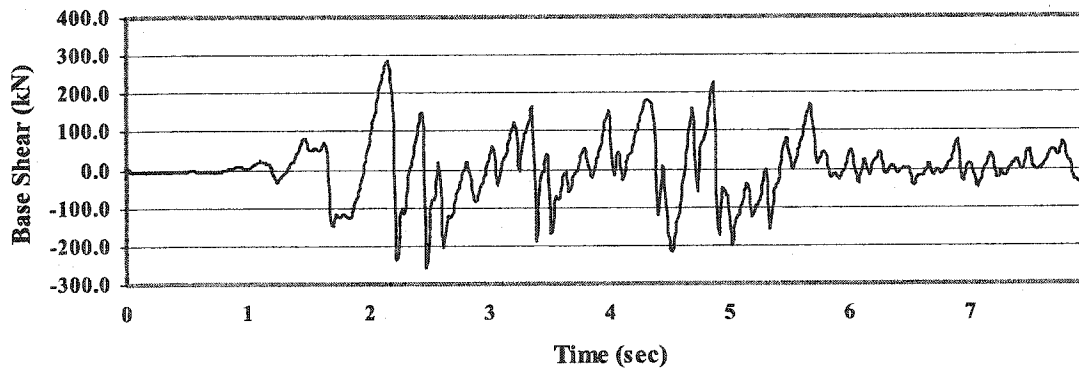
(a) Base Shear

Figure 7.13 Dynamic Response of Tall Tank - Model 6
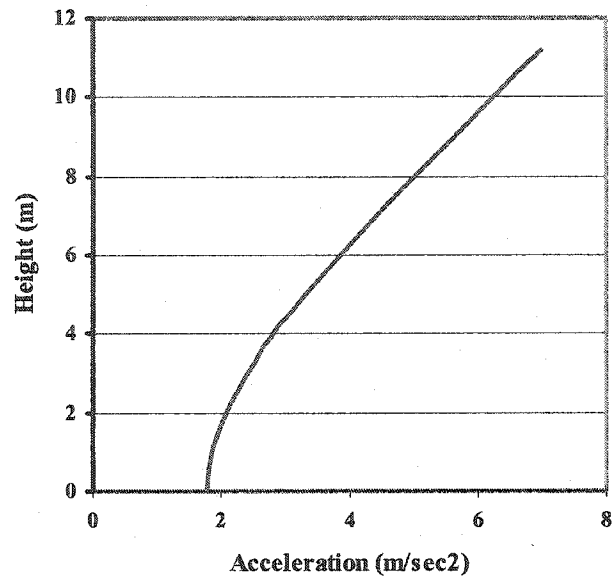
(a) Acceleration of Wall
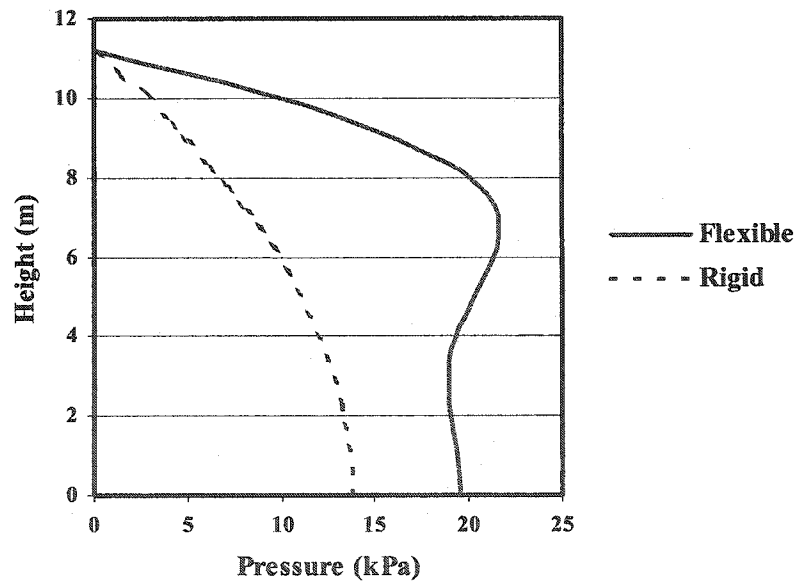
(b) Hydrodynamic Pressure

Figure 7.14 Dynamic Response of Wall and Impulsive Pressure Distribution
at Time t=4.56 sec (Model 5)
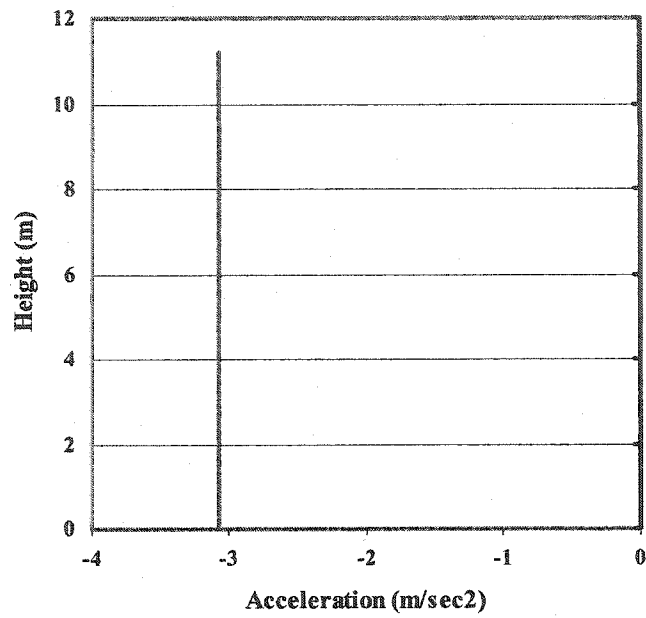
(a) Acceleration of Wall
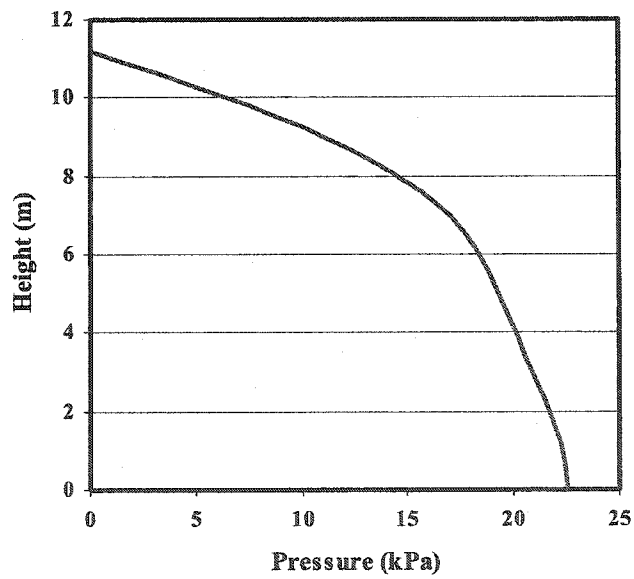
(b) Hydrodynamic Pressure

Figure 7.15 Dynamic Response of Wall and Impulsive Pressure Distribution
at Time t=2.16 sec (Model 6)
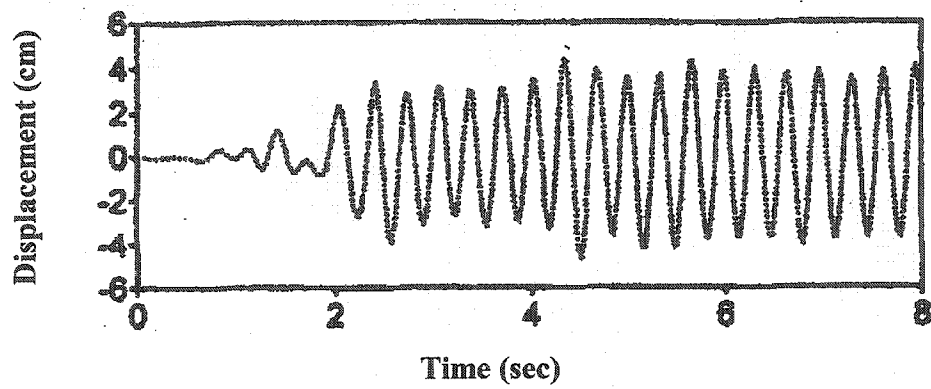
(a) Top Displacement
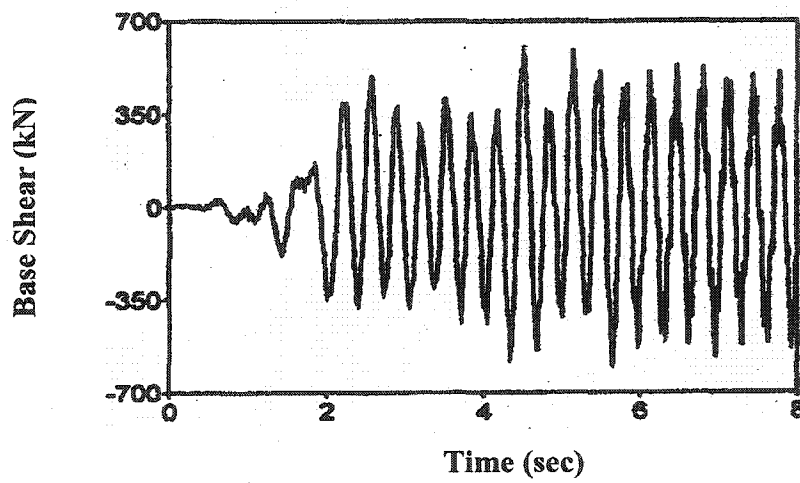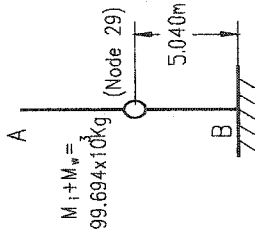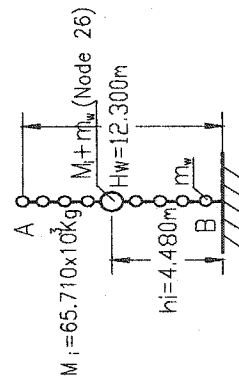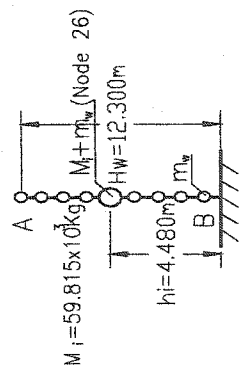
(b) Base Shear
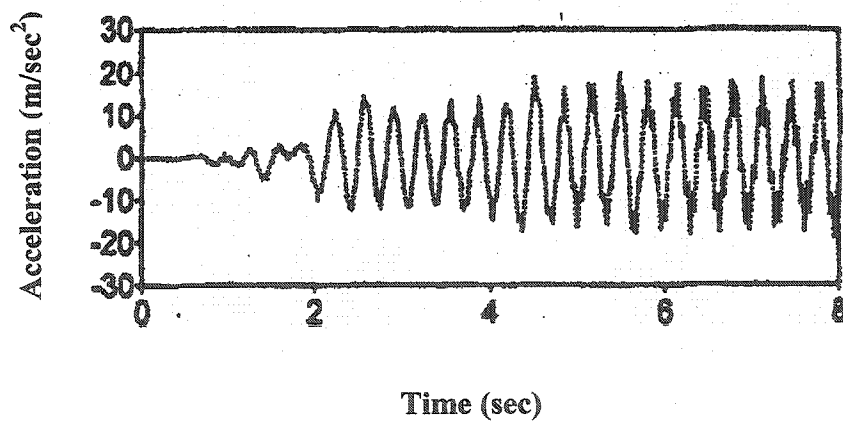
(c) Acceleration at the top of Tank Wall

Figure 7.16 Results of Analysis from Kim et al. (1996)

Table 7.2 Summary of Dynamic Response of Tall Liquid Storage Tank – Full Tank

		Model 1 (Housner)		Model 2 (Housner)		Model 3 (Proposed)	
Model							
Fluid	Impulsive Component	Lumped		Lumped		Lumped	
	Boundary Condition	Rigid		Rigid		Rigid	
Wall	Inertial Mass	Lumped		Distributed		Distributed	
	Wall Type	Flexible		Flexible		Flexible	
Analysis Method		Mode Superposition Method		Mode Superposition Method		Mode Superposition Method	
Schematic of Model							
Period (sec)		$T_1 = 0.2353$ $T_2 = 0$		$T_1 = 0.2956$ $T_2 = 0.08088$		$T_1 = 0.2923$ $T_2 = 0.07880$	
Damping Ratio		5%		5%		5%	
t_{max} (sec)		2.56	4.30	2.63	4.52	2.63	4.51
Base Shear F_B (KN)		789.960	423.840	433.800	312.840	405.960	262.320
Displacement d_A (mm)		34.73	18.63	34.54	24.97	33.24	21.54

Schematic labels:
- Model 1: $M_i + M_w = 99.694 \times 10^3$ Kg (Node 29), 5.040m, A, B
- Model 2: $M_i = 65.710 \times 10^3$ Kg, $M_i + m_w$ (Node 26), $H_w = 12.300$m, $h_i = 4.480$m, m_w, A, B
- Model 3: $M_i = 59.815 \times 10^3$ Kg, $M_i + m_w$ (Node 26), $H_w = 12.300$m, $h_i = 4.480$m, m_w, A, B

* t_{max} : the time when the peak values of dynamic response are reached

Table 7.2 Summary of Dynamic Response of Tall Liquid Storage Tank – Full Tank (continue)

		Model 4 (Proposed)		Model 5 (Proposed)		Model 6 (Proposed)	
Fluid	Impulsive Component	Distributed		Distributed		Distributed	
	Boundary Condition	Rigid		Flexible		Rigid	
Wall	Inertial Mass	Distributed		Distributed		Distributed	
	Wall Type	Flexible		Flexible		Rigid	
Analysis Method		Mode Superposition Method		Direct Step-by-Step Integration Method and Sequential Method		Direct Step-by-Step Integration Method and Sequential Method	
Schematic of Model							
Period (sec)		$T_1 = 0.3413$ $T_2 = 0.06365$		---		---	
Damping Ratio		5%		$\alpha=1.552, \beta=0.0027$		$\alpha=0, \beta=0$	
t_{max} (sec)		2.69	4.76	2.65	4.56	2.16	5.030
Base Shear F_B (KN)		314.760	290.040	318.956	338.111	283.977	202.946
Displacement d_A (mm)		32.68	30.11	23.04	26.90 (t=4.57sec)	0	0

* t_{max} : the time when the peak values of dynamic response are reached

77

As a second example, a shallow rectangular tank is analyzed to compare its response with that of the tall tank studied earlier. The dimensions of tank and parameters are:

$\rho_w = 2300 kg/m^3$ $\rho_l = 1000\ kg/m^3$ $E_c = 2.644 \times 10^4\ MPa$ $v = 0.17$

$L_x = 15\ m$ $H_w = 6.0\ m$ $H_l = 5.5\ m$ $t_w = 0.6\ m$

Figure 7.17 shows the finite element model. The same analysis procedure discussed before is first carried out. The analysis results are summarized in Table. 7.3. Time history of each model is shown in Figure 7.18-7.23.

Results of analysis show that the general trend in the behavior of the shallow tank is very similar to the tall tank. In particular a comparison in the results of time history of base shear between model 1 and 5 indicates that the values are significantly higher than Model 1. In this case, difference is 200% as compared to 230% observed in the tall tank.
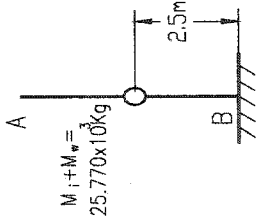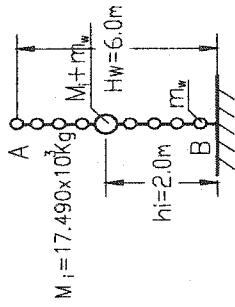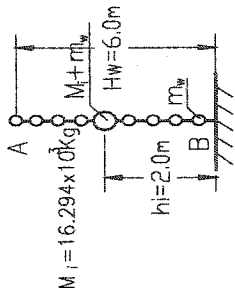
For the shallow tank, the results obtained from model 4 and model 5 are very similar. Further study shows that the hydrodynamic pressure is still amplified as a result of the flexibility of tank wall. But the maximum base shear during the entire time history does not increase as compared to the results obtained from model 4 based on rigid wall boundary condition. This is due to the hydrodynamic pressure applied as external forces in model 5. As the hydrodynamic pressure load is highly dependent on the flexibility of the wall in the model 5, the effect of the wall inertial forces during time history analysis may cancel the hydrodynamic pressure. Further research in this area could be carried out on it.

Under horizontal ground motion, the tank wall may develop cracking of concrete and yielding of reinforcement. As a result, the stiffness of the wall could be reduced considerably. For this reason, the tank wall is analyzed under different E_c values ranging from $E_c = E_0$ for the fully uncracked section up to $E_c = 0.1 E_0$. In this case, the concrete is expected to be totally damaged. It may be unrealistic to use such a small value of E_c for liquid containing structures. However, the results provide some useful information on how the flexible tank wall could behavior as compared to the more rigid walls.
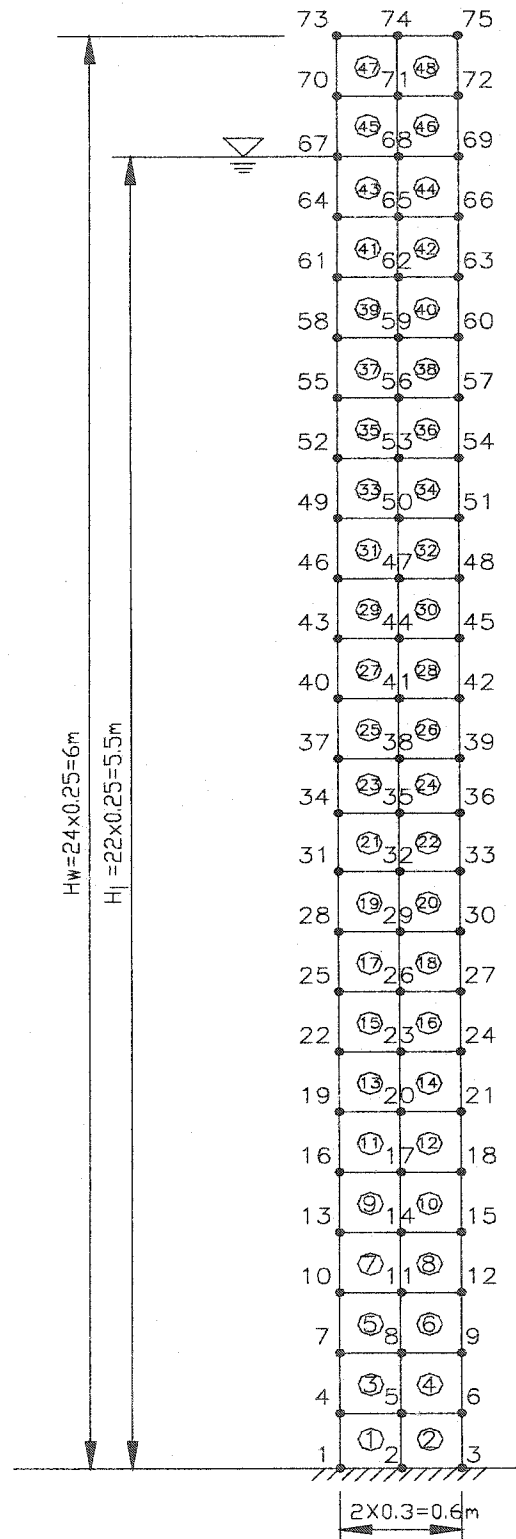
Figure 7.17 Finite Element Model – Shallow Tank

79

Table 7.3 Summary of Dynamic Response of Shallow Liquid Storage Tank – Full Tank

		Model 1 (Housner)			Model 2 (Housner)			Model 3 (Proposed same as Haroun)		
Fluid	Impulsive Component	Lumped			Lumped			Lumped		
	Boundary Condition	Rigid			Rigid			Rigid		
Wall	Inertial Mass	Lumped			Distributed			Distributed		
	Wall Type	Flexible			Flexible			Flexible		
Analysis Method		Mode Superposition Method			Mode Superposition Method			Mode Superposition Method		
Schematic of Model										
Period (sec)		$T_1 = 0.1055$ $T_2 = 0$			$T_1 = 0.1217$ $T_2 = 0.03503$			$T_1 = 0.1208$ $T_2 = 0.03430$		
Damping Ratio		5%			5%			5%		
t_{max} (sec)		2.51	3.54	4.54	2.65	3.55	5.06	2.65	3.55	5.06
Base Shear F_B (KN)		153.240	151.740	142.920	121.500	106.800	97.140	113.880	99.540	92.400
Moment M_B (KNm)		372.934	369.259	347.825	381.542	335.380	305.014	362.927	317.254	294.355
Displacement d_A (mm)		5.085	5.036	4.743	6.933	6.093	5.541	6.649	5.812	5.392

* t_{max} : the time when the peak values of dynamic response are reached

Table 7.3 Summary of Dynamic Response of Shallow Liquid Storage Tank – Full Tank (continue)

		Model 4 (Proposed)			Model 5 (Proposed)			Model 6 (Proposed)		
Fluid	Impulsive Component	Distributed			Distributed			Distributed		
	Boundary Condition	Rigid			Flexible			Rigid		
Wall	Inertial Mass	Distributed			Distributed			Distributed		
	Wall Type	Flexible			Flexible			Rigid		
Analysis Method		Mode Superposition Method			Direct Step-by-Step Integration Method and Sequential Method			Direct Step-by-Step Integration Method and Sequential Method		
Schematic of Model										
Period (sec)		$T_1 = 0.1476$ $T_2 = 0.02798$			---			---		
Damping Ratio		5%			$\alpha = 3.579,\ \beta = 0.0012$			$\alpha = 0,\ \beta = 0$		
t_{max} (sec)		2.69	3.59	4.95	2.28	3.57	4.56	2.16	3.40	4.87
Base Shear F_B (KN)		73.200	78.900	74.340	78.662	54.552	64.566	74.485	49.171	59.384
Moment M_B (KNm)		278.159	299.950	282.443	241.836	167.795	179.155	179.506	119.208	143.040
Displacement d_A (mm)		5.480	5.908	5.564	4.544	3.153	3.245	0	0	0

* t_{max} : the time when the peak values of dynamic response are reached

81

(a) Displacement (Top)

(b) Base Shear

(c) Base Moment

Figure 7.18 Dynamic Response of Shallow Tank – Model 1
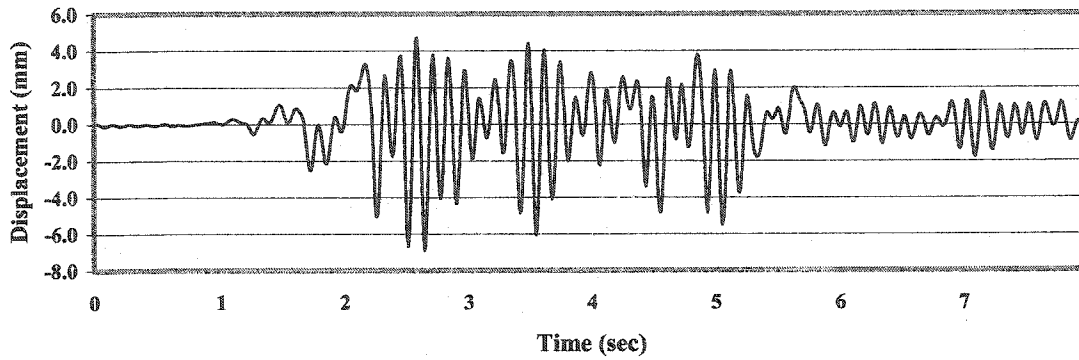
(a) Displacement (Top)
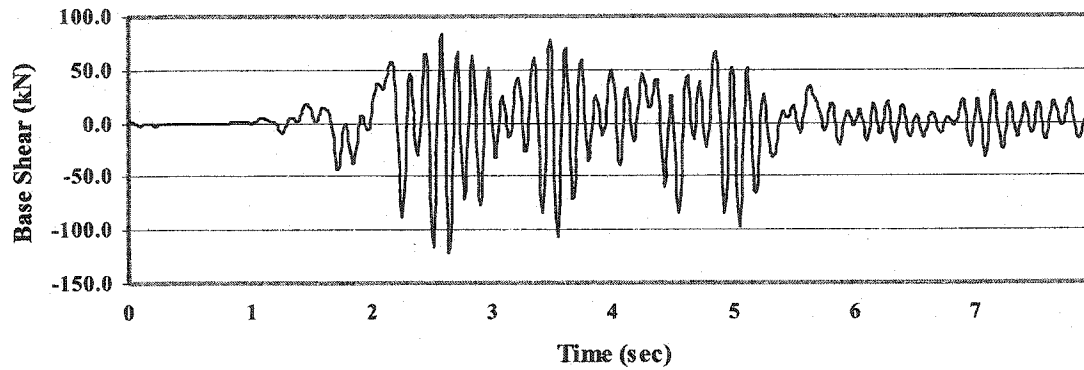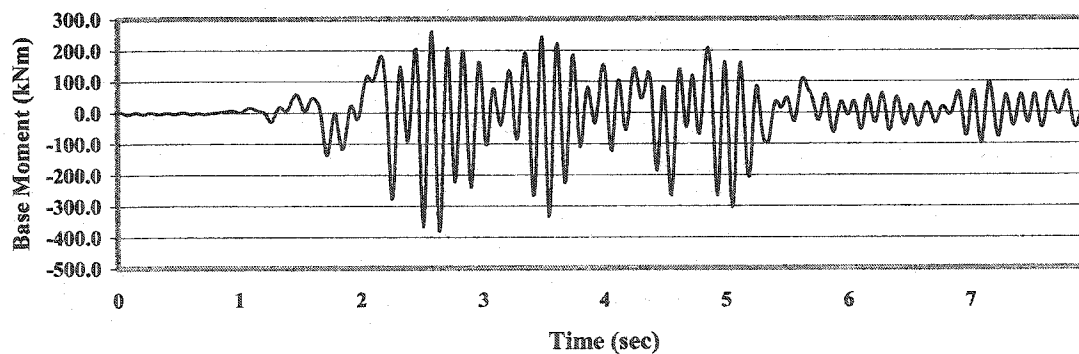
(b) Base Shear

(c) Base Moment

Figure 7.19 Dynamic Response of Shallow Tank – Model 2
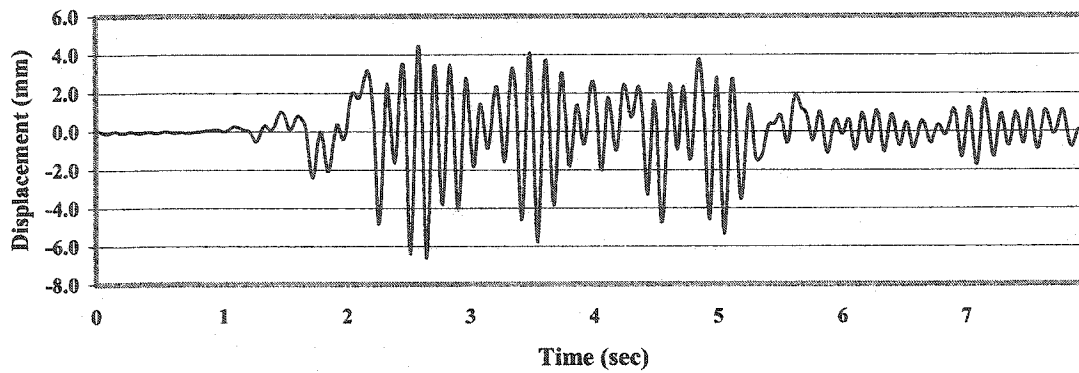
(a) Displacement (Top)
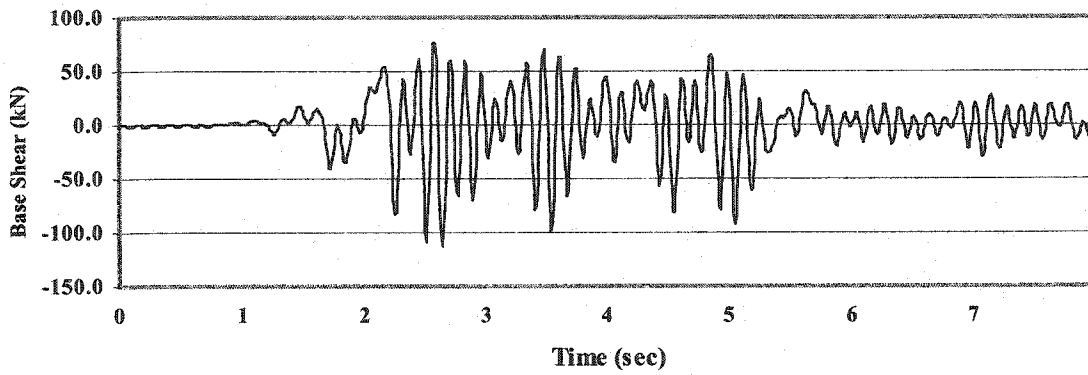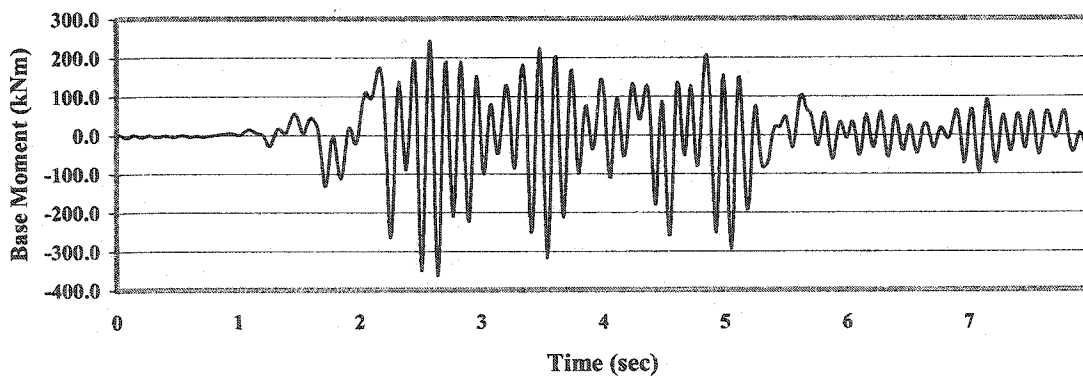
(b) Base Shear

(c) Base Moment

Figure 7.20 Dynamic Response of Shallow Tank - Model 3
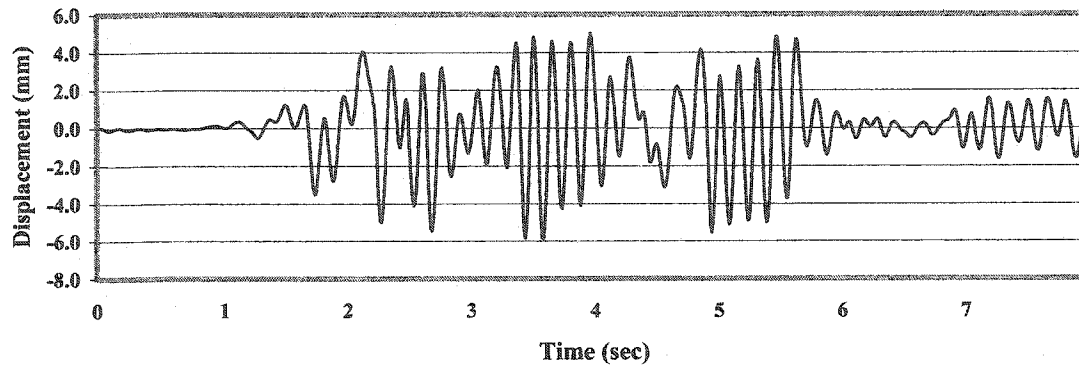
(a) Displacement (Top)
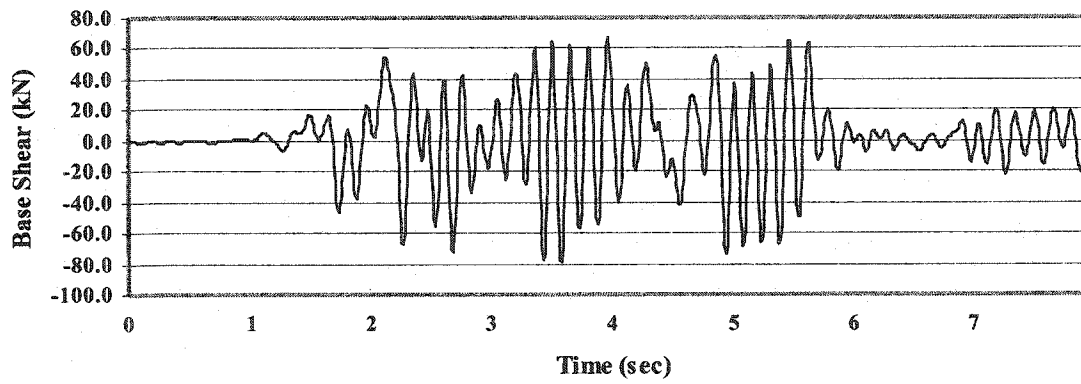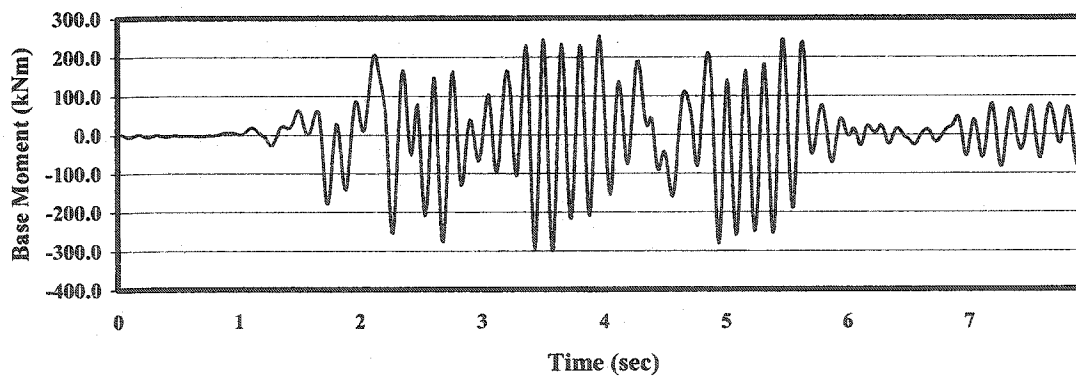
(b) Base Shear

(c) Base Moment

Figure 7.21 Dynamic Response of Shallow Tank - Model 4
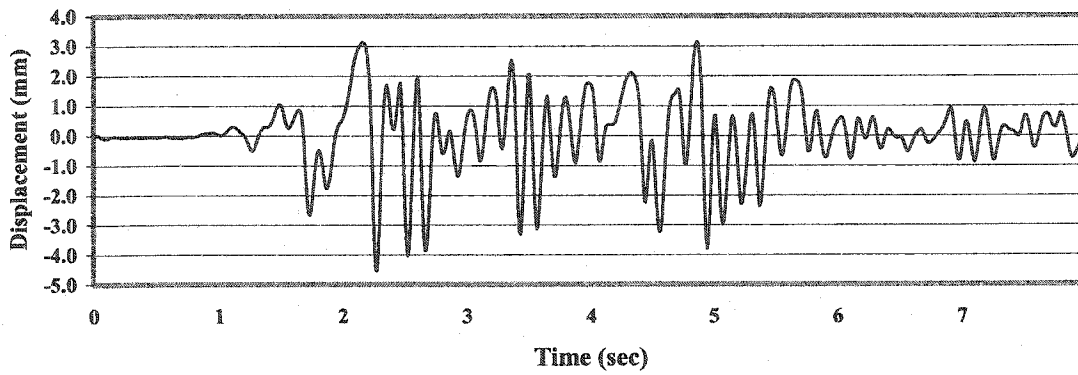
(a) Displacement (Top)
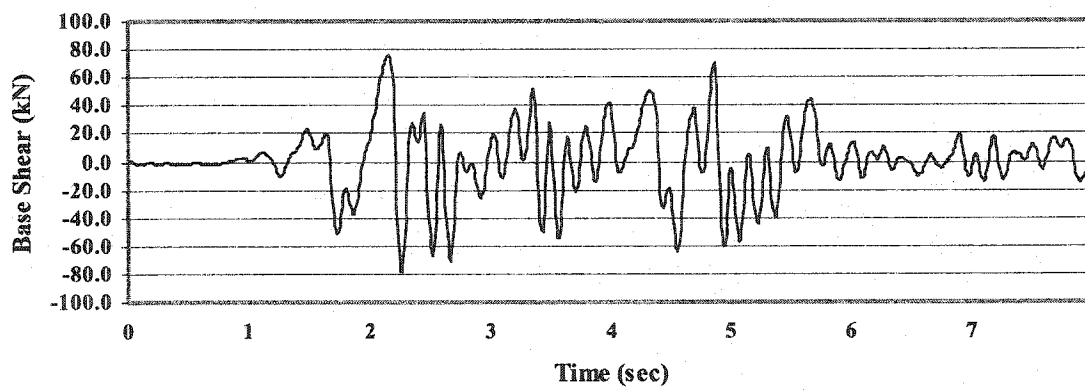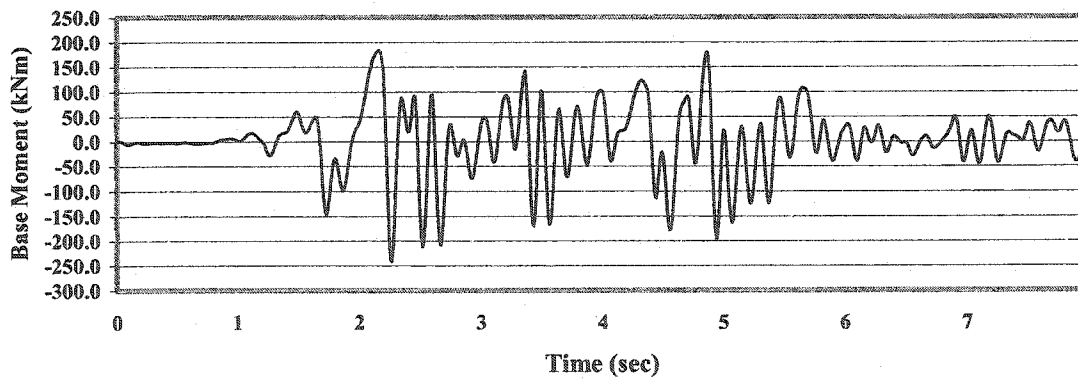
(b) Base Shear
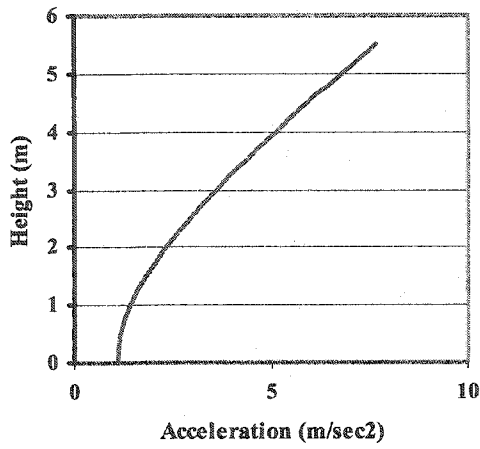
(c) Base Moment
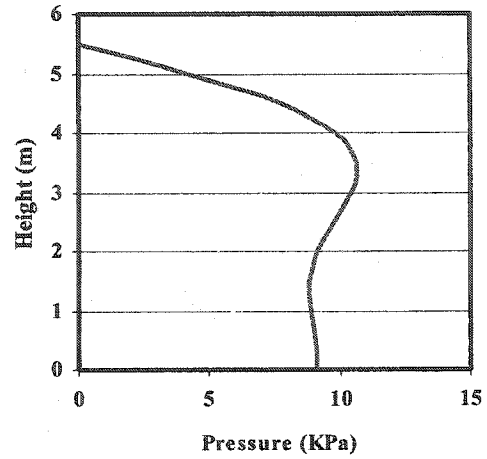
(d) Wall Acceleration   (e) Hydrodynamic Pressure

Figure 7.22 Dynamic Response of Shallow Tank - Model 5
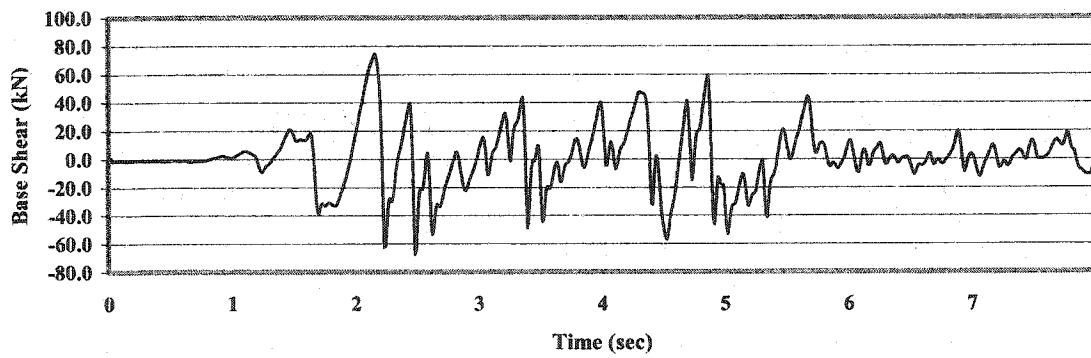
(a) Base Shear
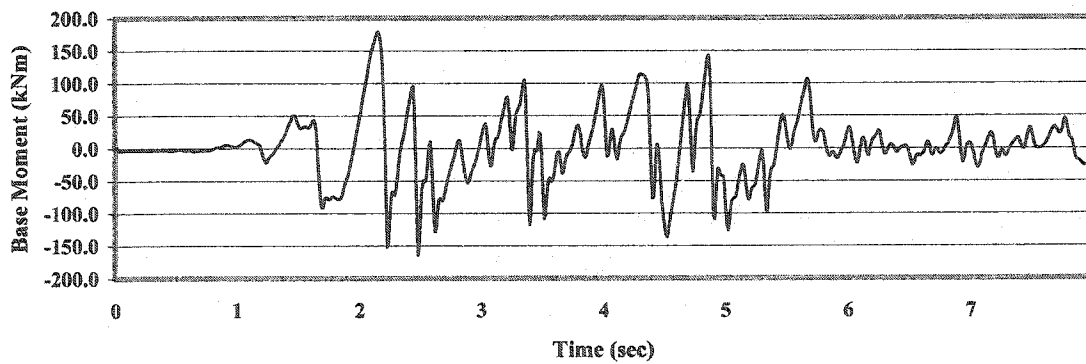
(b) Base Moment
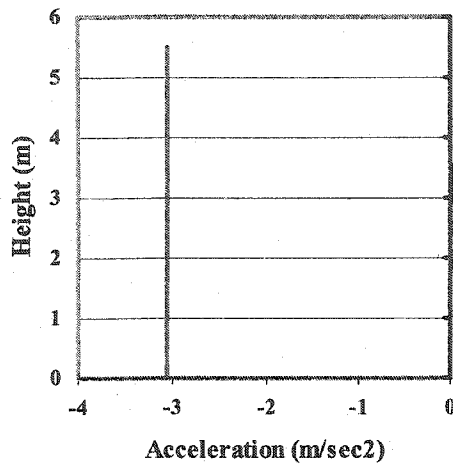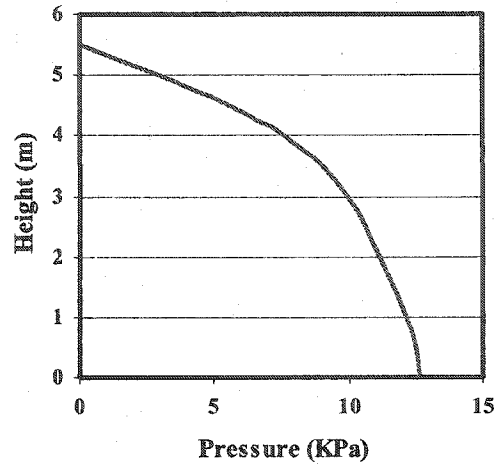
(c) Wall Acceleration   **(d) Hydrodynamic Pressure**

Figure 7.23 Dynamic Response of Shallow Tank - Model 6

The values of modules of elasticity of concrete, Poisson's ratio and the shear modules used for this study are listed in Table 7.4. The value of modules of elasticity is in proportion to the initial value for the uncracked section. The Poisson ratio v is constant and the shear modulus is calculated using the following relationship:

$$G = \frac{E_c}{2(1+v)}$$ (7.3)

Table 7.4 Different Modulus of Elasticity of Concrete

E_c / E_0	1	0. 8	0.6	0.4	0.2	0.1
$E_c \,(\times 10^4 \text{MPa})$	2.644	2.0776	1.586	1.058	0.529	0.264
v	0.17	0.17	0.17	0.17	0.17	0.17
$G \,(\times 10^4 \text{MPa})$	1.130	1.126	0.678	0.452	0.226	0.113

The summarized calculation results in terms of different E_c values are shown in Table 7.5. The maximum base shear F_B, base moment M_B and top displacement d_A are listed. Figures 7.24-7.28 show the time history response of these tanks. For the case of

$E_c = E_0$, the results are presented in earlier part. The direct step-by-step integration method and the sequential method (Model 5) are used in the dynamic analysis. The damping ratio is calculated based on the first two modes of vibration, which are obtained using the mode superposition method.

Table 7.5 Effect of Variation of Modulus of Elasticity of Concrete on Response

E_c/E_0		1	0.8	0.6	0.4	0.2	0.1
Freq. (1/sec)	f_1 (T_1)	6.78 (0.148)	6.01 (0.166)	5.25 (0.191)	4.29 (0.233)	3.03 (0.330)	2.14 (0.467)
(Period) (sec)	f_2 (T_2)	35.74 (0.028)	31.92 (0.031)	27.68 (0.036)	22.61 (0.044)	15.99 (0.063)	11.29 (0.089)
f_i/f_{io} (i=1,2)		1	0.89	0.78	0.63	0.45	0.32
Damping Ratio	α	3.579	3.179	2.772	2.264	1.601	1.131
	β	0.0012	0.0013	0.0015	0.0019	0.0026	0.0037
t_{max1}(sec)		2.28	2.28	2.30	2.56	2.64	5.10
F_B (kN)		78.662	79.685	84.514	86.338	91.884	98.780
t_{max2}(sec)		2.28	2.28	2.29	2.56	2.64	5.10
M_B (kNm)		241.836	248.573	259.463	271.826	257.726	311.475
t_{max3}(sec)		2.28	2.28	2.29	2.55	2.35	5.10
d_A (mm)		4.544	5.976	8.160	12.87	24.08	59.18

Figure 7.29 shows plots of the normalized response with respect to E_0. In order to reflect the dynamic response of the full tank system more precisely, the normalized response of these tanks can also be presented in the response spectrum form. The normalized natural frequencies of tanks with respect to f_o for the variable flexibility are used in the x coordinate as well. Both the first and the second natural frequency have the

same proportion to f_0 of which the tank has the modulus elasticity equal to E_0. Similar graphs are shown for base shear and moment.

Figure 7.29 shows that the natural frequencies of vibration decrease when the tank wall becomes more flexible. However, the base shears and moments increase with the increase of flexibility of tank wall. For the case $E_c = 0.2E_0$, the base moment decrease as compared to $E_c = 0.4E_0$, but the base shear still increase. This could be due to the higher mode effect as will be seen later.

Figure 7.30 shows the acceleration and impulsive pressure distribution along the tank wall when the maximum base shear is reached. Figure 7.30(a) indicates that as the flexibility of tank wall increases, the acceleration along the height of tank wall increases. Figure 7.30(b) shows the increase in impulsive pressure distribution with the increase of the flexibility of the tank wall.

Comparing all the cases, there is special case for $E_c = 0.2E_0$. In this case the wall acceleration reduced towards the top of tank wall. This could be due to the high mode effects as mentioned earlier. As the horizontal ground acceleration is still higher than those of others at the time when the maximum base shear is reached, the hydrodynamic pressure still increases. But the relative acceleration along the height of tank wall is small. Therefore the effect of flexibility of tank wall is not as significant as those of others. It also means that the input time history of earthquake has effect on the time history of hydrodynamic pressure load.
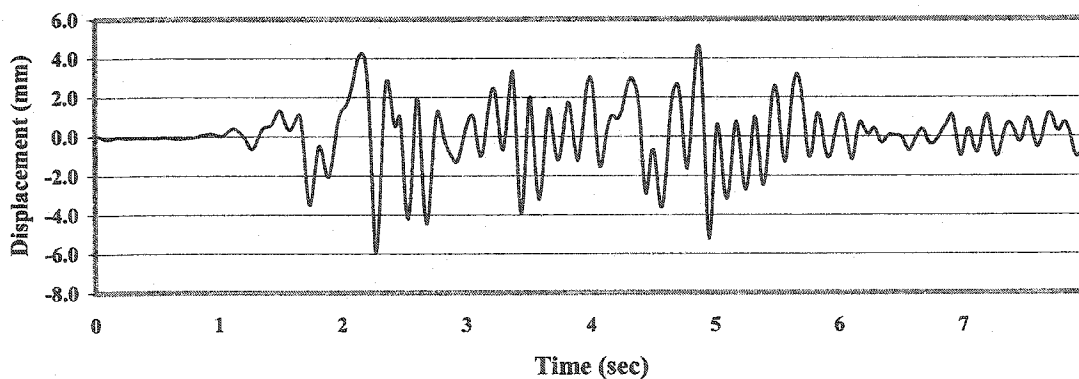
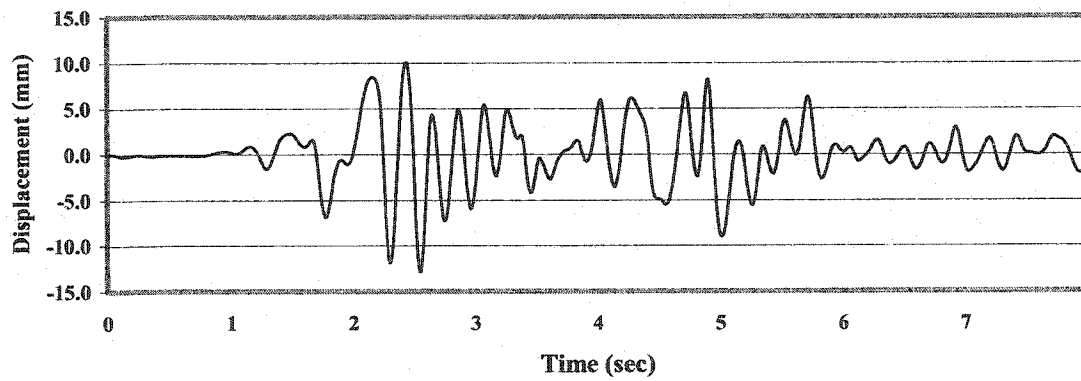(a) Displacement (Top)
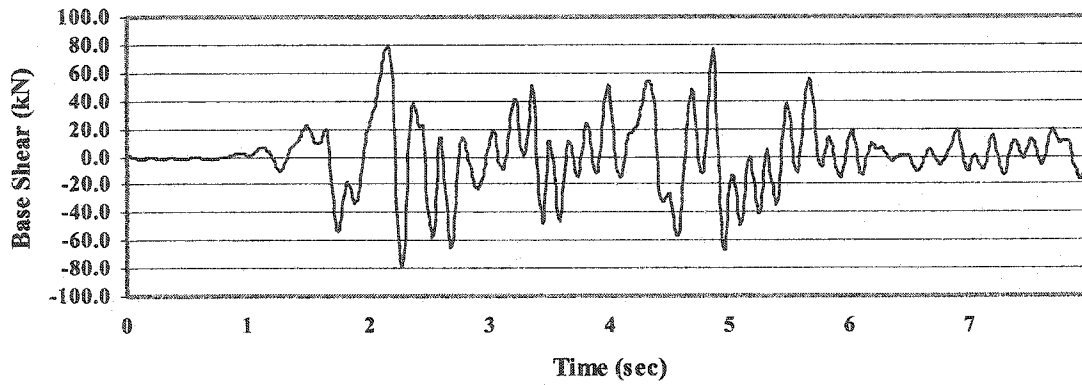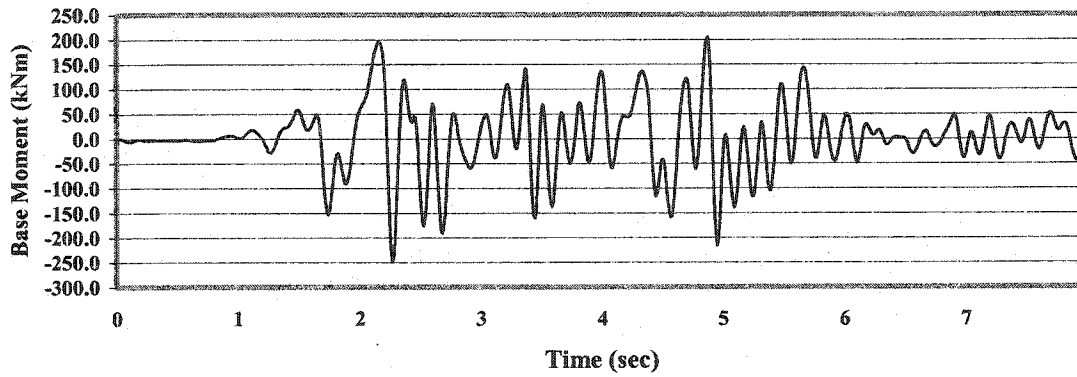
(b) Base Shear
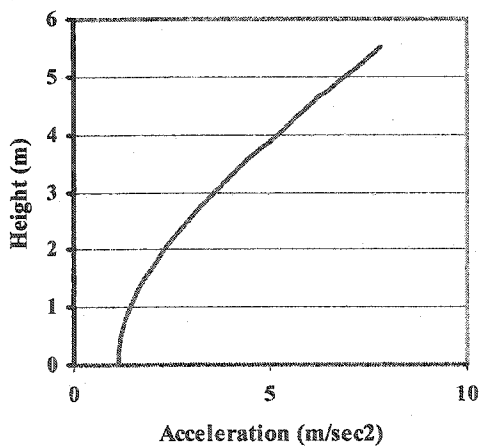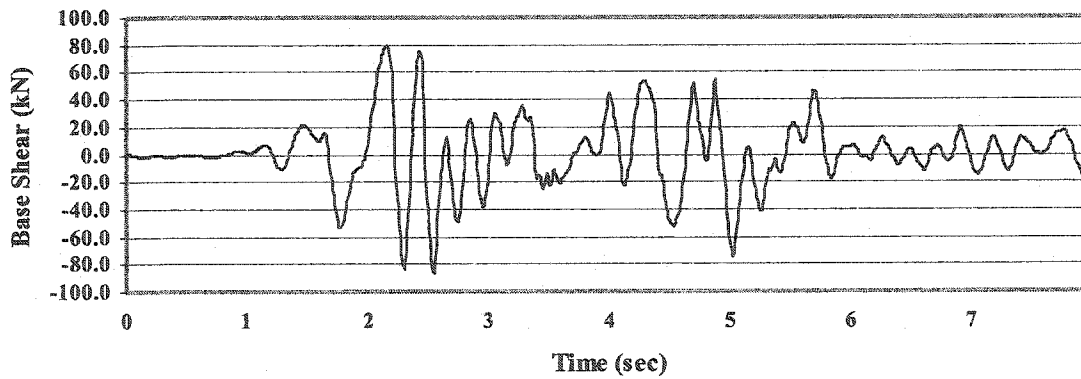

(c) Base Moment

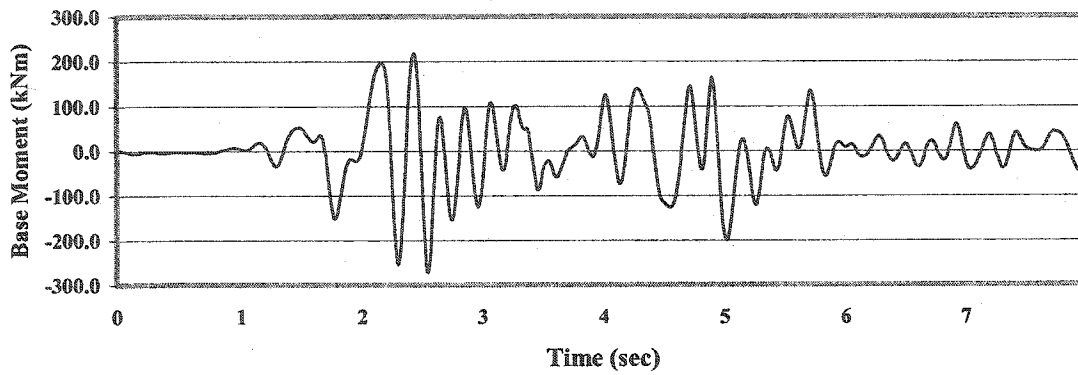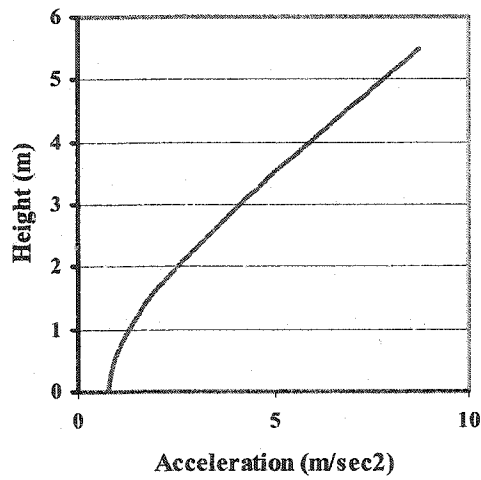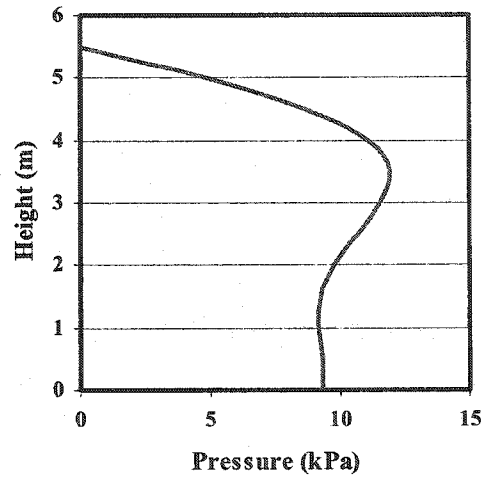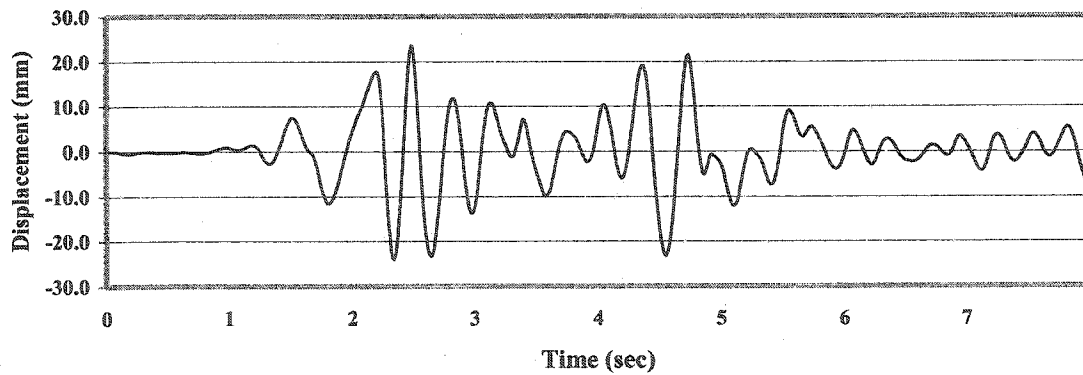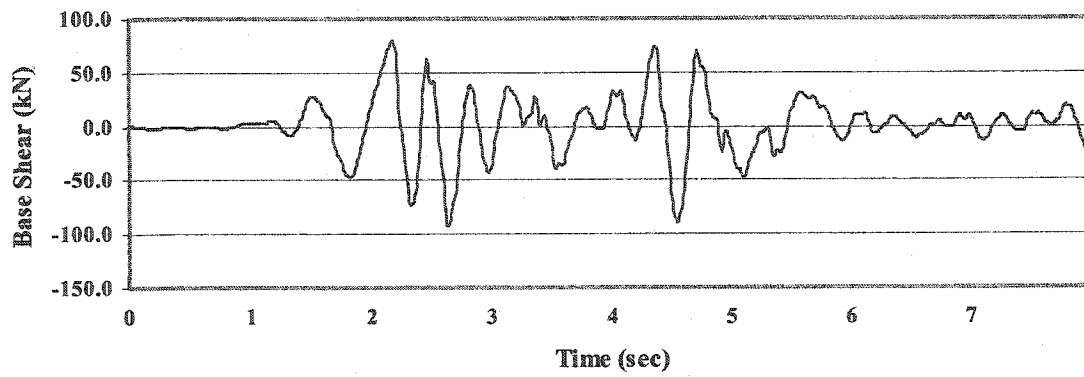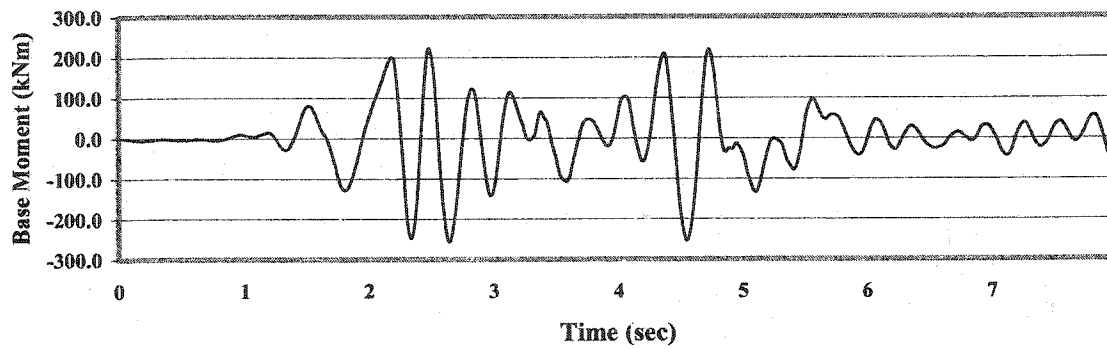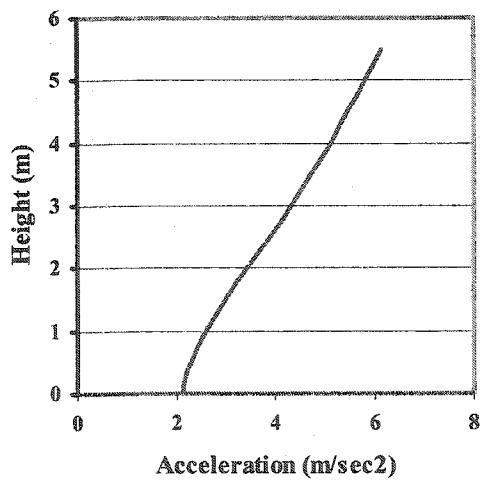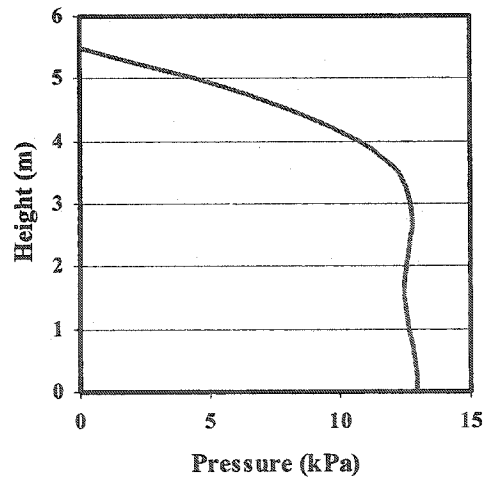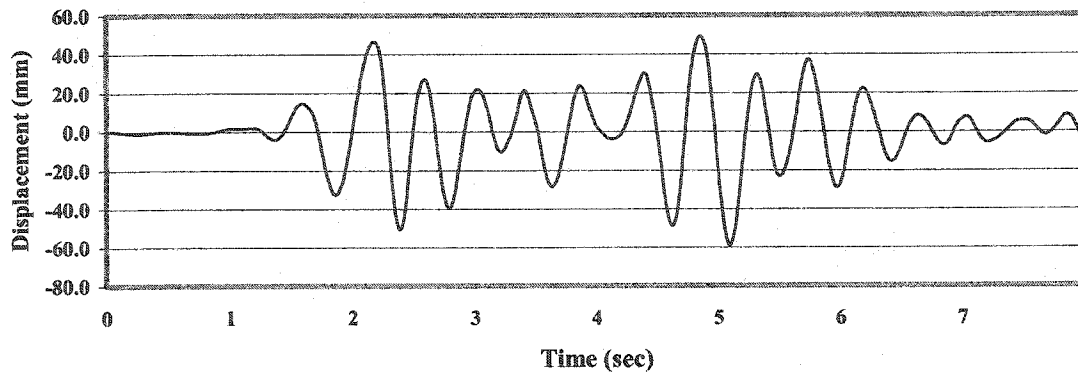(d) Wall Acceleration
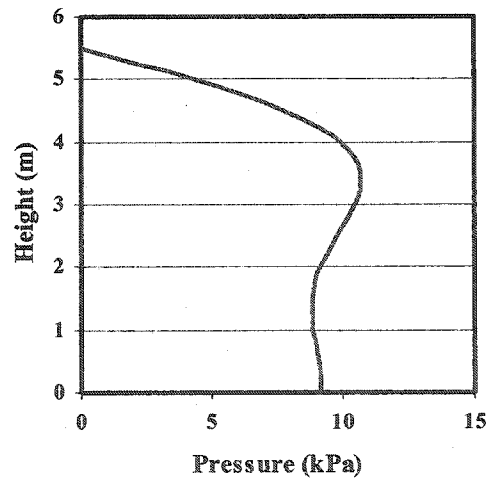
(e) Hydrodynamic Pressure

Figure 7.24 Dynamic Response of Shallow Tank - $E_c=0.8E_0$
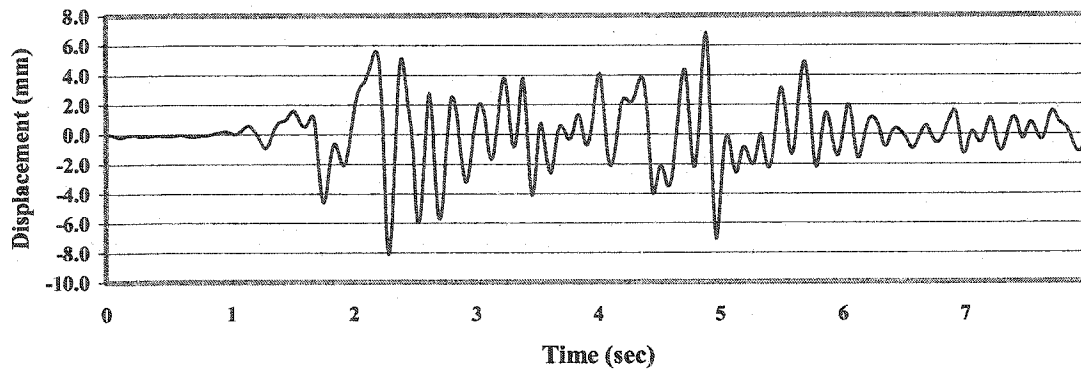
(a) Displacement (Top)
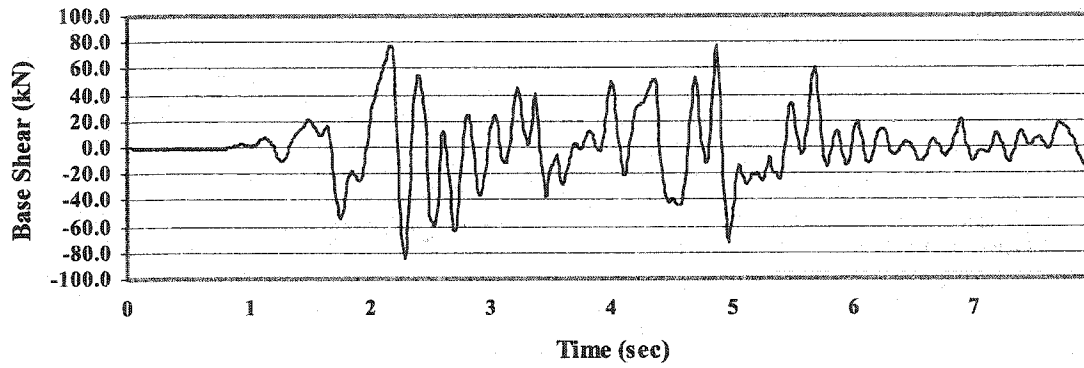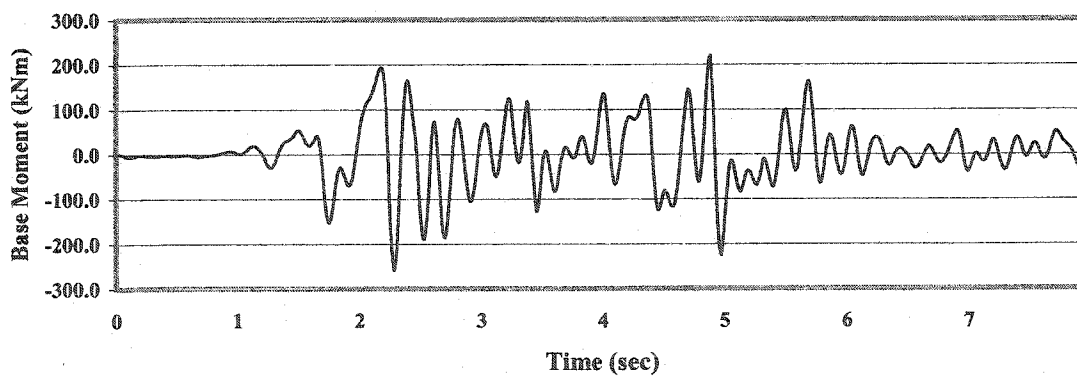
(b) Base Shear
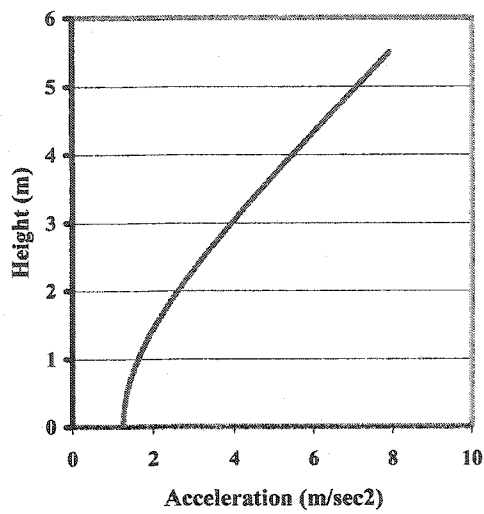
(c) Base Moment

(d) Wall Acceleration
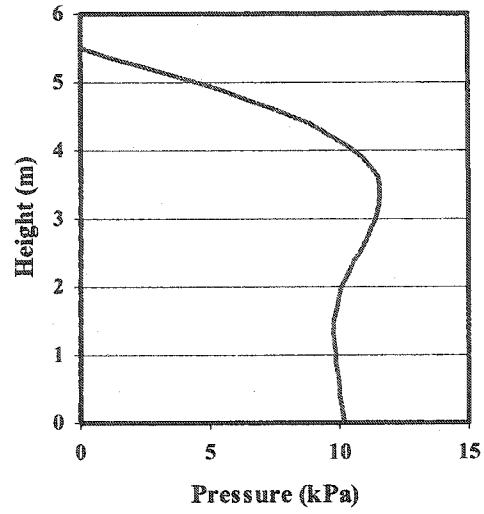
(e) Hydrodynamic Pressure

Figure 7.25 Dynamic Response of Shallow Tank - E_c=0.6E_0

(a) Displacement (Top)

(b) Base Shear

(c) Base Moment

(d) Wall Acceleration

(e) Hydrodynamic Pressure

Figure 7.26 Dynamic Response of Shallow Tank - $E_c=0.4E_0$

(a) Displacement (Top)

(b) Base Shear

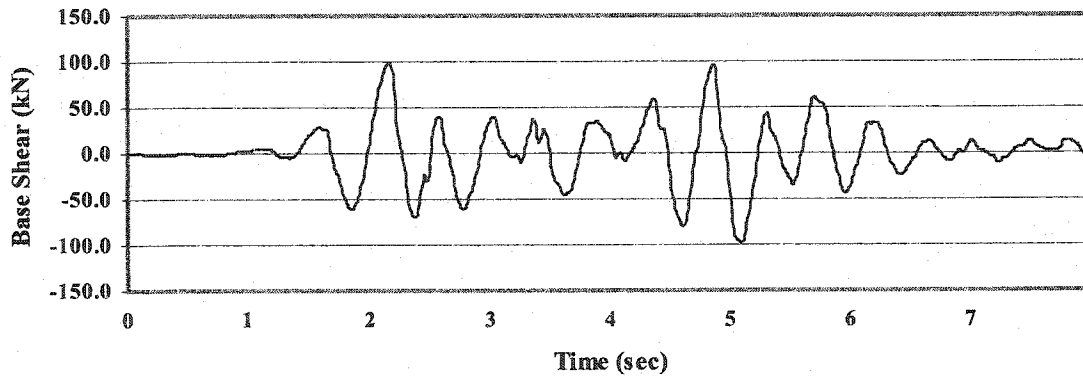

(c) Base Moment

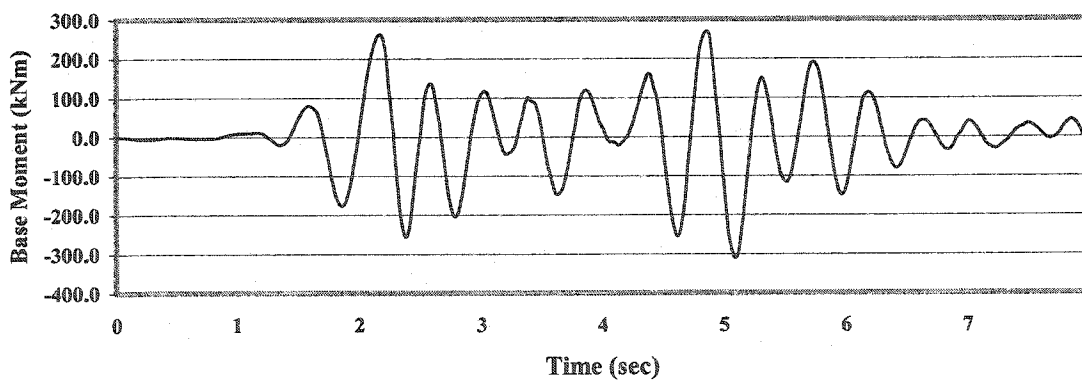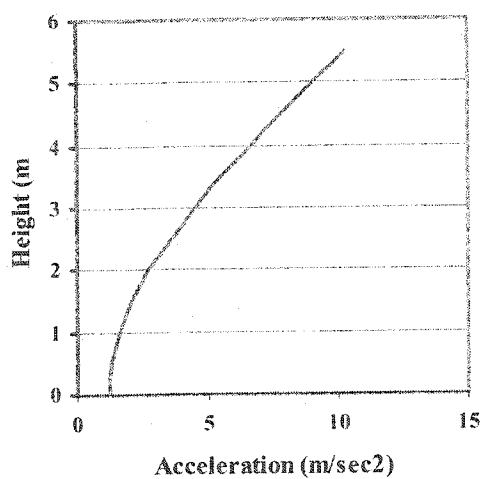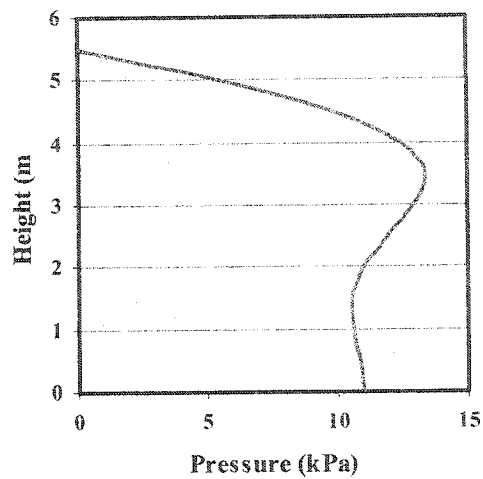(d) Wall Acceleration

(e) Hydrodynamic Pressure

Figure 7.27 Dynamic Response of Shallow Tank - $E_c=0.2E_0$

(a) Displacement (Top)
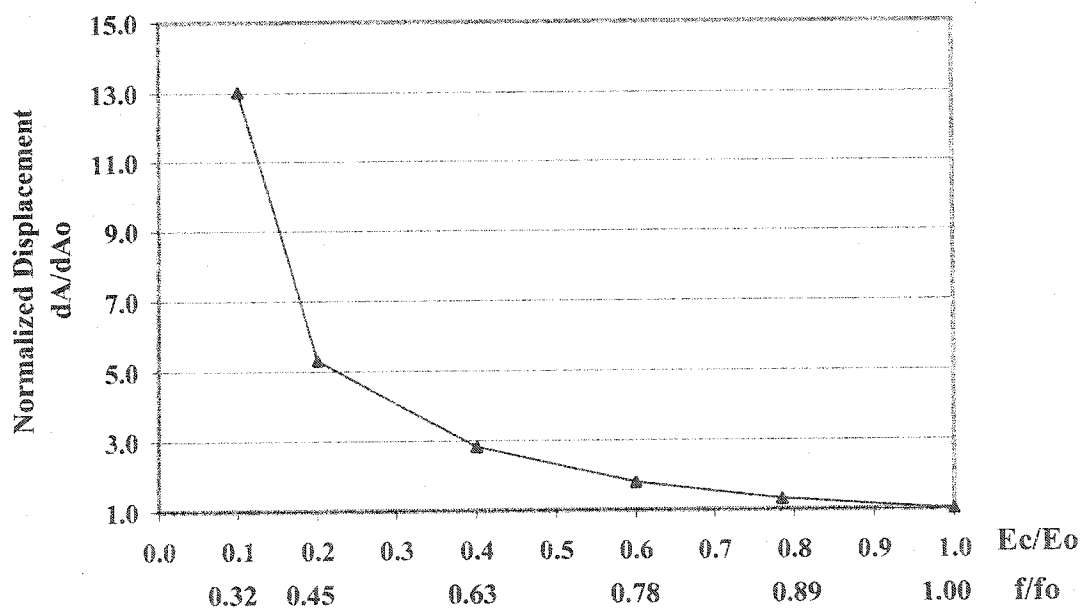

(b) Base Shear

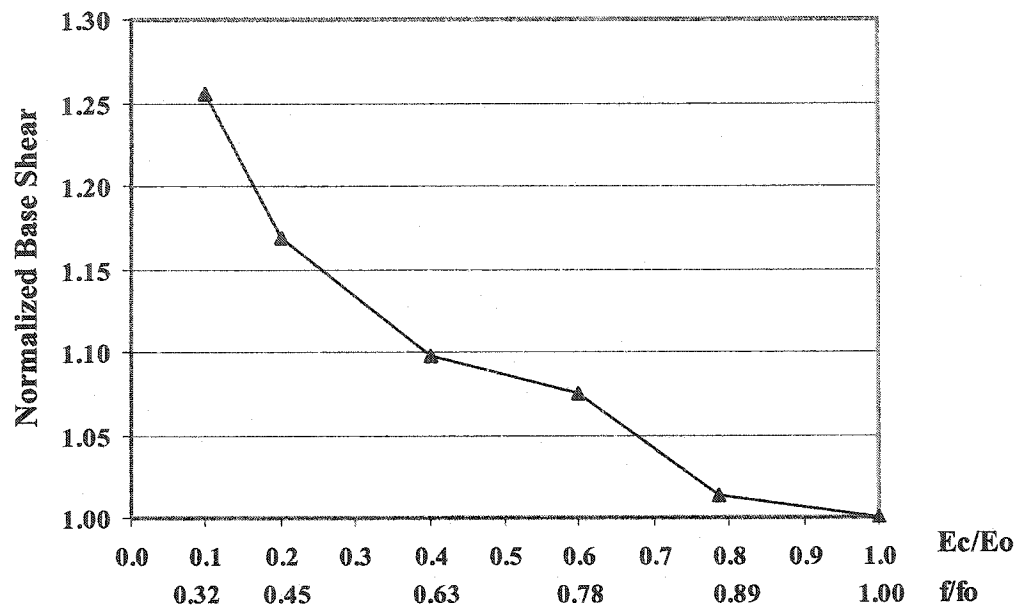

(c) Base Moment

(d) Wall Acceleration

(e) Hydrodynamic Pressure

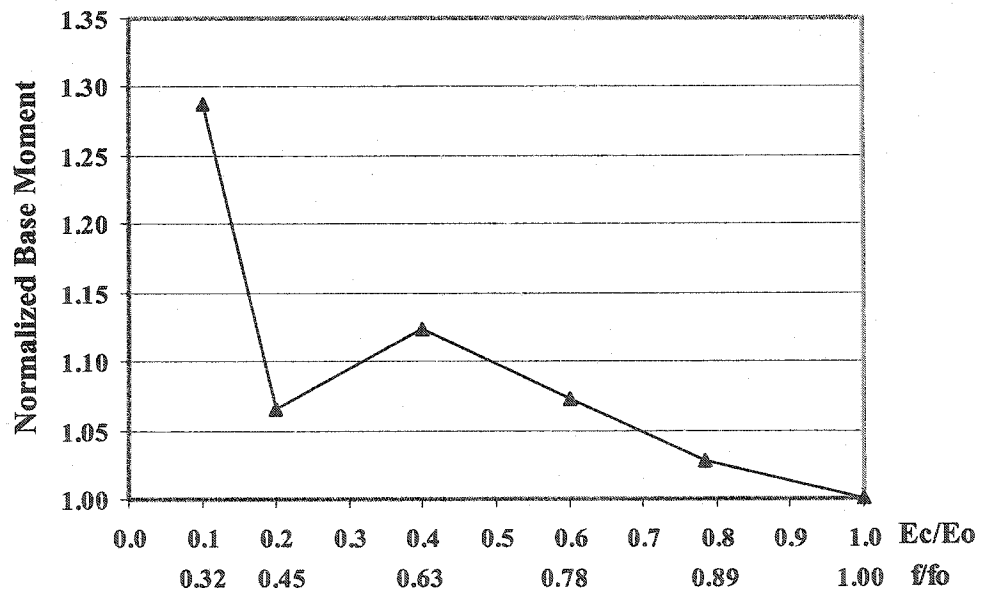**Figure 7.28 Dynamic Response of Full Shallow Tank - $E_c=0.1E_0$**

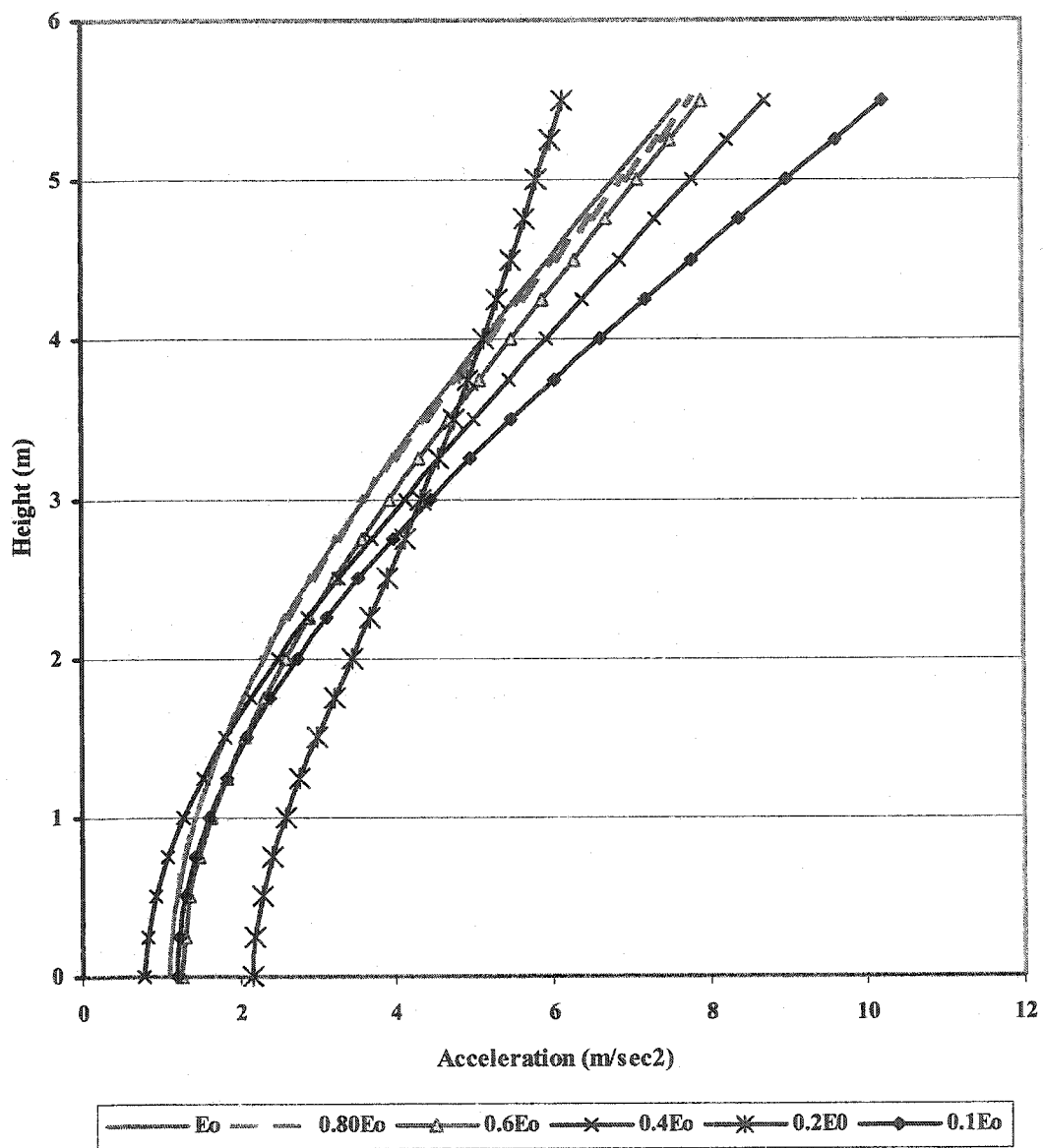
(a) Normalized Displacement Spectrum

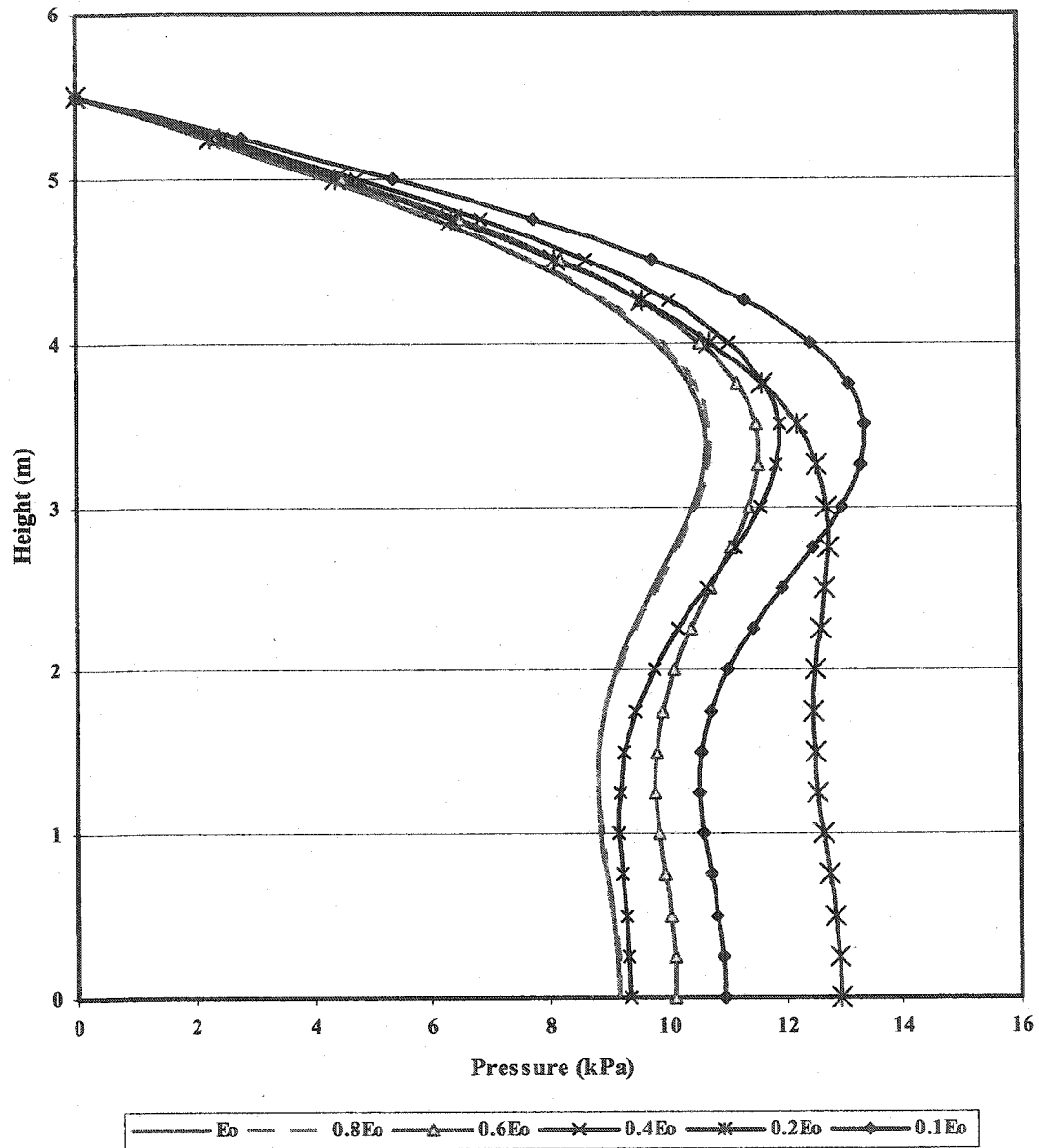**(b) Normalized Base Shear Spectrum**

(c) Normalized Base Moment Spectrum

**Figure 7.29 Effect of Flexibility of Tank Wall on Response**

(a) Wall Acceleration

(b) Hydrodynamic Pressure

Figure 7.30 Dynamic Response of Tank Wall and Impulsive
Pressure Distribution for Different E_c

7.3.2 Vertical Ground Motion

Two different vertical ground motions are used in this investigation. One is the El Centro Earthquake 1940. The horizontal component of this record was used earlier in this chapter. The second ground motion record is Northridge Earthquake 1994. Past earthquakes show that the maximum amplitude of the vertical component of ground acceleration can be significant, especially near the center of the earthquake (Collier and Elnashai, 2001). In order to study this kind of earthquake, Northridge Earthquake 1994 is chosen for the analysis. The vertical accelerograms of these two earthquakes are shown in Figures 7.31 and 7.32 respectively.
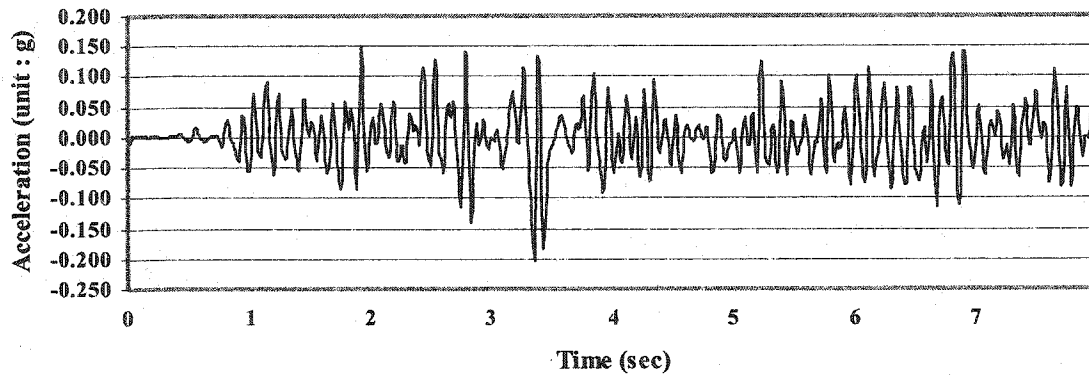

Figure 7.31 Vertical Component of El Centro Accelerogram (0-8sec):

1940 Imperial Valley Earthquake
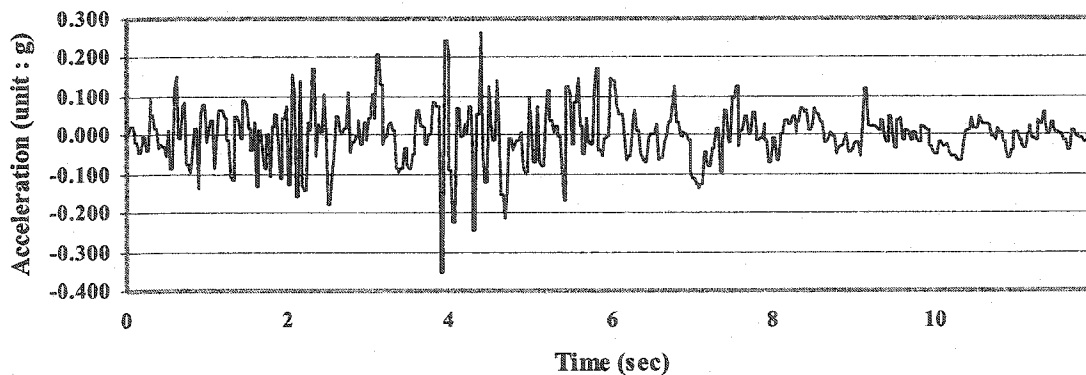
Figure 7.32 Vertical Component of Northridge Accelerogram (0-12sec):
1994 Northridge Earthquake

The dynamic response of liquid storage tanks subjected to the vertical ground motion is analyzed on the basis of theory presented in Chapter 5. Only horizontal hydrodynamic pressure induced by the vertical acceleration is considered. The horizontal dynamic response of liquid storage tanks subjected to vertical ground motion is analyzed.

Two models are used for the dynamic analysis. The first model is to analyze dynamic response of liquid storage tanks using the added mass method as shown in Figure 7.33(a). The part of hydrodynamic pressure induced by the vertical acceleration, which is equal to $p = \rho_l (H - y)\ddot{v}(t)$, is represented by the added mass $m_i(y)$. It is distributed along the tank wall. A rigid wall boundary condition is used in the hydrodynamic pressure calculation. The second model is analyzed using the combination of the added mass method and the sequential method as demonstrated in Figure 7.33(b). The added mass method which is the same as Model 1 considers the hydrodynamic pressure induced by the vertical ground acceleration, and the sequential method considers the flexibility of the tank wall in the horizontal direction. Basically Model 2 should provide more accurate results than Model 1.

(a) Model 1   (b) Model 2
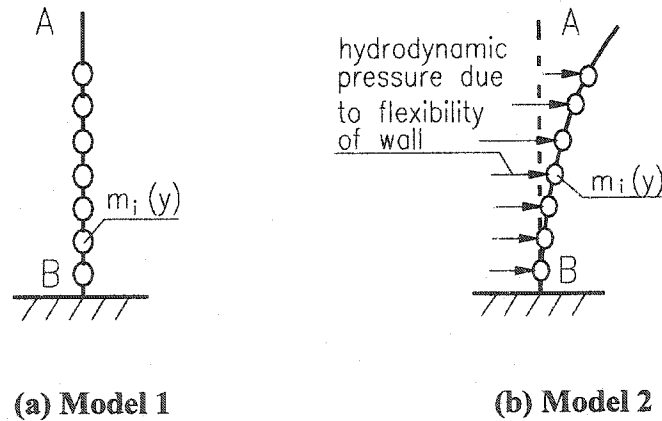
Figure 7.33 Two Models Used in the Vertical Ground Motion Calculation

Both the tall tank and the shallow tank used previously are analyzed in this study. Table 7.6 shows summary of analysis results for the different size of tanks in the different

vertical ground motions. The damping ratio is 5% for Model 1. For Model 2, the Rayleigh damping is used. The first two natural periods of liquid storage system are calculated from Model 1. The maximum dynamic responses of liquid storage tanks under vertical ground motion are listed.

It can be found that the displacement, base shear and base moment calculated using Model 2 can be either larger or smaller than those from Model 1. The reason of such phenomenon is that there are two motions resulting in the horizontal movement of flexible tank wall when the tank is subjected to the vertical ground motion. One follows the vertical ground motion, and another is horizontal motion due to the flexibility of tank wall. As the natural frequencies of these two motions are far apart from each other, the consequence of these two motions is like damping effect on each other.

The time history responses of the liquid storage tanks subjected to the vertical ground motion are shown in Figures 7.34-7.41. They are obtained through either Model 1 or Model 2. In addition, mode shape of tank wall and the corresponding distribution of hydrodynamic of Model 2 at the peak value are also demonstrated.

The time history diagrams show the responses obtained from Model 1 and Model 2 are significantly different. This is because of consideration of flexibility of tank wall as discussed before. In the diagrams of hydrodynamic pressure distribution (Figures 7.35(d), 7.37(d), 7.39(d), 7.41(d)) the hydrodynamic pressure induced by the vertical ground acceleration is demonstrated in the form of solid line. The amplitude of hydrodynamic pressure due to the flexibility of tank wall is in the form of dash curve. The total increase or decrease of hydrodynamic pressure due to the vertical ground motion is obtained by the sum of these two pressures.

Table 7.6 Summary of Dynamic Response of Liquid Storage Tanks due to Vertical Ground Motions

Earthquake Record	Model Number	Tall Tank			Shallow Tank		
		Displacement d_A (mm)	Base Shear F_B (kN)	Base Moment M_B (kNm)	Displacement d_A (mm)	Base Shear F_B (kN)	Base Moment M_B (kNm)
1940 El Centro Earthquake	Model 1	5.35	73.72	462.68	2.38	49.68	152.69
	Model 2	3.45	123.30	402.60	1.03	35.40	74.36
1994 Northridge Earthquake	Model 1	14.28	196.68	1234.25	2.07	43.19	132.73
	Model 2	5.52	116.02	516.48	1.38	51.38	99.60
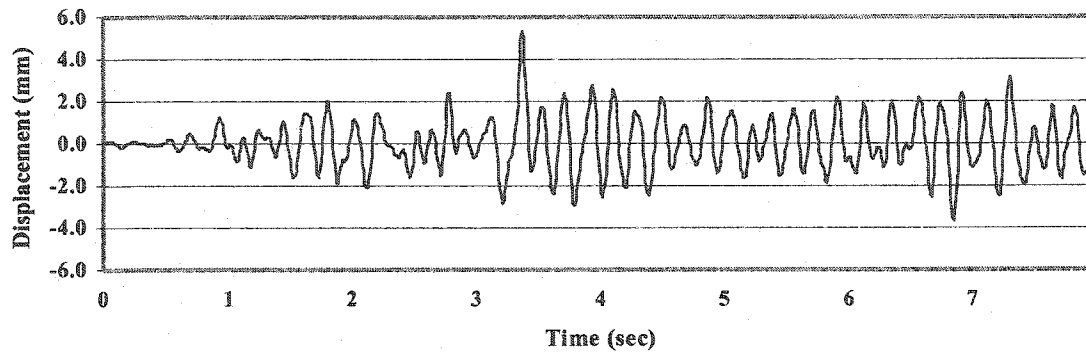
(a) Displacement (Top)
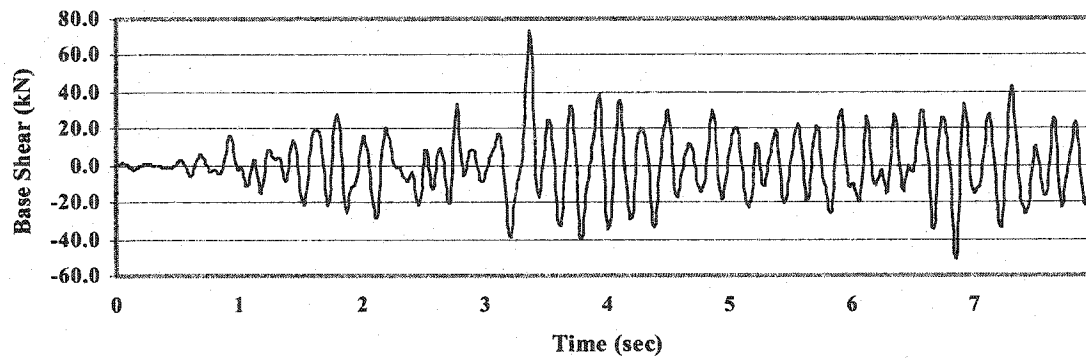
(b) Base Shear

(c) Base Moment

Figure 7.34 Dynamic Response of Tall Tank due to Vertical Ground Motion

– Model 1 (1940 El Centro Earthquake)

(a) Displacement (Top)

(b) Base Shear

(c) Base Moment

(d) Hydrodynamic Pressure

(e) Acceleration of Wall

Figure 7.35 Dynamic Response of Tall Tank due to Vertical Ground Motion
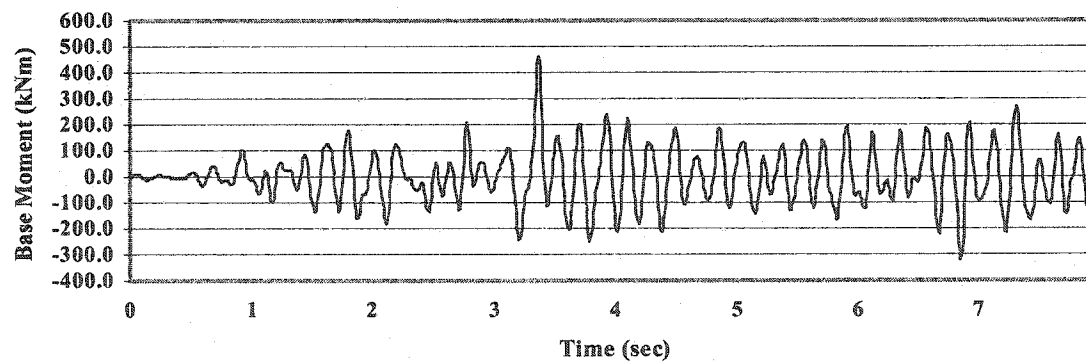
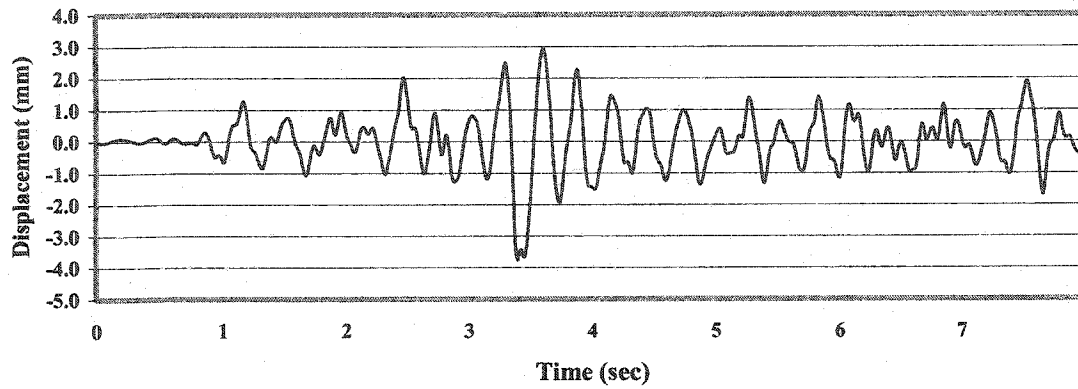– Model 2 (1940 El Centro Earthquake)

(a) Displacement (Top)

(b) Base Shear

(c) Base Moment

Figure 7.36 Dynamic Response of Shallow Tank due to Vertical Ground Motion

- Model 1 (1940 El Centro Earthquake)

(a) Displacement (Top)

(b) Base Shear

(c) Base Moment

109

(d) Hydrodynamic Pressure

(e) Acceleration of Wall

Figure 7.37 Dynamic Response of Shallow Tank due to Vertical Ground Motion
– Model 2 (1940 El Centro Earthquake)
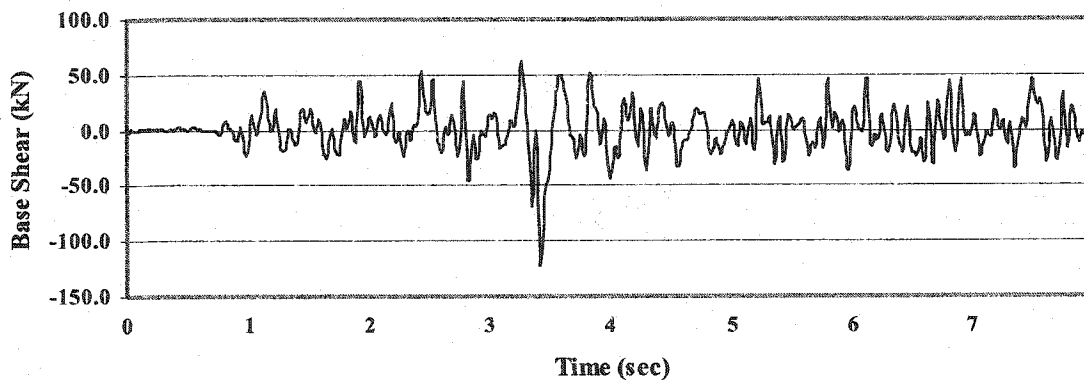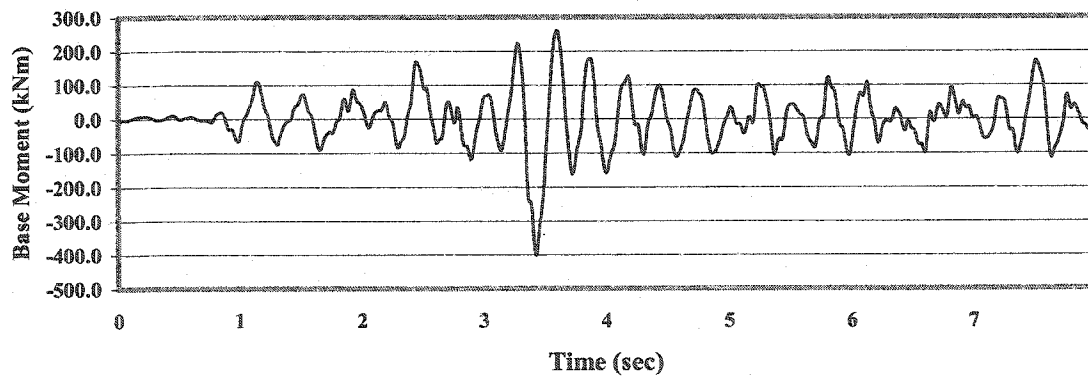
(a) Displacement (Top)
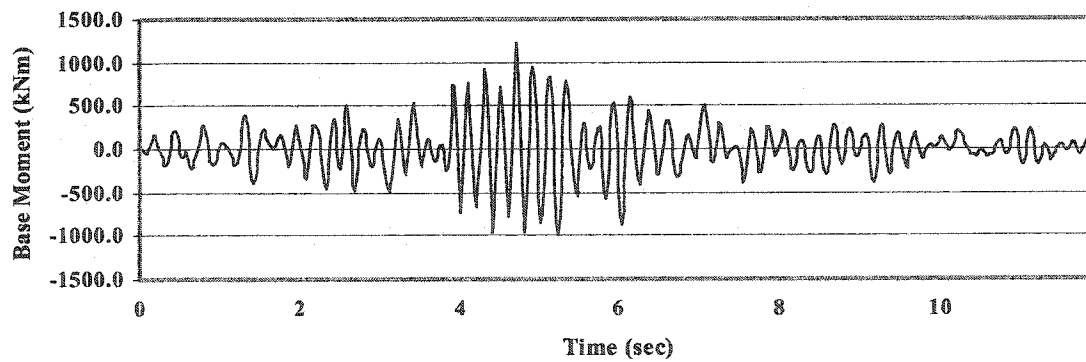
(b) Base Shear

(c) Base Moment

Figure 7.38 Dynamic Response of Tall Tank due to Vertical Ground Motion
— Model 1 (1994 Northridge Earthquake)
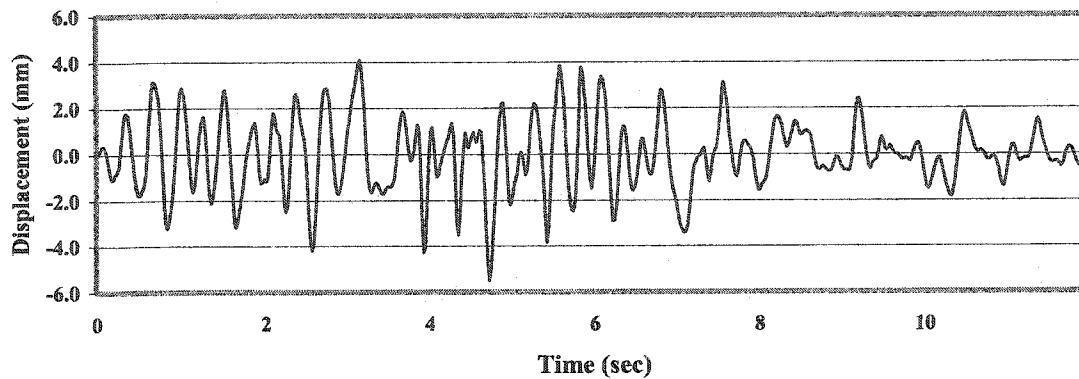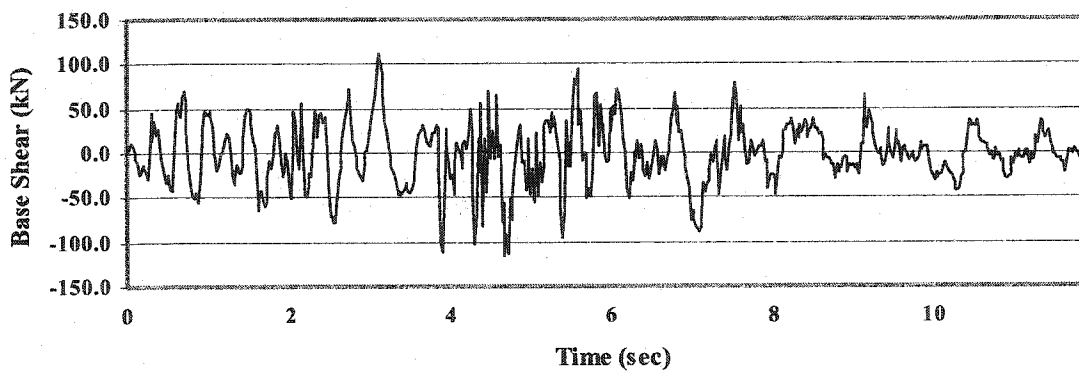
(a) Displacement (Top)
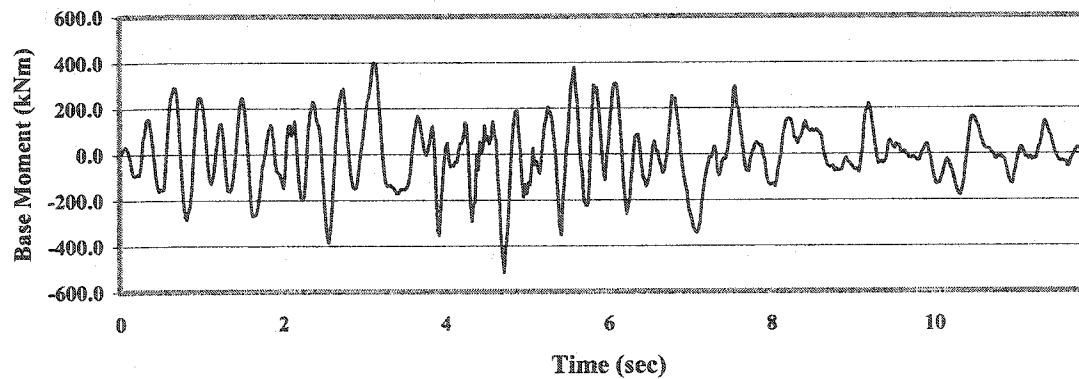
(b) Base Shear
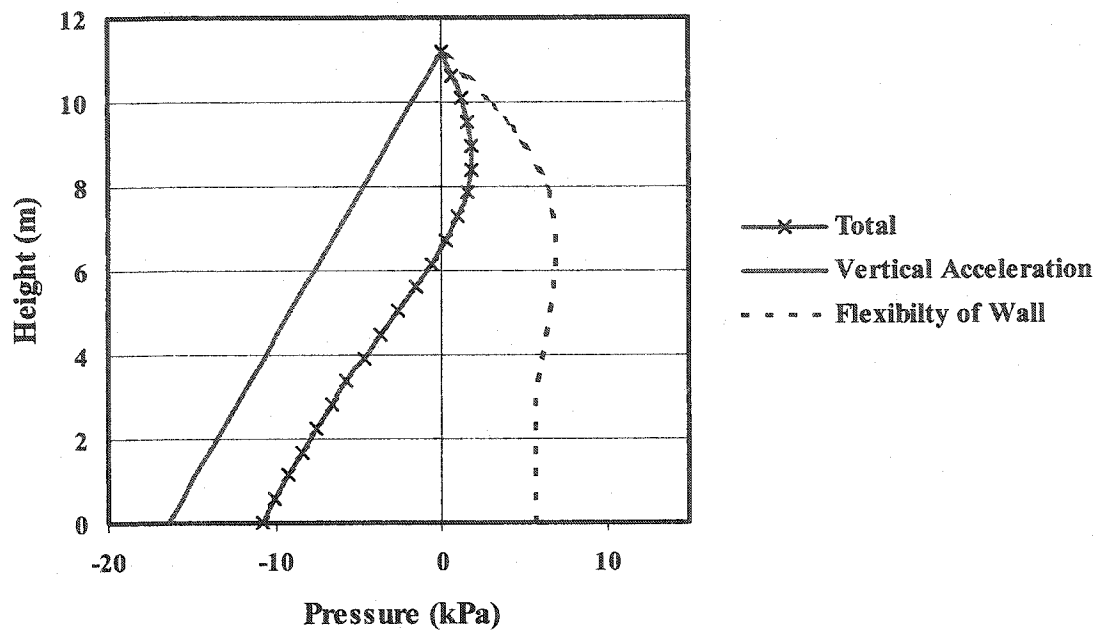
(c) Base Moment

(d) Hydrodynamic Pressure
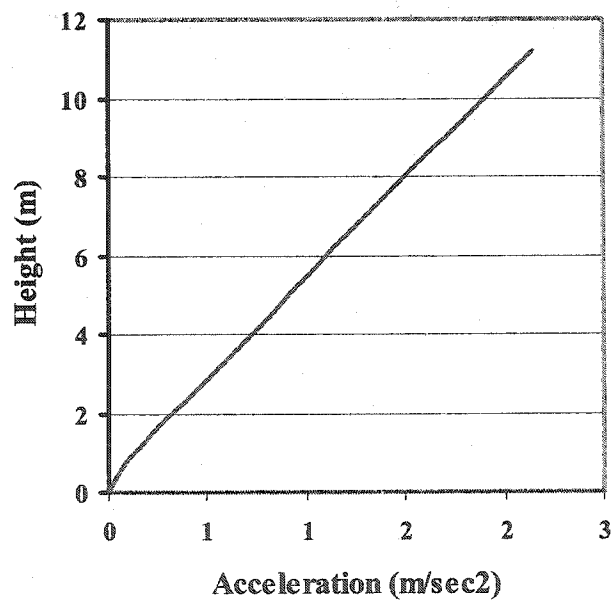
(e) Acceleration of Wall

Figure 7.39 Dynamic Response of Tall Tank due to Vertical Ground Motion

- Model 2 (1994 Northridge Earthquake)
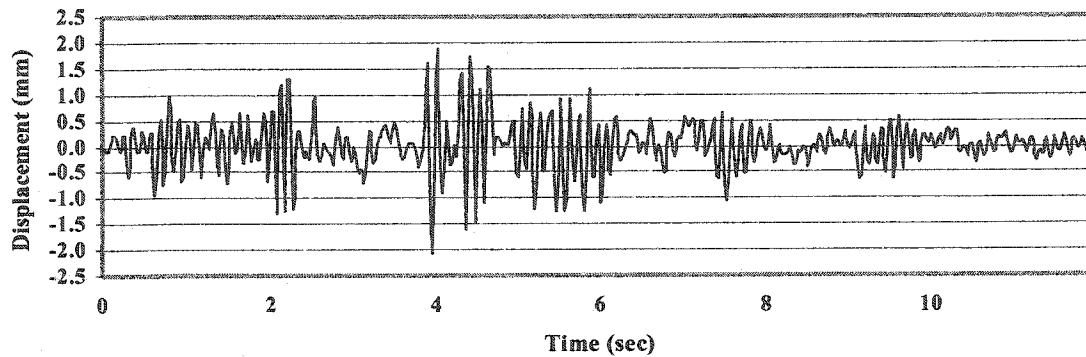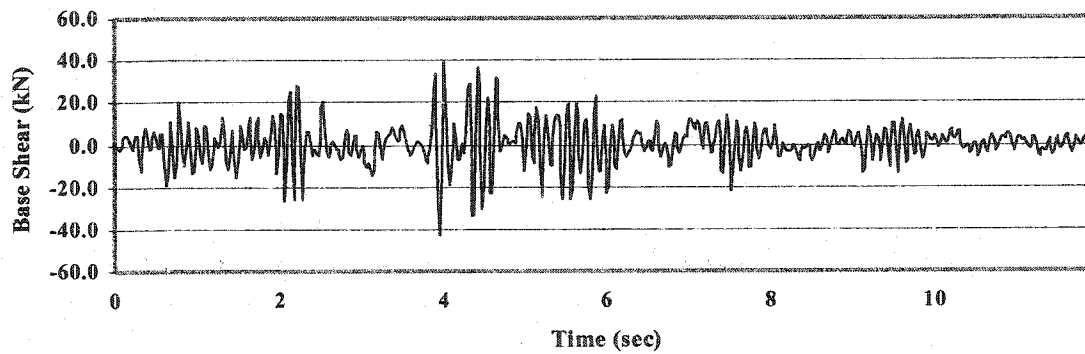
(a) Displacement (Top)
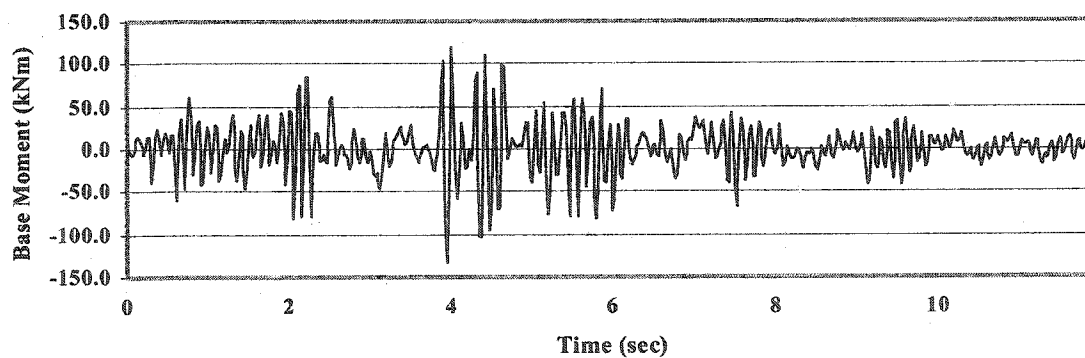
(b) Base Shear

(c) Base Moment

Figure 7.40 Dynamic Response of Shallow Tank due to Vertical Ground Motion
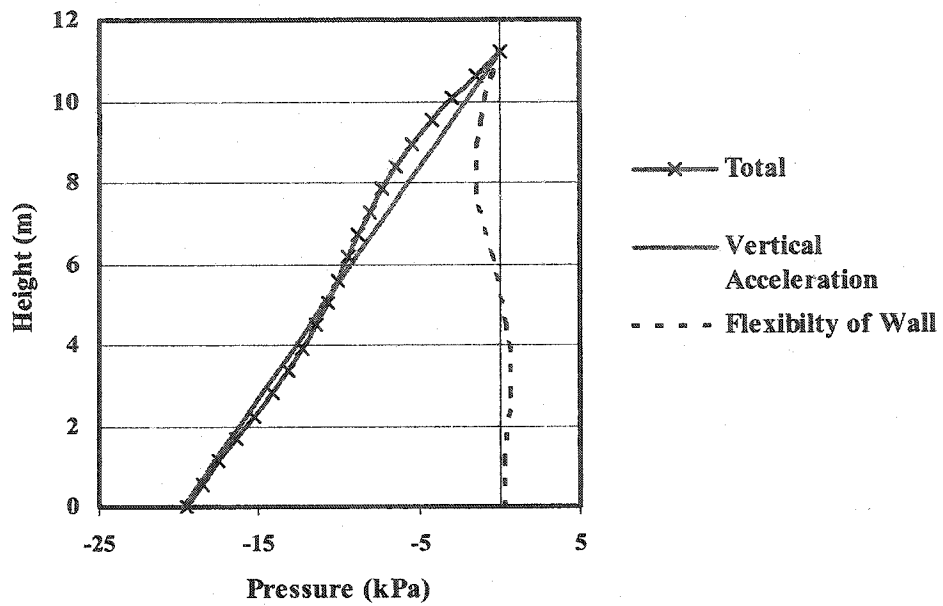— Model 1 (1994 Northridge Earthquake)
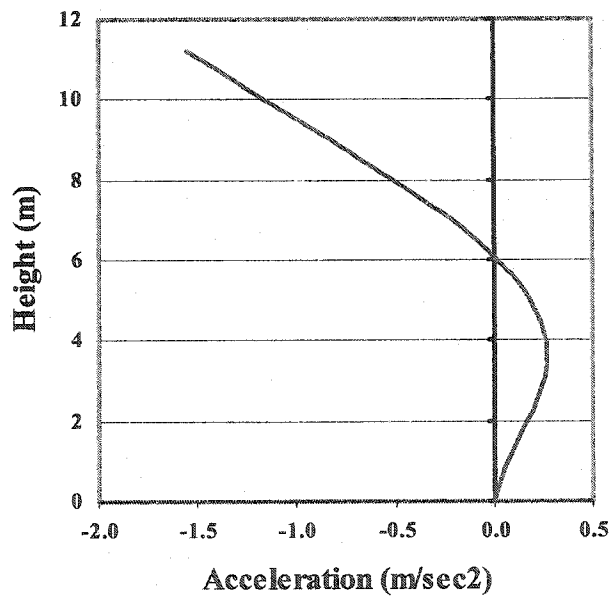
114

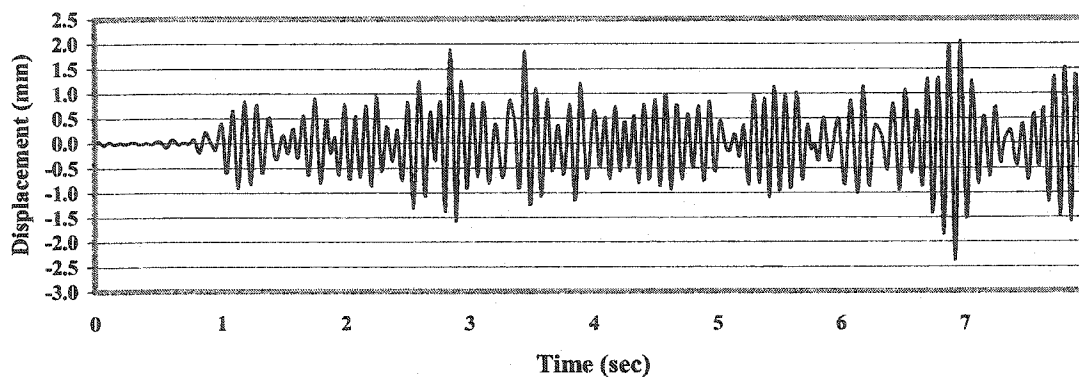(a) Displacement (Top)

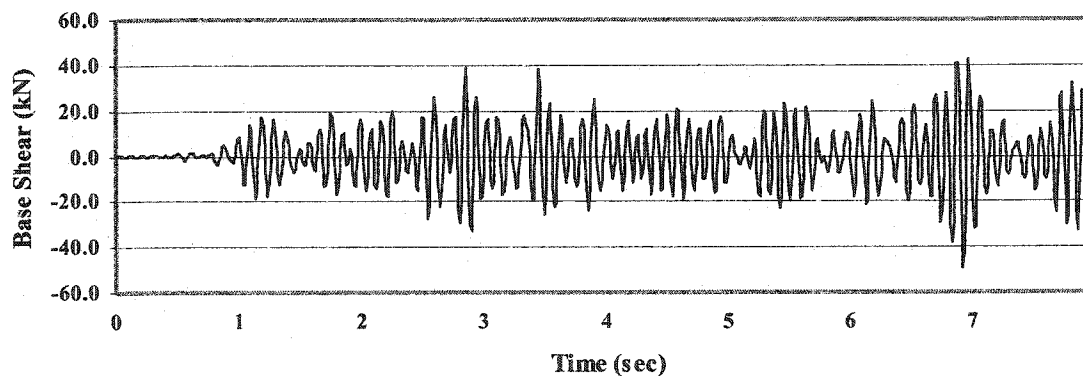(b) Base Shear

(c) Base Moment

115
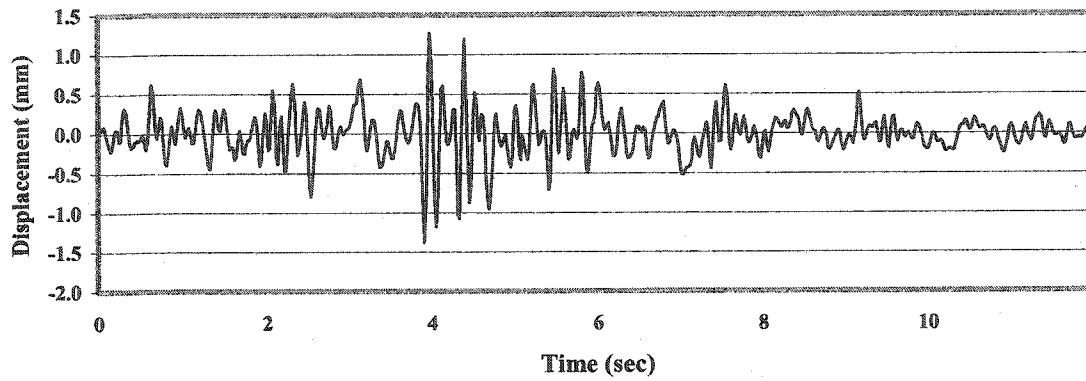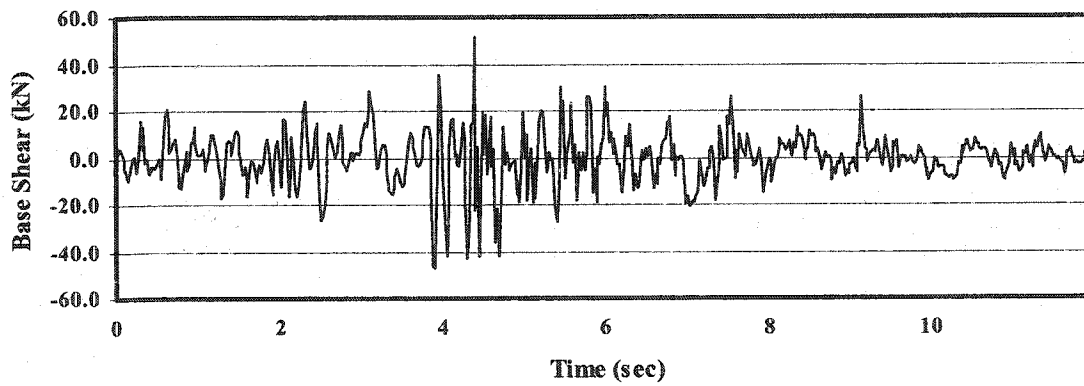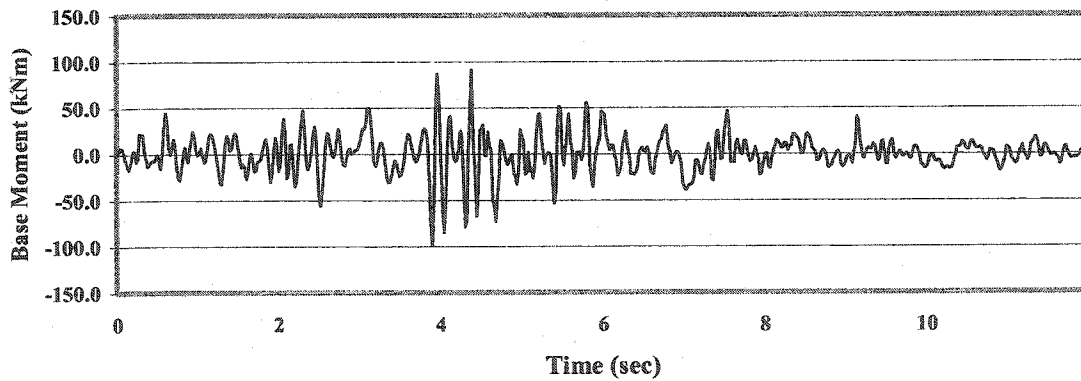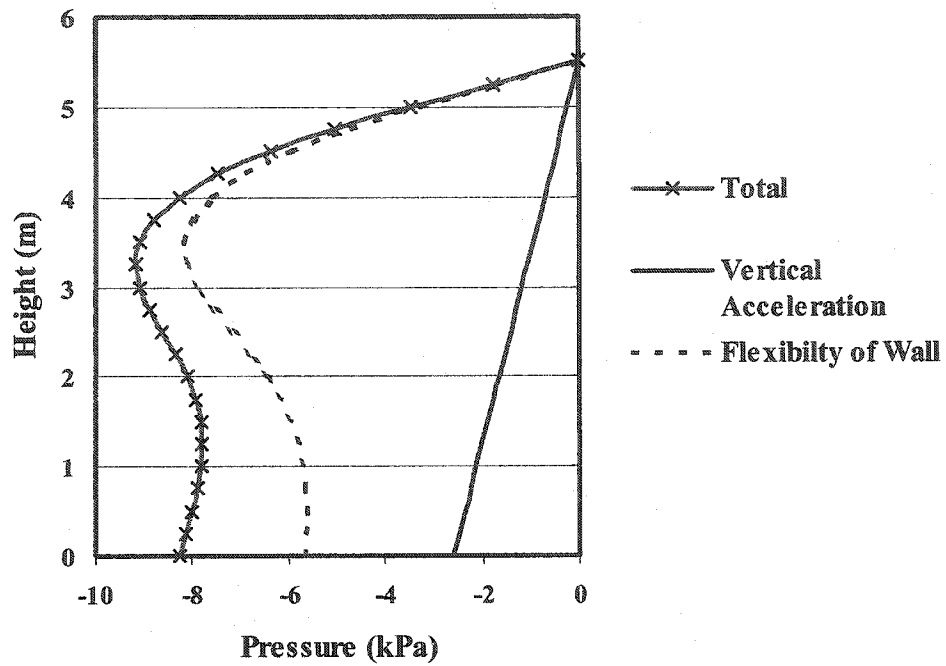
(d) Hydrodynamic Pressure
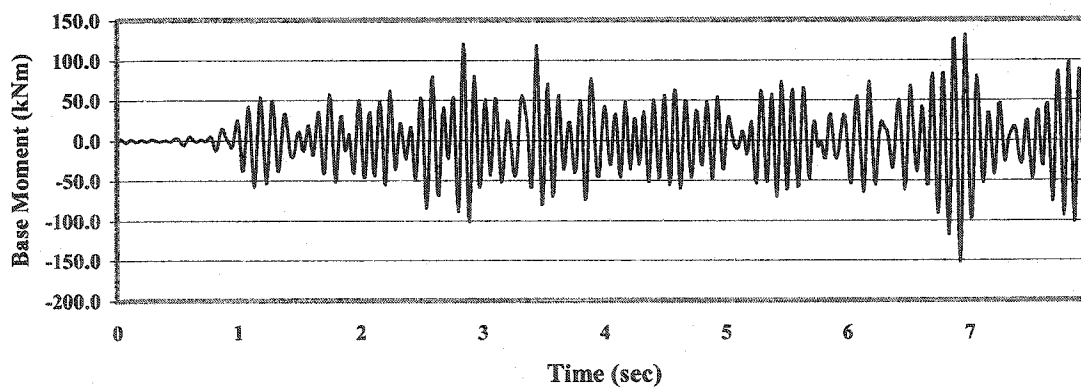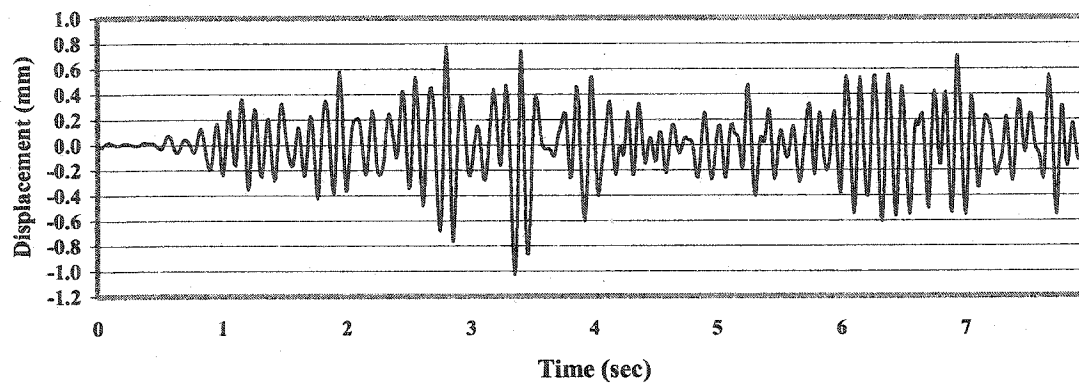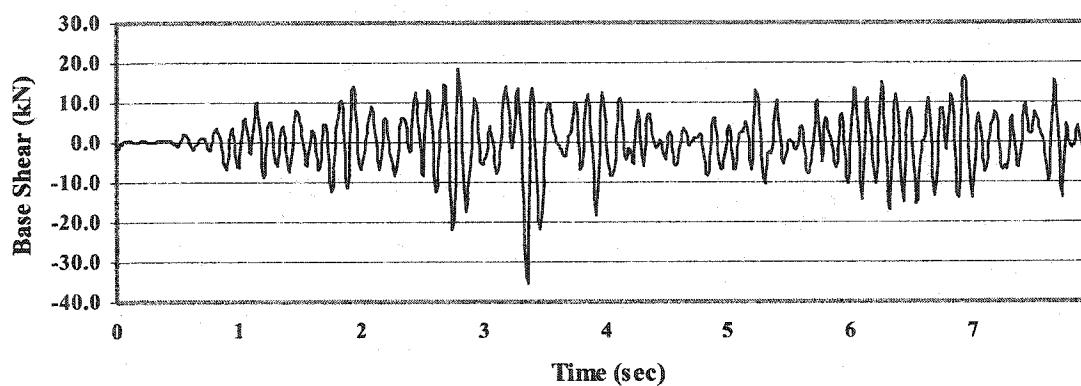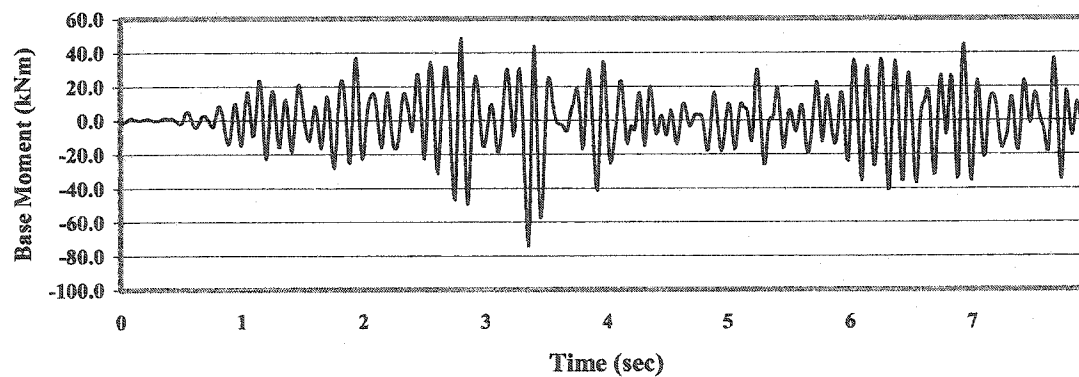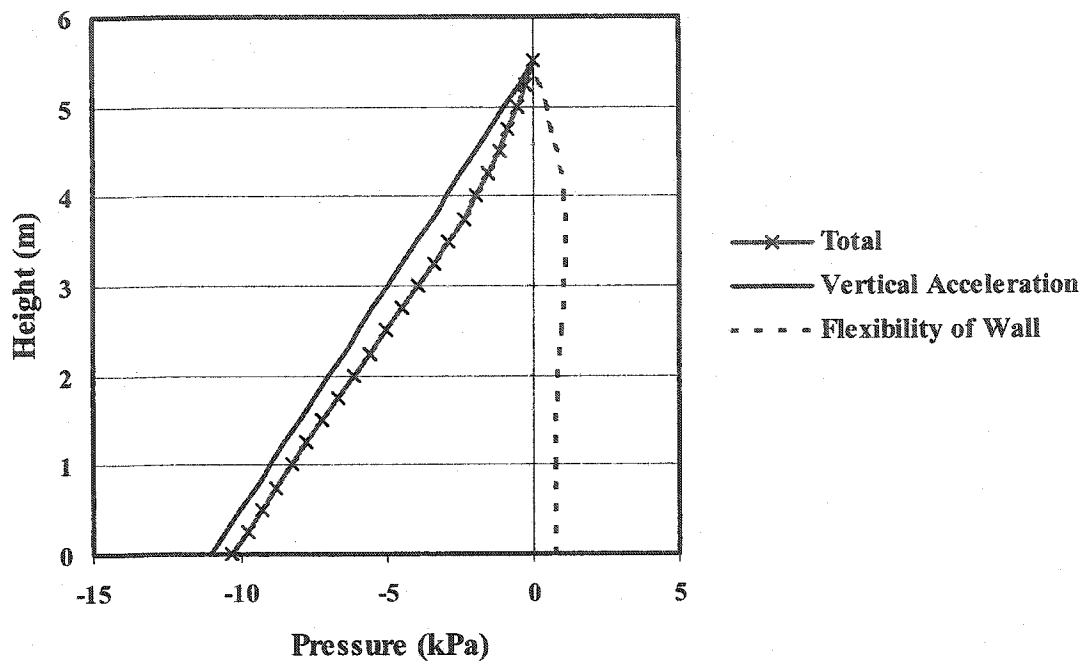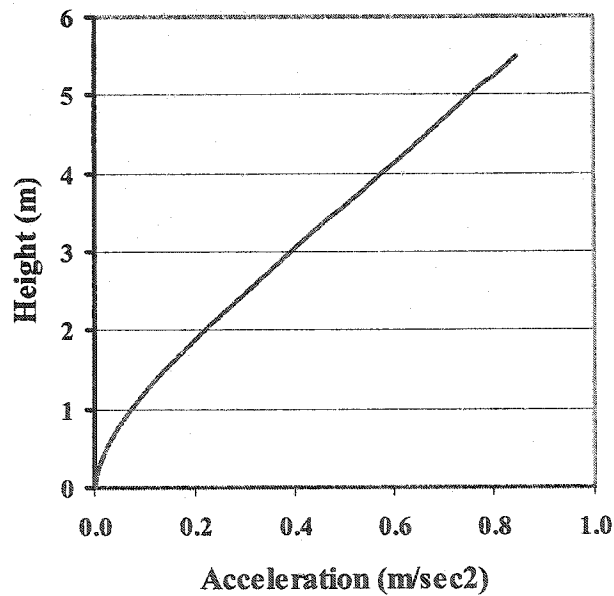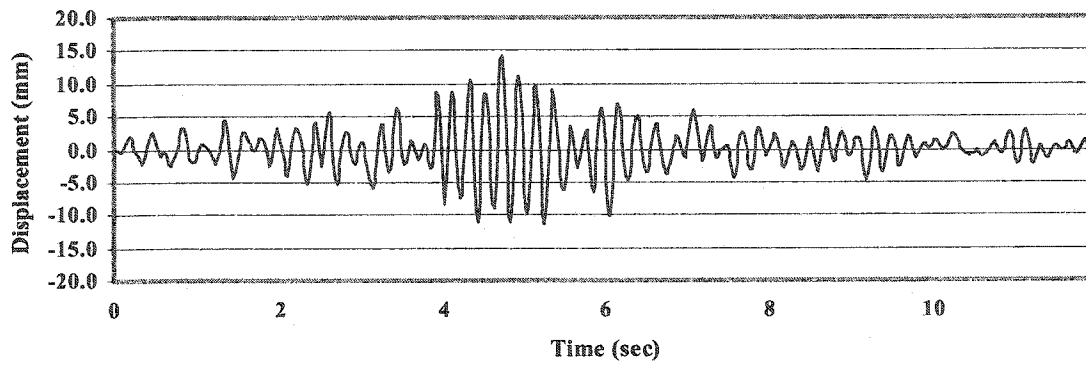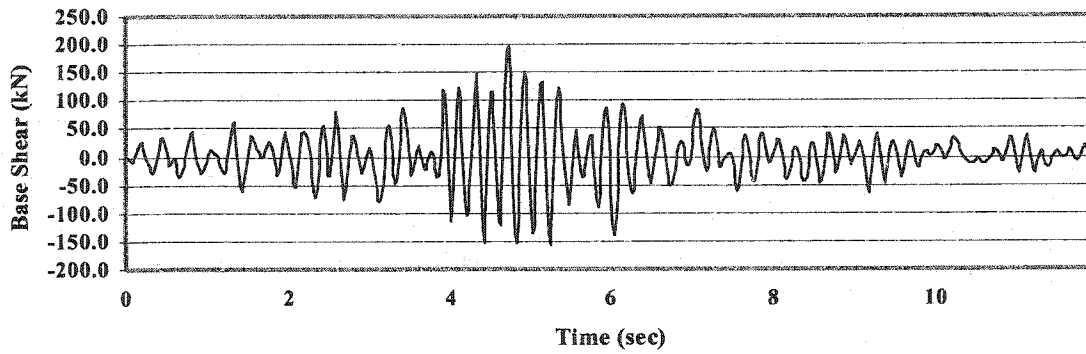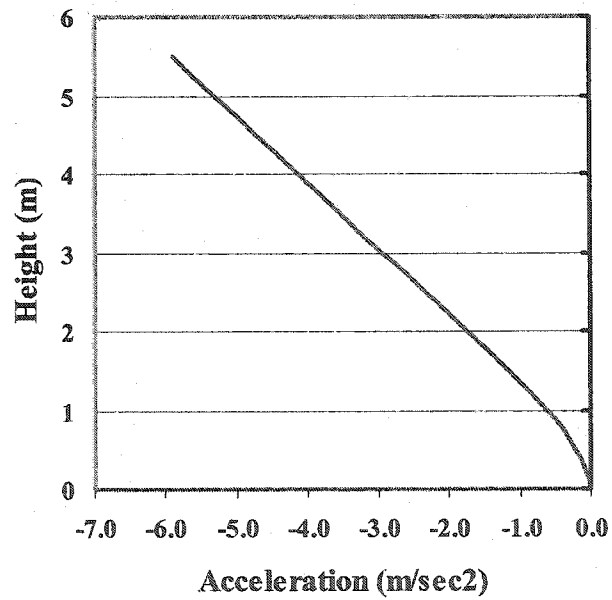

(e) Acceleration of Wall

Figure 7.41 Dynamic Response of Shallow Tank due to Vertical Ground Motion

– Model 2 (1994 Northridge Earthquake)

7.3.3 Combination of Horizontal and Vertical Ground Motion

In Section 7.3.1, dynamic response of liquid storage tanks induced by the horizontal ground motion is discussed. Also, the impulsive hydrodynamic pressure induced by the vertical ground motion is calculated in Section 7.3.2. The total dynamic response of liquid storage tanks due to the horizontal and vertical ground motions is calculated by sum of these two load cases. For the horizontal ground motion, model 5 in which the sequential method combined with the direct step-by-step integration method as discussed in Section 7.3.1 is used. For the vertical ground motion, model 2 in which the combination of the added mass and sequential method using the direct step-by-step integration method as discussed in Section 7.3.2 is used.

The horizontal component of Northridge Earthquake 1994 used in the analysis is shown in Figure 7.42.
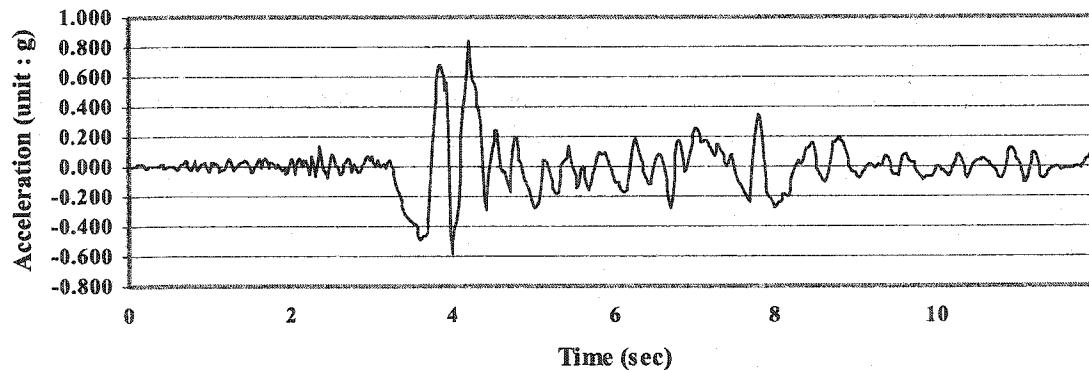
Figure 7.42 Horizontal Component (360°) of Northridge Accelerogram (0-12sec): 1994 Northridge Earthquake

Tables 7.7 – 7.10 show maximum dynamic response of tank wall and response due to the horizontal ground motion and vertical ground motion respectively. Figure 7.43 - 7.46 show the time history of such combination. From the analysis results of combination of hydrodynamic pressures, it confirms the importance of vertical ground motion in the calculation of hydrodynamic pressures induced by both vertical and horizontal ground

117

motion. It is even critical when the maximum amplitude of vertical component of ground motion exceeds peak horizontal amplitude.

Table 7.7 Combination of Dynamic Response of Tall Tank in Horizontal Direction

(1940 El Centro Earthquake)

Ground Motion	Horizontal Ground Motion	Vertical Ground Motion	Sum
Top Displacement (mm)	-26.30	-0.82	-27.12
Base Shear (KN)	-338.111	-32.850	-370.961
Base Moment (KNm)	-2018.524	-99.976	-2118.500

(a) Displacement (Top)

(b) Base Shear
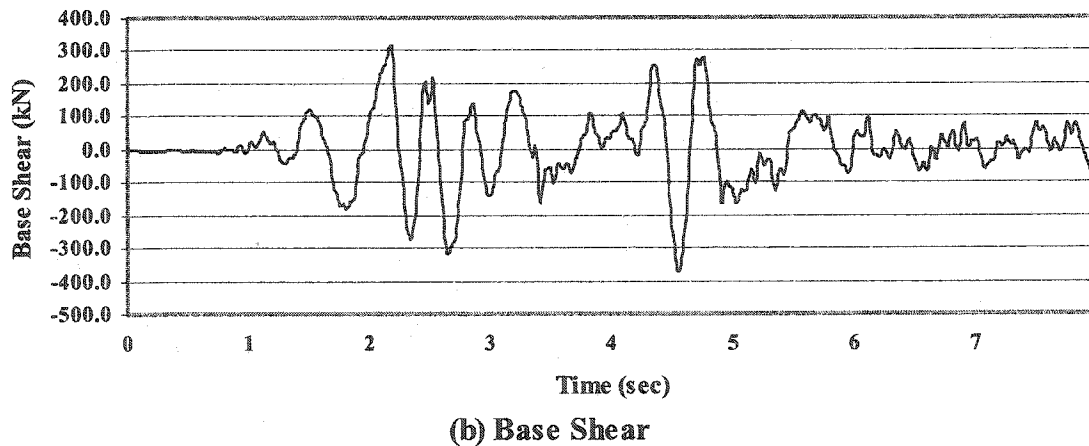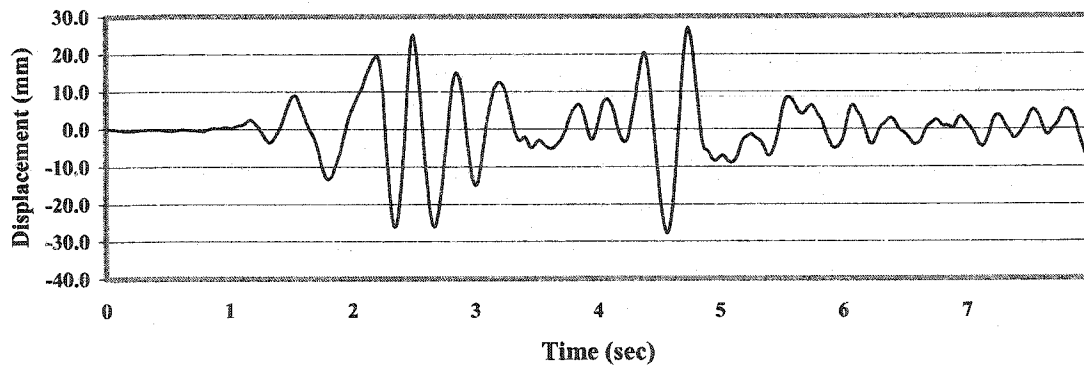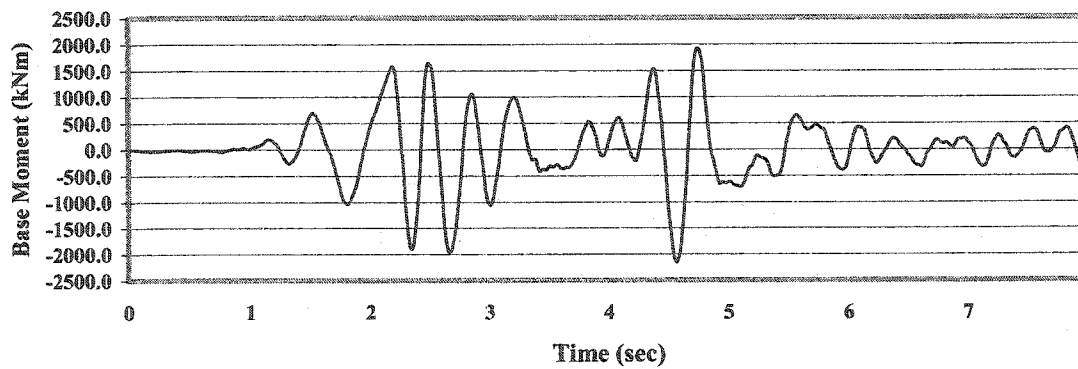
(c) Base Moment

Figure 7.43 Combination of Dynamic Response of Tall Tank in Horizontal Direction

(1940 El Centro Earthquake)

Table 7.8 Combination of Dynamic Response of Shallow Tank

in Horizontal Direction (1940 El Centro Earthquake)

Ground Motion	Horizontal Ground Motion	Vertical Ground Motion	Sum
Top Displacement (mm)	-4.544	-0.234	-4.778
Base Shear (KN)	-78.662	-8.405	-87.067
Base Moment (KNm)	-241.836	-17.042	-258.878

(a) Displacement (Top)

119
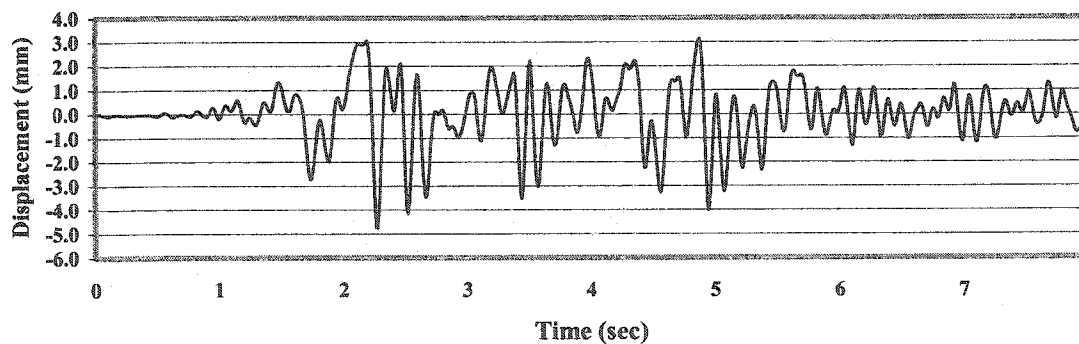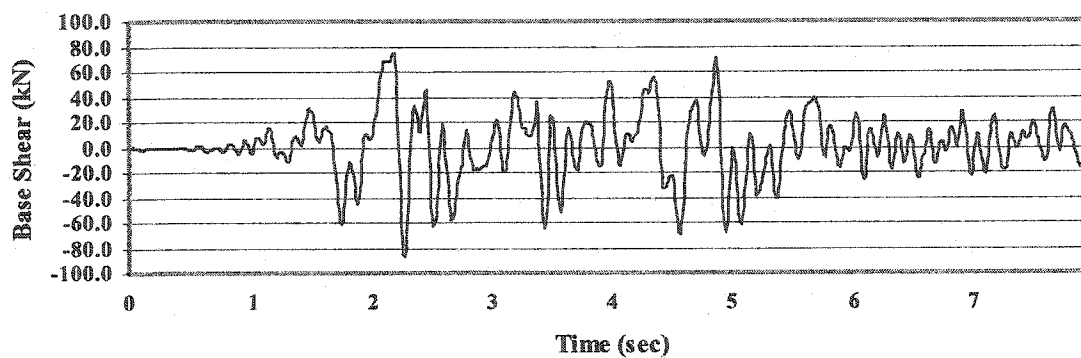
(b) Base Shear
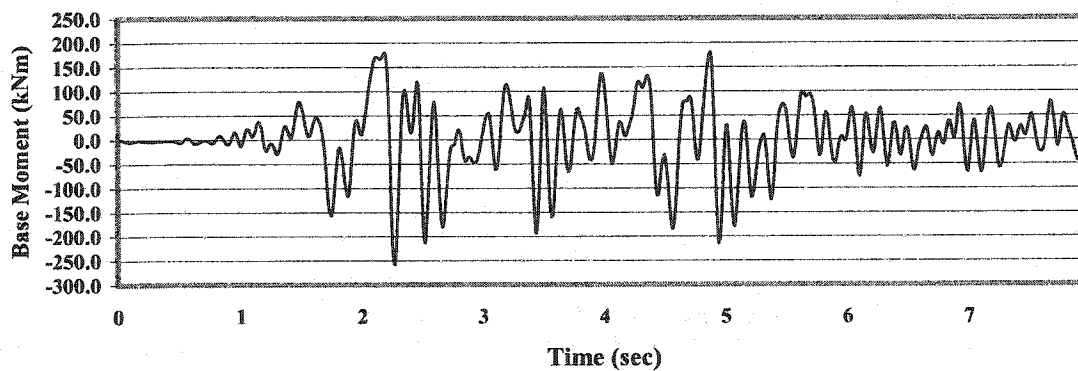
(c) Base Moment

Figure 7.44 Combination of Dynamic Response of Shallow Tank in Horizontal Direction (1940 El Centro Earthquake)

Table 7.9 Combination of Dynamic Response of Tall Tank in Horizontal Direction (1994 Northridge Earthquake)

Ground Motion	Horizontal Ground Motion	Vertical Ground Motion	Sum
Top Displacement (mm)	-98.42	1.34	-97.08
Base Shear (KN)	-1243.647	20.841	-1222.806
Base Moment (KNm)	-7857.994	125.199	-7732.795

120
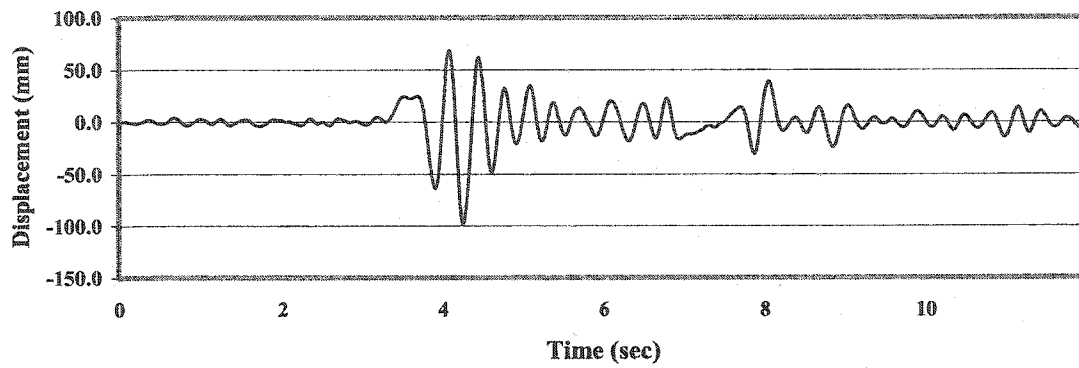
(a) Displacement (Top)
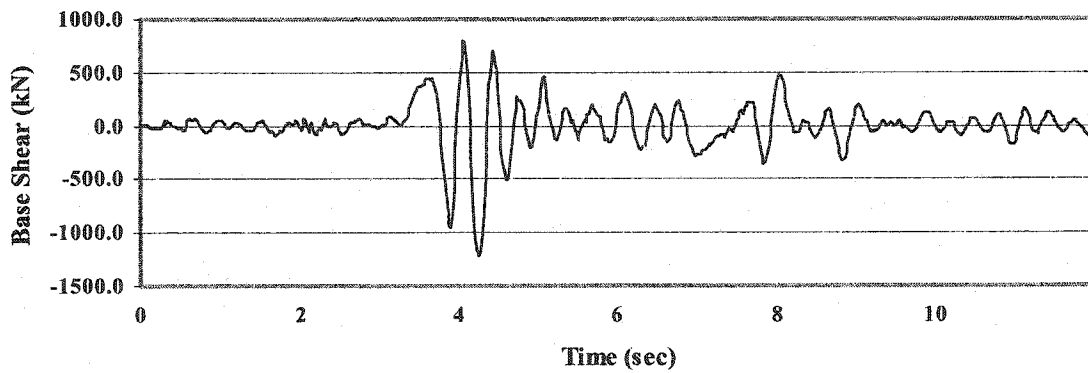
(b) Base Shear
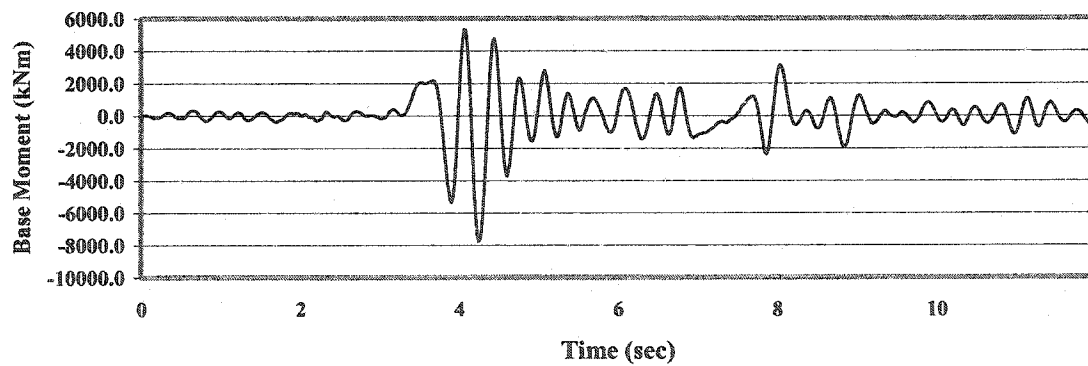
(c) Base Moment

Figure 7.45 Combination of Dynamic Response of Tall Tank

in Horizontal Direction (1994 Northridge Earthquake)

Table 7.10 Combination of Dynamic Response of Shallow Tank in Horizontal Direction (1994 Northridge Earthquake)

Ground Motion	Horizontal Ground Motion	Vertical Ground Motion	Sum
Top Displacement (mm)	-8.616	-0.093	-8.709
Base Shear (KN)	-204.283	-3.508	-207.791
Base Moment (KNm)	-501.786	-7.069	-508.855
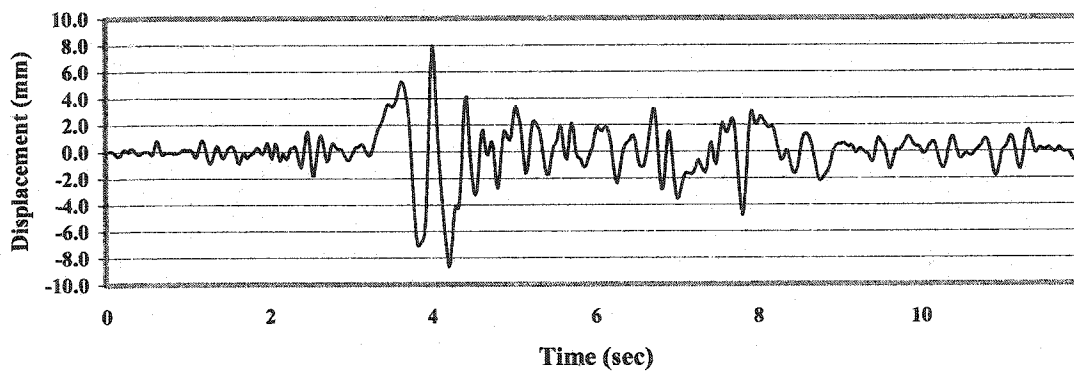
(a) Displacement (Top)
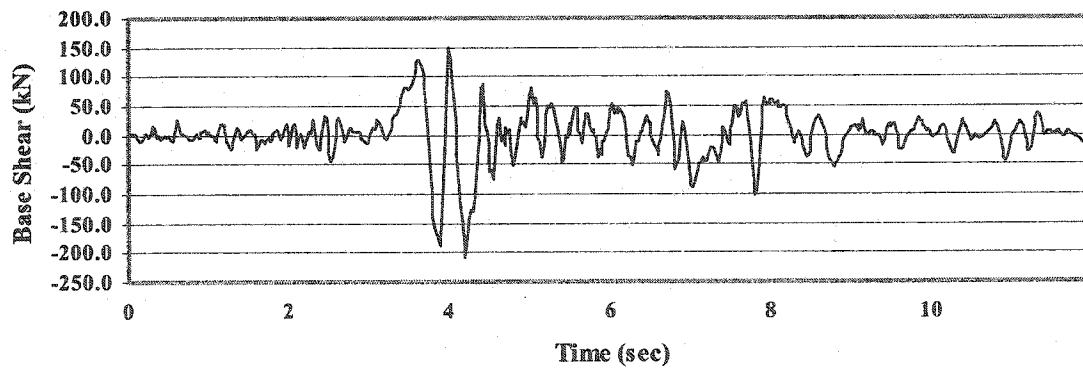
(b) Base Shear
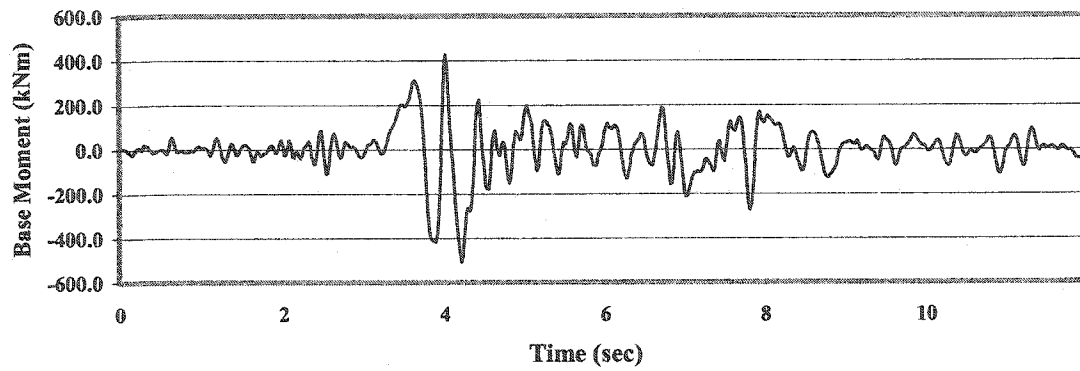
(c) Base Moment

Figure 7.46 Combination of Dynamic Response of Shallow Tank

in Horizontal Direction (1994 Northridge Earthquake)

Chapter 8

Summary, Conclusions and Recommendations

8.1 Summary

The dynamic response of concrete rectangular liquid storage tanks subjected to earthquakes is investigated in this study. Analysis is performed under both horizontal and vertical ground motions. The main purpose of study is to investigate dynamic response of such tanks.

The most important issue concerned in this study is how to calculate the hydrodynamic pressures. According to the Housner's model, the hydrodynamic pressures can be divided into two parts, convective pressure and impulsive pressure. In this study, both of them are formulated based on the potential flow theory under horizontal and vertical ground motions. The boundary conditions of fluid include the flexibility of the tank wall in the hydrodynamic pressure calculation.

The dynamic response of an empty tank is analyzed using the finite element method. It is based on the linear elastic theory. The linear structural analysis software SAPIV is used for dynamic analysis. A two-dimensional rectangular tank wall is analyzed using the mode superposition method and the direct step-by-step integration method. The time history of dynamic response of empty tank wall is demonstrated. The validity of SAPIV used for structural dynamic analysis in this study is verified.

The liquid storage tank system is analyzed using the coupled analysis method. In this study, the hydrodynamic pressures are no longer to be approximated by added masses such as that used in the Housner's model, but treated as external forces. The advantage of the proposed model is that it can consider the effect of flexibility of tank wall on both hydrodynamic pressure calculation and dynamic analysis of solid wall. In previous studies, the flexibility of concrete tank wall is considered only in the dynamic analysis of solid wall and the hydrodynamic pressure is calculated using the rigid wall boundary

condition. In order to analyze the dynamic response using the proposed model, a sequential method is applied. The sequential method can apply results from the first analysis as loads or boundary conditions for the second analysis. Through this method the fluid and the solid rectangular tank can be coupled. It is proved that except the difference time step for the calculation of hydrodynamic pressure in time history, the governing equation of motion of the proposed model is equivalent to that of the Housner's model in the dynamic analysis. If sufficient small time increment, Δt, is used in the calculation, the results obtained from sequential method can appropriately reflect the dynamic time history response.

A computer program HYDRO is developed in this study to calculate hydrodynamic pressures. As a subroutine, it is successfully incorporated into the linear structural analysis software SAPIV. Thus the dynamic response of liquid storage tank can be easily obtained.

In order to demonstrate the efficiency of the proposed model using the sequential method, a tall rectangular tank is first analyzed in this study. Different models are used to prove the validity of proposed model. It is concluded that the amplitude of hydrodynamic pressure is affected by the flexibility of the tank wall.

The response of a shallow tank is also analyzed in this study. The effect of variation in the flexibility of tank wall is studied. The acceleration along the height of tank wall and the corresponding hydrodynamic pressure distribution due to wall flexibility are demonstrated.

As the vertical ground motion is very critical in the dynamic response of liquid storage tanks, both the tall tank and the shallow tank are analyzed for two different earthquake records. They are analyzed using the combination of added mass method and the sequential method. Finally all horizontal load cases are combined by the sum of the dynamic response of liquid storage tanks obtained from the time history analysis.

8.2 Conclusions

In this study, dynamic response of liquid storage tanks is investigated. Based on the results of the investigation, the following conclusions can be made:

1. The magnitudes of hydrodynamic pressure can be amplified due to the flexibility of tank wall. It results in large hydrodynamic pressure applied on the tank wall. This may be the cause of serious damage to concrete liquid storage tanks in past earthquakes.

2. The governing equation of motion of the proposed model is equivalent to the Housner's model in the study of dynamic response of liquid storage tanks, except the difference in the time step in the dynamic analysis. If the time interval specified in the dynamic analysis is small enough, the analysis results can appropriately reflect the time history of dynamic response of liquid storage tanks.

3. The effect of flexibility of tank wall is very significant in the calculation of hydrodynamic pressures. With increase of the flexibility of wall, the hydrodynamic pressures are also increased.

4. In the calculation of hydrodynamic pressures, the flexibility of wall is ignored in the design codes and standards. Although the results obtained from the design codes and standards are still conservative, it is not accurate in the dynamic analysis of liquid storage tanks.

5. The equivalent mass model used in the design standards and codes are not accurate enough to estimate dynamic response of liquid storage tanks, such as base shear. They are overestimated using the equivalent mass model.

6. The effect of damping is very significant in the study of dynamic response of liquid storage tanks. In certain circumstance, resonance may occur resulting in extremely large stresses in the tank wall.

7. The hydrodynamic pressure due to the vertical ground motion cannot be neglected. It can also results in horizontal hydrodynamic pressures. The dynamic response of

liquid storage tanks subject to the vertical acceleration can be analyzed using the combination of the added mass method and the sequential method. The total response of structures in the horizontal direction is sum of response under both horizontal and vertical ground motions.

8.3 Recommendations for Further Research

Based on this investigation, some recommendations for the dynamic response of liquid storage tanks are presented below:

1. A simplified procedure should be established to include the effect of the flexibility of the tank wall in design codes and standards.

2. The effect of damping on the dynamic response of liquid storage tanks must be studied in further research. It may have significant effect on the behavior of liquid storage tanks.

3. As an extended application of the two-dimensional model presented in this study, three-dimensional model should be considered in future research. Therefore, more complex boundary conditions of the tank wall can be considered in the dynamic response of liquid storage tanks.

4. The effect of size of tanks and the level of liquid inside the tanks on the dynamic response of liquid storage tanks should be studied in order to consider the variable capacity of fluid containing structures.

5. This study shows that the hydrodynamic pressure load is highly dependent on the input ground motion. The effect of time history of ground motion on the hydrodynamic pressure must be studied.

6. The effect of component of convective hydrodynamic pressure under earthquakes is still not very clear. A simplified method should be used for calculation of such pressure.

References

ACI Committee 350. 2001. Seismic Design of Liquid-Containing Concrete Structures ACI 350.3. American Concrete Institute.

ANSYS Inc. ANSYS Help Manual (Version 6.1). Global Headquarters, Southpointe, 275 Technology Drive, Canonsburg, PA 15317.

ASCE Committee on Seismic Analysis of the Committee on Nuclear Structures and Materials of the Structural Division, American Society of Civil Engineers. 1984. Fluid/Structure Interaction During Seismic Excitation ISBN 0-87262-392-0.

Balendra, T., and Nash, W. A. 1978. Earthquake Analysis of Cylindrical Liquid Storage Tank with a Dome by the Finite Element Method. Engineering Research Institute, Department of Civil Engineering, University of Massachusetts, Amherst.

Balendra, T., Ang, K. K., Paramasivam, P. and Lee, S. L. 1982. Seismic Design of Flexible Cylindrical liquid Storage Tanks. Earthquake Engineering and Structural Dynamics, Vol. 10. 477-496, John Wiley & Sons, Ltd. ISSN 0098-8847/82/030477-20.

Bathe, K. J., Wilson, E. L. and Peterson, F. E. 1974. SAP IV – A Structural Analysis Program For Static and Dynamic Response of Linear System, College of Engineering, University of California, Berkeley, EERC 73-11.

Bathe, K. J. 1996. Finite Element Procedures. Englewood Cliffs, N. J., Prentice Hall, ISBN 0133014584.

Chwang, A. T. and Housner, G. W. 1978. Hydrodynamic Pressures on Sloping Dams During Earthquakes, Part 1. Momentum Method. Journal of Fluid Mechanics, vol. 87, part 2, pp. 335 – 341.

Collier, C. J. and Elnashai, A. S. 2001. A Procedure for Combining Vertical and Horizontal Seismic Action Effects. Journal of Earthquake Engineering, Vol. 5, No. 4, pp. 521-539, Imperial College Press.

Currie, I. G. 1973. Fundamental Mechanics of Fluid. McGraw-Hill, Inc., New York, N.Y.

Dogangun, A., Durmus, A. and Ayvaz, Y. 1996. Static and Dynmaic Analysis of Rectangular Tanks by Using the Lagrangian Fluid Finite Element. Computers & Structures Vol.59, No. 3, pp. 547-552

Epstein, H. I. 1976. Seismic Design of Liquid-Storage Tanks. Journal of the Structural Division, Proceedings of the American Society of Civil Engineers, Vol. 102, No. ST9, September.

Haroun, M. A. and Housner, G. W. 1981. Seismic Design of Liquid Storage Tanks. Journal of the Technical Councils of ASCE, April.

Haroun, M. A. and Ellaithy, H. M. 1983. Seismically Induced Fluid Forces on Elevated Tanks. Journal of Technical Topics in Civil Engineering, Vol. 111, No.1, December, ASCE, ISSN 0733-9461/85/0001-0001.

Haroun, M. A. 1983. Vibration Studies and Tests of Liquid Storage Tanks. Earthquake Engineering and Structural Dynamics, Vol. 11, 19-206, John Wiley & Sons, Ltd., ISSN 0098-8847/83/020179-28.

Haroun, M. A. 1984. Stress Analysis of Rectangular Walls Under Seismically Induced Hydrodynamic Loads. Bulletin of the Seismological Society of America, Vol. 74, No. 3, June.

Haroun, M. A. and Tayel, M.A. 1985. Response of Tanks to Vertical Seismic Excitations. Earthquake Engineering and Structural Dynamic, Vol. 13, pp. 583-5895

Haroun, M. A. and Abou-Izzeddine, W. 1992A. Parametric Study of Seismic Soil-Tank Interaction. I: Horizontal Excitation. Journal of structural Engineering, Vol. 118, No. 3, March, ASCE, ISSN 0733—9445/92/0003-0783.

Haroun, M. A. and Abou-Izzeddine, W. 1992B. Parametric Study of Seismic Soil-Tank Interaction. II: Vertical Excitation. Journal of structural Engineering, Vol. 118, No. 3, March, ASCE, ISSN 0733—9445/92/0003-0798.

Housner, G. W. 1957. Dynamic Pressures on Accelerated Fluid Containers. Bulletin of the Seismological Society of American, Vol.47, No.1, January, pp. 15 – 37.

Housner, G. W. 1963. The Dynamic Behavior of Water Tanks. Bulletin of the Seismological Society of American, Vol. 53, No. 2, February.

Housner, G. W. and Haroun, M. A. 1979. Vibration Tests of Full Scale Liquid Storage Tanks. Earthquake Engineering Research Institute from Proceedings of the Second U.S. National Conference on Earthquake Engineering, Stanford, California, August, pp. 137 – 145.

Housner, G. W. and Haroun, M. A. 1980. Dynamic Analyses of Liquid Storage Tanks. The Turkish National Committee on Earthquake Engineering from Proceedings of 7th Conference on Earthquake Engineering, Istanbul, Turkey, vol. 8, pp. 431 – 438.

Jacobson, L. S. and Ayre, R.S. 1949. Impulsive Hydrodynamics of Fluid Inside a Cylindrical Tank. Bulletin of the Seismological Society of America, Vol.39, pp.189-203

Kana, D. D. 1979. Seismic Response of Flexibility Cylindrical Liquid Storage Tanks. Nuclear Engineering and Design, 52, pp. 185-199.

Kim, J. K., Koh, H. M. and Kwahk, I. J. 1996. Dynamic Response of Rectangular Flexible Fluid Containers. Journal of Engineering Mechanics, Vol.122, No. 9, September, ASCE, ISSN 0733-9399/96/0009-0807-0817.

Munshi, J. A. 2002. Design of Liquid-Containing Concrete Structures for Earthquake Forces, Portland Cement Association, ISBN 0-89312-219-X.

Murphy, L. M. 1973. San Fernando, California, Earthquake of February 9. National Oceanic and Atmospheric Administration, U.S. Department of Commerce.

Nachtigall, I., Gebbeken, N. and Urrutia-Galicia, J. L. 2003. On the Analysis of vertical Circular Cylindrical Tanks under Earthquake Excitation at its Base. Engineering Structure 25, pp. 201-213.

New Zealand Standards Association. 1986. NZS3106: The New Zealand Code of Practice for Concrete Structures for the Storage of Liquids.

Park, J. H., Koh, H. M., and Kim, J. 1990. Liquid-Structure Interaction Analysis by

Coupled Boundary Element-Finite Element Method in Time Domain. Proc., 7th International Conference on Boundary Element Technology, BE-TECH/92, Computational Mechanics Publication, Southampton, England, 89-92.

Petyt, M. 1990. Introduction to Finite Element Vibration Analysis. Cambridge University Press, ISBN0-521-26607-6.

Priestley, M. J. N., Hood, J. H. and Davidson, B. J. 1986. Seismic Design of Storage Tanks. Bulletin of the New Zealand National Society for the Earthquake Engineering, Vol. 19, No. 4, December.

Reddy, J. N. and Gartling, D. K. 2001. The Finite Element Method in Heat Transfer and Fluid Dynamics (second Edition), CRC Press LLC, ISBN 0-8493-2355-X

Reddy, J. N. 1993. An Introduction to the Finite Element Method. McGraw-Hill, second edition.

SAP2000. 1998. Three dimensional Static and Dynamic Finite Element Analysis and Design of Structures (Analysis Reference), CSI.

Shaaban, S. H. and Nash, W. A. 1975. Response of an Empty Cylindrical Ground Supported Liquid Storage Tank to Base excitation. Engineering Research Institute, Department of Civil Engineering, University of Massachusetts, Amherst, August.

Tsang, S.K. and Harding, J.E. 1987. Ring-Stiffened Cylinders under Interactive Loading. Journal of Structural Engineering, Vol. 113, No. 9, September, ASCE, ISSN 0733-9445/87/0009-1977.

Veletsos, A. S. and Tang, Yu. 1986. Dynamics of Vertically excited Liquid Storage Tanks. Journal of Structural Engineering Vol. 112, No. 6, June, ASCE, ISSN 0733-9445/86/0006-1228.

Veletsos, A. S. and Tang, Yu. 1987. Rocking Response of Liquid Storage Tanks. Journal of Engineering Mechanics, Vol. 113, No.11, November, ASCE, ISSN 0733-9399/87/0011-1774.

Veletsos, A. S. and Tang, Yu. 1990. Soil-Structure Interaction Effects for Laterally

Excited Liquid Storage Tanks. Earthquake Engineering And Structural Dynamics, Vol. 19, 473-496, John Wiley & Sons, Ltd. ISSN 0098-8847/90/040473-24.

Veletsos, A. S., Tang, Y. and Tang, H. T. 1992A. Dynamic Response of Flexibly Supported Liquid –Storage Tanks. Journal of Structural Engineering, Vol. 118, No.1, January, ASCE, ISSN 0733-9445/92/0001-0264.

Veletsos, A. S., and Tang, Y. and Tang, H. T. 1992B. Dynamic Response of Flexibly Supported Liquid –Storage Tanks. Journal of Structural Engineering, Vol. 118, No.1, January, ASCE, ISSN 0733-9445/92/0001-0264.

Veletsos, A. S. and Shivakumar, P. 1996. Dynamic Response of Tanks Containing Liquids or Solids. Computer Analysis and Design of Earthquake Resistant Structures, Computational Mechanics Publications Earthquake Engineering Series, Vol. 2, December.

Wei Yi and Natsiavas, S. 1992. Seismic Response of Unanchored Fluid-Filled Tanks Using Finite Elements. Journal of Pressure Vessel Technology, Transaction of ASME, February, Vol. 114, pp. 74- 79.

Westergaard, H. M. 1933. Water Pressures on Dams During Earthquakes. Transaction, American Society of Civil Engineers, Vol. 98.

Wilson, E. L. 1998. Three Dimensional Static and Dynamic Analysis of Structures – A Physical Approach With Emphasis on Earthquake Engineering. CSI.

Yang, J. Y. and Veletsos, A. S. 1976. Dynamic Behavior of Fluid-Tank System. Ph.D Thesis, Civil Engineering, Rice University Houston, Texas, March.

Yu, Baoqing, Nash, W. A. and Kirchhoff, R. H. 1987 Finite Element-Perturbation Analysis of A Cylindrical Liquid Storage Tank With Dome. Department of Civil Engineering, University of Massachusetts, Amherst, December.

Appendix A Derivation of Equation - Impulsive Pressure (Horizontal)

The velocity potential function ϕ_I is solved by separation of variables method. ϕ_I can be expressed in the form that:

$$\phi_1 = X(x) \cdot Y(y) \cdot T(t) \tag{A.1}$$

Substituting ϕ_I into two-dimensional Laplace's Eq. 3.11, we can get:

$$\frac{X(x)''}{X(x)} + \frac{Y(y)''}{Y(y)} = 0 \tag{A.2}$$

According to the boundary conditions indicated in Eq.3.18-3.20 they result in:

$$y = H_1 \quad \frac{\partial \phi_1}{\partial t} = 0 \Rightarrow X(x) \cdot Y(y) \cdot T(t)' = 0 \Rightarrow Y(H_1) = 0 \tag{A.3.1}$$

$$y = 0 \quad \frac{\partial \phi_1}{\partial y} = 0 \Rightarrow X(x) \cdot Y(y)' \cdot T(t) - 0 \Rightarrow Y(0)' = 0 \tag{A.3.2}$$

$$x = \pm L_x \quad \frac{\partial \phi_1}{\partial x} = -\dot{u}(t) \Rightarrow X(x)' \cdot Y(y) \cdot T(t) = -\dot{u}(t) \tag{A.3.3}$$

The Eq.A.2 can be transformed as:

$$\frac{X(x)''}{X(x)} = -\frac{Y(y)''}{Y(y)} = \lambda_i^2 \tag{A.4}$$

The solution for $Y(y)$ can be expressed as:

$$Y(y) = B_1 \cos(\lambda_i \cdot y) + B_2 \sin(\lambda_i \cdot y) \tag{A.5}$$

Where B_1 and B_2 are unknown constant. From boundary condition Eq.A.3.2, it results in $B_2 = 0$ and from the boundary condition A.3.1, it result in:

$$\lambda_i = \frac{(2n-1)\pi}{2H_1} \tag{A.6}$$

The solution for $X(x)$ can be expressed as:

$$X(x) = A_1 \cosh(\lambda_i \cdot x) + A_2 \sinh(\lambda_i \cdot x) \tag{A.7}$$

Where A_1 and A_2 are unknown constant. From boundary condition Eq.A.3.3, as the symmetric condition, it leads to $A_1 = 0$. Thus the velocity potential ϕ_I can be expressed as

133

that:

$$\phi_1 = \sum_{n=1}^{\infty} A_{2n} \sinh(\lambda_{i,n} \cdot x) \cdot B_{1n} \cos(\lambda_{i,n} \cdot y) \cdot T(t) \qquad (A.8)$$

Substituting ϕ_1 into the Eq.A.3.3 it results in:

$$\sum_{n=1}^{\infty} A_{2n} \cdot B_{1n} \cdot \lambda_{i,n} \cdot \cosh(\lambda_{i,n} L_x) \cdot \cos(\lambda_{i,n} y) \cdot T(t) = -\ddot{u}(t) \qquad (A.9)$$

Multiplying Eq.A.9 by $\cos(\lambda_i y)$ and integrating with respect to y from 0 to H_l, we can get that:

$$\sum_{n=1}^{\infty} A_{2n} \cdot B_{1n} \cdot T(t) = -\sum_{n=1}^{\infty} \frac{2}{\lambda_{i,n} \cdot H_l \cdot \cosh(\lambda_{i,n} L_x)} \int_0^{H_l} \cos(\lambda_{i,n} y) \, \ddot{u}(t) dy \qquad (A.10)$$

Therefore ϕ_1 can be expressed as that:

$$\phi_1 = -\sum_{n=1}^{\infty} \frac{2 \cdot \sinh(\lambda_{i,n} x)}{\lambda_{i,n} \cdot H_l \cdot \cosh(\lambda_{i,n} L_x)} \cos(\lambda_{i,n} y) \int_0^{H_l} \cos(\lambda_{i,n} y) \, \dot{u}(t) dy \qquad (A.11)$$

The hydrodynamic pressure is:

$$p = -\rho_l \frac{\partial \phi_1}{\partial t} = \sum_{n=1}^{\infty} \frac{2 \cdot \rho_l \cdot \sinh(\lambda_{i,n} x)}{\lambda_{i,n} \cdot H_l \cdot \cosh(\lambda_{i,n} L_x)} \cos(\lambda_{i,n} y) \int_0^{H_l} \cos(\lambda_{i,n} y) \cdot \ddot{u}(t) dy \qquad (A.12)$$

The impulsive pressure distribution at the surface of the wall $x=\pm L_x$ is:

$$p = -\rho_l \frac{\partial \phi_1}{\partial t} = \sum_{n=1}^{\infty} \frac{2 \cdot \rho_l}{\lambda_{i,n} \cdot H_l} \tanh(\lambda_{i,n} L_x) \cos(\lambda_{i,n} y) \int_0^{H_l} \cos(\lambda_{i,n} y) \, \ddot{u}(t) dy \qquad (A.13)$$

For the rigid wall condition, $\ddot{u}(t) = \ddot{u}_g(t)$ which means that the velocity along the height of wall is same as the velocity of ground motion, we can obtain that:

$$\phi_1 = -\sum_{n=1}^{\infty} \frac{2 \cdot (-1)^n \sinh(\lambda_{i,n} x)}{\lambda_{i,n}^2 \cdot H_l \cdot \cosh(\lambda_{i,n} L_x)} \cos(\lambda_{i,n} y) \cdot \dot{u}_g(t) \qquad (A.14)$$

The hydrodynamic pressure is:

$$p = -\rho_l \frac{\partial \phi_1}{\partial t} = \sum_{n=1}^{\infty} \frac{2 \cdot (-1)^n \cdot \rho_l \cdot \sinh(\lambda_{i,n} x)}{\lambda_{i,n}^2 \cdot H_l \cdot \cosh(\lambda_{i,n} L_x)} \cos(\lambda_{i,n} y) \cdot \ddot{u}_g(t) \qquad (A.15)$$

At the surface of wall $x=\pm L_x$, it becomes:

$$p = -\rho_l \frac{\partial \phi_1}{\partial t} = \sum_{n=1}^{\infty} \frac{2 \cdot (-1)^n \cdot \rho_l}{\lambda_{i,n}^2 \cdot H_l} \tanh(\lambda_{i,n} L_x) \cdot \cos(\lambda_{i,n} y) \cdot \ddot{u}_g(t) \qquad \text{(A.16)}$$

This result is same as the formula of impulsive hydrodynamic pressure for the rigid wall derived by Haroun in reference.

Appendix B Derivation of Equation - Convective Pressure (Horizontal)

The velocity potential function ϕ_2 is solved by the separation of variables method. For the harmonic condition $\ddot{u}_g(t) = \dot{u}_0 \cdot \sin(\omega \cdot t)$, the solution ϕ_2 can be expressed as:

$$\phi_2 = X(x) \cdot Y(y) \cdot \dot{u}_0 \cdot \sin(\omega \cdot t) \qquad \text{(B.1)}$$

Substituting ϕ_2 into two-dimensional Laplace's equation Eq. 3.11, we can get:

$$\frac{X(x)''}{X(x)} + \frac{Y(y)''}{Y(y)} = 0 \qquad \text{(B.2)}$$

According to the boundary conditions indicated in Eq.3.21-3.23, they result in:

$$y = H_1 \quad [-\omega^2 \cdot Y(y) + g \cdot Y(y)'] \cdot X(x) \cdot \dot{u}_0 \sin(\omega \cdot t) = -g \frac{\partial \phi_1}{\partial y} \qquad \text{(B.3.1)}$$

$$y = 0 \quad \frac{\partial \phi_2}{\partial y} = 0 \Rightarrow X(x) \cdot Y(y)' \cdot T(t) = 0 \Rightarrow Y(0)' = 0 \qquad \text{(B.3.2)}$$

$$x = \pm L_x \quad \frac{\partial \phi_2}{\partial x} = 0 \Rightarrow X(x)' \cdot Y(y) \cdot T(t) = 0 \Rightarrow X(x)' = 0 \qquad \text{(B.3.3)}$$

The Eq. B.2 can be transformed as:

$$-\frac{X(x)''}{X(x)} = \frac{Y(y)''}{Y(y)} = \lambda_c^2 \qquad \text{(B.4)}$$

The solution for $Y(y)$ can be expressed as:

$$Y(y) = B_1 \cosh(\lambda_c y) + B_2 \sinh(\lambda_c y) \qquad \text{(B.5)}$$

Where B_1 and B_2 are unknown constant. From boundary condition Eq.B.3.2, it results in $B_1 = 0$

The solution for $X(x)$ can be expressed as:

$$X(x) = A_1 \sin(\lambda_c x) + A_2 \cos(\lambda_c x) \qquad (B.7)$$

Where A_1 and A_2 are unknown constant. From boundary condition Eq.B.3.3, it leads to:

$$A_1 \cos(\lambda_c L_x) \pm A_2 \sin(\lambda_c L_x) = 0 \qquad (B.8)$$

This boundary condition may be satisfied by setting $A_1 = A_2 = 0$, but then $\phi_2 = 0$, which is the trivial solution. For a nontrivial solution either A_1 or A_2 at least, must be different from zero. In addition from the boundary condition Eq.3.1 related to ϕ_1 it must anti-symmetric to x=0, thus $A_1 \neq 0$, $A_2 = 0$. It results in:

$$\cos(\lambda_c L_x) = 0 \qquad (B.9)$$

in which:

$$\lambda_c = \frac{(2m-1)\pi}{2L_x} \qquad (B.10)$$

Then ϕ_2 becomes:

$$\phi_2 = \sum_{m=1}^{\infty} A_1 \cdot \sin(\lambda_{c,m} x) \cdot B_2 \cdot \cosh(\lambda_{c,m} y) \cdot \dot{u}_0 \cdot \sin(\omega \cdot t) \qquad (B.11)$$

Substituting into Eq.B.3.1, we can obtain that:

$$\sum_{m=1}^{\infty} A_{1m} \cdot B_{2m} \left[-\omega^2 \cdot \cosh(\lambda_{c,m} H_l) + g \cdot \lambda_{c,m} \cdot \sinh(\lambda_{c,m} H_l) \right] \cdot \sin(\lambda_{c,m} x) \cdot \dot{u}_0 \cdot \sin(\omega \cdot t) = -g \frac{\partial \phi_1}{\partial y}$$

$$(B.12)$$

If the right hand side is specified to zero, we can get natural frequencies of sloshing liquid:

$$\omega_{c,m}^2 = \lambda_{c,m} \cdot g \cdot \tanh(\lambda_{c,m} H_l) \qquad (B.13)$$

Eq.B.12 can also be transform into following form:

$$\sum_{m=1}^{\infty} A_{1m} \cdot B_{2m} \left[-\omega^2 + \omega_{c,m}^2 \right] \cdot \cosh(\lambda_{c,m} H_l) \cdot \sin(\lambda_{c,m} x) \cdot \dot{u}_0 \sin(\omega \cdot t) = -g \frac{\partial \phi_1}{\partial y} \qquad (B.14)$$

The solution of ϕ_1 in Eq. B.14 only considers for the rigid wall boundary condition as the

flexibility of the wall has little effect on the convective pressure. Then it can be expressed that:

$$-g \frac{\partial \phi_1}{\partial y}\bigg|_{y=H_l} = -g \sum_{n=1}^{\infty} \frac{2 \cdot \sinh(\lambda_{i,n} x)}{\lambda_{i,n} \cdot H_l \cdot \cosh(\lambda_{i,n} L_x)} \cdot \dot{u}_g(t) \quad (B.15)$$

Multiplying both sides in Eq.B.14 by $\sin(\lambda_{c,m} x)$ and integrating with respect to x from -L$_x$ to +L$_x$ and substituting Eq.B15 into it, the left hand side becomes

$$left = \sum_{m=1}^{\infty} A_{1m} \cdot B_{2m} \cdot L_x \cdot [-\omega^2 + \omega_{c,m}^2] \cdot \cosh(\lambda_{c,m} H_l) \cdot \dot{u}_0 \sin(\omega \cdot t) \quad (B.16)$$

The right hand side becomes:

$$right = -\sum_{n=1}^{\infty} \sum_{m=1}^{\infty} \frac{2 \cdot g}{\lambda_{i,n} \cdot H_l \cdot \cosh(\lambda_{i,n} L_x)} \cdot \dot{u}_g(t) \int_{-Lx}^{+Lx} \sinh(\lambda_{i,n} x) \cdot \sin(\lambda_{c,m} x) dx \quad (B.17)$$

The integration part can be solved as following result:

$$\int_{-Lx}^{+Lx} \sinh(\lambda_{i,n} x) \cdot \sin(\lambda_{c,m} x) dx$$

$$= \frac{2}{\lambda_{i,n}^2 + \lambda_{c,m}^2} [\lambda_{i,n} \cdot \cosh(\lambda_{i,n} x) \cdot \sin(\lambda_{c,m} x) - \lambda_{c,m} \sinh(\lambda_{i,n} x) \cdot \cos(\lambda_{c,m} x)]\bigg|_0^{Lx}$$

$$= \frac{2}{\lambda_{i,n}^2 + \lambda_{c,m}^2} [(-1)^m \cdot \lambda_{i,n} \cdot \cosh(\lambda_{i,n} L_x) - \lambda_{c,m} \sinh(\lambda_{i,n} L_x)]$$

$$(B.18)$$

Then we can get unknown constant in terms of harmonic condition $\dot{u}_g(t) = \dot{u}_0 \cdot \sin(\omega \cdot t)$:

$$\sum_{m=1}^{\infty} A_{1m} \cdot B_{2m}$$

$$= \sum_{m=1}^{\infty} \sum_{n=1}^{\infty} \frac{1}{(\omega^2 - \omega_{c,m}^2) \cdot \cosh(\lambda_{c,m} H_l) \cdot L_x} \cdot \frac{2 \cdot g}{\lambda_{i,n} \cdot H_l \cdot \cosh(\lambda_{i,n} L_x)} \cdot \frac{2}{\lambda_{i,n}^2 + \lambda_{c,m}^2} \cdot$$

$$[(-1)^m \cdot \lambda_{i,n} \cdot \cosh(\lambda_{i,n} L_x) - \lambda_{c,m} \sinh(\lambda_{i,n} L_x)]$$

$$(B.19)$$

Therefore the velocity potential ϕ_2 can be expressed as that:

$$\phi_2 = \dot{u}_0 \cdot \sin(\omega \cdot t) \cdot \sum_{m=1}^{\infty} \sum_{n=1}^{\infty} \frac{1}{(\omega^2 - \omega_{c,m}^2) \cdot \cosh(\lambda_{c,m} H_l) \cdot L_x} \cdot \frac{2 \cdot g}{\lambda_{i,n} \cdot H_l \cdot \cosh(\lambda_{i,n} L_x)} \cdot$$

$$\frac{2}{\lambda_{i,n}^2 + \lambda_{c,m}^2} \cdot [(-1)^m \cdot \lambda_{i,n} \cdot \cosh(\lambda_{i,n} L_x) - \lambda_{c,m} \sinh(\lambda_{i,n} L_x)] \cdot \sin(\lambda_{c,m} x) \cdot \cosh(\lambda_{c,m} y)$$

$$(B.20)$$

Appendix C Derivation of Equation - Impulsive Pressure (Vertical)

In this research the hydrodynamic pressures for the vertical acceleration consider two components. One is related to the vertical motion of rigid tank. It can obtained by:

$$p_1 = \rho_l (H_l - y) \cdot \ddot{v}_g(t) \tag{C.1}$$

The other is associated with the flexibility of the wall. For this component, the velocity potential function ϕ_3 can be assumed as:

$$\phi_3 = X(x) \cdot Y(y) \cdot T(t) \tag{C.2}$$

Substituting ϕ_3 into two-dimensional Laplace's equation Eq. 3.11, we can get:

$$\frac{X(x)''}{X(x)} + \frac{Y(y)''}{Y(y)} = 0 \tag{C.3}$$

According to the boundary conditions indicated in Eq.3.39-3.41, they result in:

$$y=H_l \qquad \frac{\partial \phi_3}{\partial t} = 0 \Rightarrow Xx) \cdot Y(y) \cdot T(t)' = 0 \Rightarrow Y(H_l) = 0 \tag{C.4.1}$$

$$y=0 \qquad \frac{\partial \phi_3}{\partial y} = \dot{v}_g(t) \Rightarrow X(x) \cdot Y(y)' \cdot T(t) = \dot{v}_g(t) \tag{C.4.2}$$

$$x=\pm L \qquad \frac{\partial \phi_3}{\partial x} = \pm \dot{u}(t) \Rightarrow X(x)' \cdot Y(y) \cdot T(t) = \pm \dot{u}(t) \tag{C.4.3}$$

The Eq.C.3 can be transformed as:

$$\frac{X(x)''}{X(x)} = -\frac{Y(y)''}{Y(y)} = \lambda_i^2 \tag{C.5}$$

The solution for $Y(y)$ can be expressed as:

138

$$Y(y) = B_1 \cos(\lambda_i y) + B_2 \sin(\lambda_i y) \qquad (C.6)$$

Where B_1 and B_2 are unknown constant. For symmetric of the structure by axis of $x=0$ in the vertical acceleration condition, it results in $B_2=0$ and from the boundary condition Eq.C.4.1, it result in:

$$\lambda_i = \frac{(2n-1)\pi}{2H_l} \qquad (C.7)$$

The solution for $X(x)$ can be expressed as:

$$X(x) = A_1 \cosh(\lambda_i x) + A_2 \sinh(\lambda_i x) \qquad (C.8)$$

Where A_1 and A_2 are unknown constant. From boundary condition Eq.C.4.3, for the symmetric, it leads to $A_1=0$.

Thus the velocity potential ϕ_3 can be expressed as that:

$$\phi_3 = \sum_{n=1}^{\infty} A_{1n} \cosh(\lambda_{i,n} x) \cdot B_{1n} \cos(\lambda_{i,n} y) \cdot T(t) \qquad (C.9)$$

Substituting ϕ_3 into the Eq.C.4.3 it results in:

$$\sum_{n=1}^{\infty} A_{2n} \cdot B_{1n} \cdot \lambda_{i,n} \cdot \sinh(\lambda_{i,n} L_x) \cdot \cos(\lambda_{i,n} y) \cdot T(t) = \pm \ddot{u}(t) \qquad (C.10)$$

Here we can find that the hydrodynamic pressure related to the flexibility of the wall can be calculated as same as the procedure used in the horizontal acceleration, except that the boundary conditions in the horizontal acceleration is anti-symmetric while in the vertical acceleration they are symmetric. From the same derivation procedure considering the flexibility of wall in horizontal acceleration condition, the hydrodynamic pressure due to the flexibility of wall in vertical acceleration is that:

$$p_2 = -\rho_l \frac{\partial \phi_3}{\partial t} = \sum_{n=1}^{\infty} \frac{2 \cdot \rho_l \cdot \cosh(\lambda_{i,n} x)}{\lambda_{i,n} \cdot H_l \cdot \sinh(\lambda_{i,n} L_x)} \cos(\lambda_{i,n} y) \int_0^{H_l} \cos(\lambda_{i,n} y) \ddot{u}(t) dy \qquad (C.11)$$

At the surface of the wall $x=\pm L$ it becomes that:

$$p_2 = -\rho_l \frac{\partial \phi_1}{\partial t} = \sum_{n=1}^{\infty} \frac{2 \cdot \rho_l}{\lambda_{i,n} \cdot H_l} \coth(\lambda_{i,n} L_x) \cos(\lambda_{i,n} y) \int_0^{H_l} \cos(\lambda_{i,n} y) \ddot{u}(t) dy \qquad (C.12)$$

Therefore the total hydrodynamic pressure in the vertical acceleration condition is that:

$$p = p_1 + p_2 = \rho_l(H_l - y) \cdot \ddot{v}_g(t) + \sum_{n=1}^{\infty} \frac{2 \cdot \rho_l}{\lambda_{i,n} \cdot H_l} \coth(\lambda_{i,n} L_x) \cos(\lambda_{i,n} y) \int_0^{H_l} \cos(\lambda_{i,n} y) \ddot{u}(t) dy$$

$$(C.13)$$

Appendix D Format of Input File PRE.DAT

The PRE.DAT is input file for subroutine HYDRO. It provides information for calculation of hydrodynamic pressure. The format is list below:

Part 1. Analysis Information

Notes	Columns	Variables	Type of Data	Entry
(1)	1 - 5	NSYN	I5	Number of required analysis
				EQ.1 Including hydrodynamic analysis
				NE.1 Empty Tank

Part 2. Control Information (4F10.0, 3I5)

Notes	Columns	Variables	Type of Data	Entry
(1)	1 - 10	FDEN	F10.0	The mass density of fluid
(2)	11 – 20	XL	F10.0	The half width of rectangular tank
(3)	21 - 30	YL	F10.0	The height of rectangular tank wall
(4)	31 - 40	HL	F10.0	The height of fluid.
(5)	41 - 45	MF	I5	Number of nodes calculated in SAPIV
(6)	45 - 50	NHOV	I5	Number of required earthquake

calculation

EQ.1 Horizontal

NE.1 Vertical

Notes	Columns	Variables	Type of Data	Entry
(7)	51 - 55	NEAR	I5	Number of earthquake record

Part 3. Nodes Information (I5, F10.0)

Notes	Columns	Variables	Type of Data	Entry
(1)	1 - 5	NODF(I)	I5	The equation number applied hydrodynamic pressure
(2)	6 – 15	Y(I)	F10.0	The Y-coordinate of node applied hydrodynamic pressure

Part 4. Earthquake Time Function Information (12F6.0)

Notes	Columns	Variables	Type of Data	Entry
(1)	1 – 6	TIM(1)	F6.0	Time values at point 1, TIM(1)
	7 – 12	ACE(1)	F6.0	Function value at point 2, ACE(TIM1)
	13 – 18	TIM(2)	F6.0	Time values at point 1, TIM(2)
	19 - 24	ACE(2)	F6.0	Function value at point 2, ACE(TIM2)
		etc.	etc.	etc.